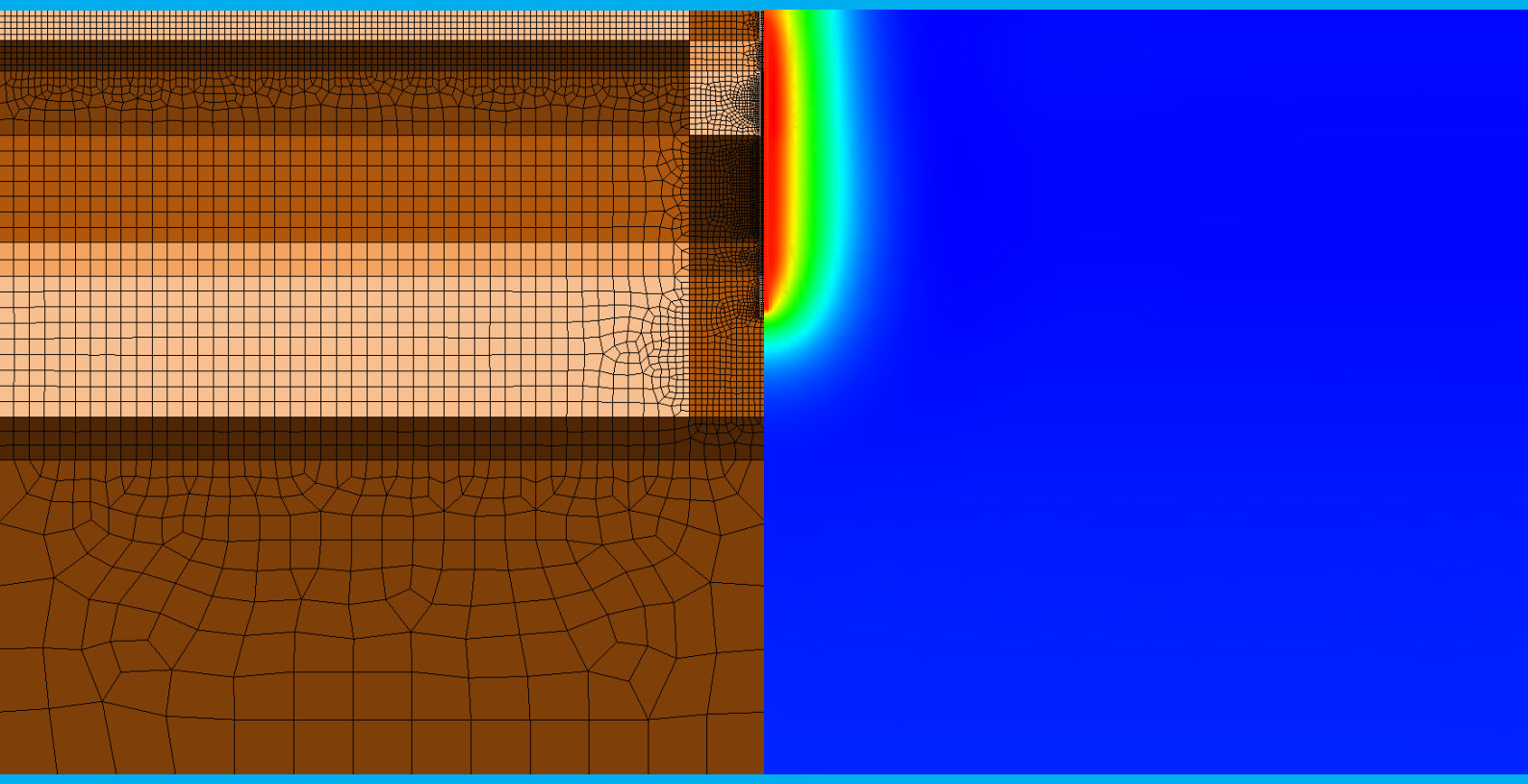
# Numerical modelling of an experimental energy pile

D. Bot



TU Delft

# Numerical modelling of an experimental energy pile

by

D. Bot

to obtain the degree of Master of Science
at the Delft University of Technology,


| | | |
|---|---|---|
| Student number: | 1376187 | |
| Project duration: | November 6, 2016 – August 30, 2017 | |
| Thesis committee: | Dr. P. J. Vardon, | TU Delft, supervisor |
| | Prof. Dr. M. A. Hicks, | TU Delft, professor |
| | Dr. R. I. N. Al-Khoury, | TU Delft |
| | Ir. I. A. Pantev, | TU Delft |
| | Ir. W. P. Kikstra, | DIANA FEA BV. |


An electronic version of this thesis is available at `http://repository.tudelft.nl/`.

TU Delft

# Preface

Before you lies the thesis "Numerical modelling of an experimental energy pile", the culmination of 8 months of hard work. It is also the end of an academic career spanning, very nearly, a decade. This graduation project has everything I was looking for, a numerical investigation grounded in practice with the possibility of using measurements to validate the model. So back in November I did not need to think for long before taking on this challenge. The field measurements did not take place in the end, but the fact that my work will be used in future research is enough validation for me. The challenges in this work for me lied partly in the subject matter and partly in the executional aspects of conducting research. After a slow start I picked up pace in January and progressed steadily from there.

I would like to use this preface to thank my graduation committee. My daily supervisor Dr Phil Vardon for answering my many questions and offering new perspectives. Prof. Michael Hicks and Dr. Rafid Al-Khoury for the critical feedback and the help in getting this finished on time. Wijtze-Pieter Kikstra for all the instruction for DIANA, without it I would not have understood the model in the way I do now. Also for sometimes echoing the sounds of frustration I was making, moments before I came asking for help. I would like to thank Ivo Pantev as well, for answering questions to which you did not know the answer and acting as a soundboard when I needed to bounce some ideas off of you. Sorry to leave before the experiment is in progress, but I did start before you did. I would like to see some results soon.

I owe gratitude to my friends who read this thesis and found quite a few mistakes and helped to improve it significantly. To my fellow master students from geo-engineering who made the coffee breaks fun and frequent during the last weeks of this project. To my parents who supported me through all these years even though I frustrated them by taking a bit too long to finish my studies, I am glad to share this moment with them. And finally to my wife Isis for helping me through this time, with support, motivation to continue and timely distraction.

*D. Bot*
*Delft, August 2017*

# Abstract

Geothermal energy is a way of reducing the cost of energy. Deep geothermal energy systems extract heat from very deep soil layers where the temperatures are very high. Shallow geothermal energy systems are about 150 metres deep and they are used to store heat in the soil, to extract it later and use it for space heating. These shallow geothermal systems are generally embedded in a borehole, but they can also be cast into structures, which are called thermo-active foundations. An example of such a foundation is the energy pile, a foundation pile with a heat exchanger embedded in it, connected to a heat pump. There is no need to drill an extra hole in the ground, but the downside is that it is not well known how the bearing capacity of the pile is affected by the heating/cooling cycles. An energy pile experiment is planned to investigate the thermo-mechanical behaviours of the pile and the goal of this thesis is a numerical investigation of the pile. It serves as an estimate of the pile and soil behaviour prior to installation and the results will be used to confidently design the experiment.

The model was built with DIANA FEA software, that is capable of coupling thermo-mechanical behaviour. Firstly an experiment in London clay was recreated in order to verify and validate the model and modelling approach. The experiment in Delft was modelled using site investigation that was done at the location where it will be built. Along with old Cone Penetration Test (CPT) data the subsurface was mapped and soil parameters used in the material model were chosen. The thermal cycle that was imposed on the pile was chosen on the basis of preliminary modelling done at different temperature increments. The temperatures were chosen such that the pile was affected to a significant degree of its capacity. It was cooled for three weeks to 0 °C and then heated to 24 °C for three weeks, this was repeated for 6 years.

The research focussed on finding which thermo-mechanical effects can be expected and what the scale of those effects could be. The effect directly linked to an increase in temperature is thermal strain. Materials tend to expand and contract with the temperature at different rates and so do the pile and the soil. The gradient of the heat flow is also an important factor as the pile is subjected to the temperature before the soil is. The pile will expand first and this will be resisted by the soil, the strain that is resisted by the soil is called the restrained strain and that is responsible for the change in stress in the pile. A pile that is heated will have more stress than with just a mechanical load and a pile that is cooled will see a reduction in stress. The pile will expand vertically around a null-point somewhere along the pile, this is the point that does not move. In principle, an unrestrained pile will have a null-point in the centre of the pile, but because some soil layers resist the pile movement more than others the null-point is closer to the stronger layers. In the Delft experiment model the null-point was halfway down the pile at first, but as the amount of cycles progressed it moved down. This is due to a decrease in resistance from the weaker layers and an increase in resistance in the strong sand layer on which the pile is based. The amount of stress that is generated is also less in these later cycles as the resistance of the soil became less. With that reduced resistance an increase in settlement is also seen. This can lead to differential settlements of structures that are built on such a pile, possibly damaging them.

The results of the modelling are used to give an advice on the experiment details, such as geometry, thermal cycle and pile layout. An advice to the layout of the sensors is included as well as a prediction of the results.

# Contents

**List of Figures** ix

**List of Tables** xiii

**1 Introduction** 1
- 1.1 Project description . . . 1
- 1.2 Research questions . . . 2
- 1.3 Overview of thesis. . . . 2

**2 Literature study and relevant background** 5
- 2.1 Geothermal energy . . . 5
  - 2.1.1 Shallow geothermal energy . . . 5
  - 2.1.2 Energy foundations . . . 5
  - 2.1.3 Heat pump. . . . 6
- 2.2 Thermomechanics . . . 7
  - 2.2.1 Steady state heat flow . . . 7
  - 2.2.2 Infinite line source model . . . 8
  - 2.2.3 Thermal conductivity . . . 9
  - 2.2.4 Mechanical effects . . . 10
- 2.3 Experiments . . . 10
  - 2.3.1 EPFL experiment. . . . 10
  - 2.3.2 Lambeth College experiment . . . 11
- 2.4 Mechanisms . . . 14
- 2.5 Cyclic behaviours . . . 16
  - 2.5.1 Remoulding clay . . . 16
  - 2.5.2 Ratcheting . . . 16
- 2.6 Numerical modelling of energy piles . . . 17
  - 2.6.1 EPFL simulation . . . 17
  - 2.6.2 Lambeth College simulation . . . 17
- 2.7 Pile displacement calculations . . . 19
  - 2.7.1 GSHPA standard . . . 19
  - 2.7.2 Design considerations . . . 19
- 2.8 Conclusions. . . . 21
  - 2.8.1 Applicability to the Delft experiment. . . . 21
  - 2.8.2 Comments on the experiments from literature. . . . 21
  - 2.8.3 Numerical modelling . . . 22

**3 Model building, verification and validation** 23
- 3.1 Introduction . . . 23
- 3.2 Modelling strategy . . . 23
  - 3.2.1 Effects to investigate . . . 24
- 3.3 Domain and material parameters. . . . 25
  - 3.3.1 Modelled domain . . . 25
  - 3.3.2 Material parameters . . . 26
- 3.4 Heat flow analysis. . . . 27
- 3.5 Structural analysis . . . 28
- 3.6 Coupled THM analysis . . . 29
  - 3.6.1 Replicating previous numerical study . . . 32
- 3.7 3D modelling of cooling pipes . . . 36
- 3.8 Discussion . . . 37
- 3.9 Conclusion . . . 38

**4 Modelling the experimental energy pile** **39**
4.1 Introduction . . . 39
4.2 Structural pile design . . . 39
4.3 Site investigation and material parameters . . . 40
4.4 Thermal cycle . . . 42
4.5 Results . . . 44
4.5.1 Temperatures . . . 44
4.5.2 Axial strain, stress and shear stress . . . 44
4.5.3 Vertical displacement . . . 49
4.5.4 Null-point . . . 50
4.5.5 Transient and cyclic effects . . . 51
4.5.6 Measurement ranges . . . 52
4.6 3D modelling . . . 53
4.7 Conclusion . . . 55

**5 Discussion** **57**
5.1 Thermomechanical effects . . . 57
5.1.1 Vertical pile displacement . . . 57
5.1.2 Axial strain . . . 58
5.1.3 Axial stress . . . 58
5.1.4 Shear stress . . . 58
5.1.5 Cyclic effects . . . 58
5.1.6 Other effects . . . 59
5.1.7 Scales of the effects . . . 59
5.2 Experiment design . . . 60
5.2.1 Pile geometry . . . 60
5.2.2 Thermal cycle . . . 60
5.2.3 Heat pump . . . 60
5.2.4 Sensor measurements and placement . . . 60
5.3 Numerical modelling . . . 62
5.3.1 Material models . . . 62
5.3.2 Hydraulic behaviour . . . 63

**6 Conclusions** **65**

**7 Recommendations** **67**

**Bibliography** **69**

**A CPT data** **71**

**B Results for 24 degrees** **77**

# List of Figures


2.1 Heat pump schematic [Brandl, 2006] . . . 6
2.2 Ground sources heat pump system [Brandl, 2006] . . . 6
2.3 Heat flow through a slab [Spakovszky, 1993] . . . 7
2.4 Steady state [Spakovszky, 1993] . . . 7
2.5 Radial heat flow [Brandl, 2006] . . . 8
2.6 Thermal cell test [Clarke et al., 2008] . . . 10
2.7 Vertical stress EPFL experiment [Laloui et al., 2006] . . . 11
2.8 Vertical strain Lambeth College [Bourne-Webb et al., 2009] . . . 12
2.9 Axial load and shaft resistance when cooling [Bourne-Webb et al., 2009] . . . 13
2.10 Axial load and shaft resistance when heating [Bourne-Webb et al., 2009] . . . 13
2.11 Response mechanism load only [Amatya et al., 2012] . . . 15
2.12 Response mechanism cooling only [Amatya et al., 2012] . . . 15
2.13 Response mechanism combined load and cooling . . . 15
2.14 Response mechanism heating only [Amatya et al., 2012] . . . 15
2.15 Response mechanism combined load and heating [Amatya et al., 2012] . . . 15
2.16 Ratcheting of energy piles in a centrifuge, EP-D is jacked-in and EP-R is whished-in-place [Ng et al., 2016] . . . 16
2.17 Thermomechanical vertical stresses in the pile at EPFL:(a) experimental results (b) numerical results [Laloui et al., 2006] . . . 17
2.18 Vertical pile head displacement over time [Gawecka et al., 2016] . . . 18
2.19 Axial stress over time in the pile [Gawecka et al., 2016] . . . 18
2.20 Load-transfer curves [Knellwolf et al., 2011] . . . 19
2.21 Additional considerations for geotechnical design of thermal piles [GSHP Association, 2012] . . . 20

3.1 Modelled domain . . . 26
3.2 Temperature contour after 30 days . . . 27
3.3 Temperature contour after 360 days . . . 27
3.4 Temperature contour after 720 days . . . 27
3.5 Two years of temperature cycles in the pile . . . 28
3.6 Temperature at set distance in time . . . 28
3.7 Temperature contour at cold point 243 days . . . 28
3.8 Temperature contour at hot point 426 days . . . 28
3.9 Temperature contour at cold point 608 days . . . 28
3.10 Axial stress, preliminary analysis . . . 29
3.11 Vertical displacement, preliminary analysis . . . 29
3.12 Shear stress, preliminary analysis . . . 29
3.13 Temperature curve in cooling phase . . . 30
3.14 Temperature curve in heating phase . . . 30
3.15 Axial stress with depth after cooling phase, material 1 . . . 31
3.16 Axial stress with depth after cooling phase, material 2 . . . 31
3.17 Axial stress with depth after heating phase, material 1 . . . 31
3.18 Axial stress with depth after heating phase, material 2 . . . 31
3.19 Vertical displacement, material 1 . . . 32
3.20 Vertical displacement, material 2 . . . 32
3.21 Vertical displacement from Gawecka et al. [2016] . . . 32
3.22 Shear stress envelope [I.A. Pantev] . . . 33
3.23 Shear stress on the interface, material 1 . . . 33
3.24 Shear stress on the interface, material 2 . . . 33
3.25 Shear stress on the interface from Gawecka et al. [2016] . . . 33

3.26 Axial stress with depth, material 1 . . . 34
3.27 Axial load with depth, material 2 . . . 34
3.28 Axial stress from Gawecka et al. [2016] . . . 34
3.29 Thermally induced radial stress with depth, material 1 . . . 34
3.30 Thermally induced radial stress with depth, material 2 . . . 34
3.31 Therally induced radial stress from Gawecka et al. [2016] . . . 34
3.32 Thermally induced normal stresses . . . 35
3.33 Pile head vertical displacement . . . 35
3.34 Soil temperature at 1.5 m distance for cooling pipes and heating line . . . 37

4.1 Meshed model with soil layers . . . 41
4.2 Maximum thermally induced axial stress in heating . . . 43
4.3 Maximum thermally induced axial stress in coolinge . . . 43
4.4 Temperature in the soil at 1.5 m from the pile, halfway down the pile in heating . . . 43
4.5 Temperature in the soil at 1.5 m from the pile, halfway down the pile in cooling . . . 43
4.6 Temperature distribution of the pile and soil on day 7 of the cooling cycle . . . 44
4.7 Temperature distribution of the pile and soil on day 28, the end of the cooling cycle . . . 44
4.8 Temperature distribution of the pile and soil on day 40, start of the heating cycle . . . 44
4.9 Temperature distribution of the pile and soil on day 61, end of the heating cycle . . . 44
4.10 Axial strain in the pile, mechanical load . . . 45
4.11 Axial strain in the pile, cooling cycle . . . 45
4.12 Axial strain in the pile, heating cycle . . . 45
4.13 Axial stress in the pile, mechanical load . . . 46
4.14 Axial stress in the pile, cooling cycle . . . 46
4.15 Axial stress in the pile, heating cycle . . . 46
4.16 Axial strain, and strain increment, cooling cycle . . . 47
4.17 Axial stress, and stress increment, cooling cycle . . . 47
4.18 Shear stress, and shear stress increment, cooling cycle . . . 47
4.19 Axial strain, and strain increment, heating cycle . . . 47
4.20 Axial stress, and stress increment, heating cycle . . . 47
4.21 Shear stress, and shear stress increment, heating cycle . . . 47
4.22 Vertical movement, pile and soil, only mechanical load . . . 49
4.23 Vertical movement, pile and soil, cooling cycle . . . 49
4.24 Vertical movement, pile and soil, heating cycle . . . 49
4.25 Vertical pile displacement, 1st cycle . . . 49
4.26 Vertical pile displacement, 10th cycle . . . 49
4.27 Vertical pile displacement, 60th cycle . . . 49
4.28 Null-point location over time . . . 50
4.29 Shear stress on the interface on day 40 and day 2020 . . . 50
4.30 Axial stress on day 40 and day 2020 . . . 50
4.31 Maximum thermally induced axial stress, first 500 days . . . 51
4.32 Vertical pile head displacement, first 500 days . . . 51
4.33 Ground level displacement 1.0 m from the pile . . . 52
4.34 Output temperature cooling pipe for 0 °C input . . . 53
4.35 Output temperature cooling pipe for 24 °C input . . . 53
4.36 Output temperature cooling pipe for 0 °C input in cycle . . . 54
4.37 Output temperature cooling pipe for 24 °C input in cycle . . . 54

5.1 Sensor layout within a pile cross-section . . . 61
5.2 Sensor layout in a longitudinal cross-section of the pile . . . 62

A.1 CPT 1, cone resistance . . . 71
A.2 CPT 1, sleeve friction/cone resistance . . . 71
A.3 CPT 1, pore water pressure . . . 72
A.4 CPT 2, cone resistance . . . 72
A.5 CPT 2, sleeve friction/cone resistance . . . 72
A.6 CPT 2, pore water pressure . . . 73

A.7 CPT 3, cone resistance . . . 73
A.8 CPT 3, sleeve friction/cone resistance . . . 73
A.9 CPT 3, pore water pressure . . . 74
A.10 CPT 4, cone resistance . . . 74
A.11 CPT 4, sleeve friction/cone resistance . . . 74
A.12 CPT 4, pore water pressure . . . 75

B.1 Axial strain, heating and cooling . . . 78
B.2 Axial stress, heating and cooling . . . 78
B.3 Shear stress, heating and cooling . . . 78
B.4 Vertical pile displacement, heating and cooling . . . 78
B.5 Maximum thermally induced axial stress, first 500 days . . . 79
B.6 Pile head displacement, first 500 days . . . 79
B.7 Ground level displacement 1.0 m from the pile, first 500 days . . . 79

# List of Tables

2.1 Mechanism parameters . . . . . 15

3.1 Material parameters initial simulation . . . . . 26
3.2 Material parameters pile-soil interface . . . . . 26
3.3 Material parameters Lambeth pile . . . . . 27

4.1 Soil layers based on Dinoloket CPT's. [MWH B.V., 2015] . . . . . 41
4.2 Soil layers based on 2017 CPT's . . . . . 41
4.3 Material parameters for the Delft model . . . . . 41
4.4 Annotations to figure 4.1 . . . . . 41
4.5 Theoretical versus numerical axial stress . . . . . 42
4.6 Theoretical versus numerical axial stress Delft pile . . . . . 48
4.7 Expected measurements of various parameters . . . . . 52
4.8 Cooling pipe and thermal fluid parameters . . . . . 53
4.9 Output temperatures of cooling pipes in DIANA . . . . . 54

5.1 Expected measurements of various parameters . . . . . 59

# 1 Introduction

The heating of houses represents a large portion of energy consumption and most of that energy is supplied from non-renewable sources. Domestic heating is a sector where changes are needed in order to facilitate a climate neutral economy. Right now district heating is a good option where a large scale is required [Mimouni, 2014] such as biomass, however this is not feasible everywhere. Geothermal energy can be an answer, it is the storage or extraction of heat from the subsurface. Deep geothermal energy, where energy is drawn from large depths, requires large investments not feasible for single users. Shallow geothermal energy of up to 500 m is cheaper, but it requires careful planning with potential neighbouring geothermal systems. Embedding these heat exchangers into foundation structures can give a further reduction of both cost and scale, making it a good potential solution for smaller users. Of the thermoactive foundations the energy pile is the most used type. It gives the option of fitting a large foundation with a lot of energy piles so the energy demand of bigger buildings can be met.

Energy piles, or thermal piles, are a good method to use the soil as an energy storage. The pile can store heat that is in excess in the summer into the soil by heating it up and in the winter this heat is extracted for heating houses. This can be done because the soil has a large heat capacity and volume. Fluctuations in the ambient air temperature only affect the top 5-15 m, below which for every 100 m, the soil temperature goes up by ~1 °C. This is a steady state as nothing else influences the temperature, because of this it is a suitable medium for storing energy, when compared to water or air. It is a way to make heating living spaces more sustainable and in that way contributes to the concept of climate neutral buildings. The integration of a heat pump with a foundation element is cost and time saving, when comparing it to a separate system, making it more easily available for consumers. Ground source heat pumps are widely used already, and foundation piles as well. However the influence that the temperature change has on the load capacity of the pile is not well known.

The heat stored in the summer will expand the pile, and when that heat is used in the winter the pile will contract again. Because this does not happen in the pile at the same rate it does in the soil, these thermal cycles result in cyclic stresses on the pile and the pile-soil interface. In order to assure safe structures, the effects of this operational regime on the bearing capacity of foundation piles as well as the accumulation of displacements need to be investigated. Both the short term and long term effects will be investigated as these effects will continue for years.

## 1.1. Project description

In the larger project two PhD students and a post-doctoral researcher are researching energy piles and thermal effects on the soil. Within this project this master's thesis investigates the experimental pile numerically with the goal of helping design the experiment with confidence. The pile will be designed on the basis of the Dutch geotechnical design code NEN 9777-1 and the British standard on thermal pile design of the Ground Source Heat Pump Association [GSHP Association, 2012]. These codes together make a good start for designing the pile. The experimental pile will be built on the site of the TU Delft Green Village, a variety of measurements will be done during the building process and during use. To find the full effect that temperature changes have on the pile and the soil a lot of heating/cooling cycles must be done. For efficiency the

experimental pile must be as small as possible, but a foundation element needs to be large enough to ensure enough bearing capacity. A balance must be found between collecting a large quantity of measurement (high number of cycles) and having a representative foundation pile with realistic loading conditions.

The part of the project this thesis will focus on is a numerical simulation of the experimental energy pile. This model can help design the pile through predicting its behaviour. It is made with DIANA, a finite element program capable of modelling coupled thermo-hydro-mechanical behaviour. After interpretation of the model results, combined with the knowledge from previous experiments an advice is written concerning the piles size, thermal cycle and sensor placement and sensitivity.

## 1.2. Research questions

The main goal of this thesis is to model the proposed energy pile. This numerical model will aid the design of this experimental pile. The goal of the modelling is to find an answer to the following questions:

I. Which thermomechanical and thermo-hydro-mechanical effects can be expected?

II. What are the scales of the thermal effects on the soil and the pile?

III. How do the temperature cycles affect the soil-structure interaction?

IV. How will this affect the pile in terms of vertical displacement?

V. What is a good design of the experiment, pile geometry, optimal length of thermal cycle and energy consumption?

VI. What are the optimal sensor placements and expected range of measurements?

## 1.3. Overview of thesis

The thesis consists of the following chapters wherein the posed research questions will be answered.

**Literature and relevant background**

The second chapter contains the literature study. Consulting available published literature was essential to constructing a detailed conceptual model, general thermodynamics were investigated as well. The first of the research questions can be answered mostly from the literature. Research has been done on investigating thermal effects on soil as well as experimental energy piles. The results from the previous energy pile experiments and their applicability to the Delft pile could give an estimation on what to expect. These pile experiments however have been done in different soil conditions, either in the hard soils in Switzerland [Laloui et al., 2006] or the stiff London clay formation [Amis et al., 2008, Bourne-Webb et al., 2009]. The soft Dutch soils offer different challenges, like negative shaft friction, thermally induced consolidation and stiff a load bearing layer. The review of these experiments will include their assumptions and recommendations, including some shortcomings that do not translate well to the conditions in Delft.

**Model building, verification and validation**

In the third chapter the numerical model is described. The initial tests that were run were used to verify and validate the model. The design entails finding out which measurements must be done, what the appropriate sensors are to install in and around the pile and what the optimal geometry of the pile is. This is done by separate mechanical and thermal models that are superimposed onto each other. Initially the model is simple and in time complexity is added, this includes investigating pore water pressures and cooling pipes as a way to impose temperature change in the pile. The more complex a model becomes the more information can be gathered, the problem herein is that mistakes add up and then the source of those mistakes is no longer clear. That's why it is a deliberate and controlled process where each step is understood before going on to the next.

**Experimental pile**

Chapter four contains the modelling of the energy pile as it will be built in Delft. The model, as it was in the previous chapter, is changed to fit the Delft site. Both the site investigation that was done for this project as

well as previous desk studies have been used to make material models for each of the soil layers present. The experiment will include heating and mechanical loading, and the addition of sufficient sensors to measure the full effects in the soil and pile. The numerical simulations have given an indication of the changes in pile working stresses due to temperature increments as well as the rate of propagation of the heat front in the soil. This allowed the design of an experimental program that was short enough, while still collecting representative measurements. A short thermal cycle allows for more heating/cooling, and perhaps a faster accumulation of cyclic effects, however some time dependent effects might be missed. The thermal cycle was optimised, and with that the necessary heat pump can be chosen.

**Discussion, conclusion and recommendations**
A critical look at the modelling and the results is given in the fifth chapter. The observations from the numerical modelling and the answers to the research questions based on them are found in chapter 6 and chapter 7 contains recommendations for future research.

# 2

# Literature study and relevant background

## 2.1. Geothermal energy

Geothermal energy refers to the process of storing or extracting heat from the subsurface. Different types of geothermal energy exist and the largest distinction is between shallow and deep geothermal energy systems. This section will contain an overview of the different types and their applications. In the Netherlands deep geothermal energy starts at 500 m [Rijksdienst voor Ondernemend Nederland, 2016], everything above that is considered to be shallow. Deep geothermal energy systems makes use of temperatures of 70 °C to 120 °C or higher in order to produce steam to drive turbines and generate electricity. Soil layers with these temperatures are between 3 and 5 km from the surface and because of this deep geothermal energy systems require a large investment. In other locations such as Iceland the earth's crust is less thick and higher soil temperatures are found closer to the surface. In these locations deep geothermal energy systems are a feasible option because the water will be hot enough (often in the form of steam) to make energy with. Shallow geothermal energy systems are generally used for energy storage or space heating as they take advantage of the smaller temperature difference between the top soil layers and ambient temperature.

### 2.1.1. Shallow geothermal energy

Shallow geothermal projects typically operate between 0 °C and 32 °C [Boënnec and Maunsell, 2008]. This means that a shallow system can be used by any single user as well as aid in the heating of large office buildings. Shallow geothermal energy can again be divided into open and closed systems. In an open system water is pumped from aquifers, heated and pumped back into the aquifer, leaving it there until the energy is needed. For this to work hot and cold sources are needed, in the summer the cold source is depleted and the hot source is replenished, vice versa in the winter. The downside of open systems is that the groundwater is directly affected, there is a risk of contamination and a disturbance of groundwater meant for consumption, as well as the possibility of interfering with neighbouring geothermal systems. If a cold source is adjacent to a hot source from a different system, the efficiency goes down for both. If the groundwater in the aquifer has a gradient it can advectively transport the heat, reducing the efficiency

Closed systems consist of pipes going into the ground through which a thermal transfer fluid flows. This fluid is pumped through the pipes suspended in a grout filled borehole, heating up the soil, or taking heat from the soil. Instead of heating groundwater, the entire soil body is heated and for this reason there is no need for an isolated aquifer that keeps the water at a consistent depth. The entire profile of soil along the length of the pipe is used for heat storage. The circuit that goes through the foundation elements is called the primary circuit (figure 2.1), the secondary circuit is the network of pipes through the building that needs to be cooled or heated.

### 2.1.2. Energy foundations

A subset of closed systems are energy foundations (or thermoactive geostructures), which use pipes directly embedded in structural elements to circulate coolant and exchange heat with the surrounding soil. This can be any foundation type, from diaphragm walls to slabs and piles. The thermal properties of concrete are better than grout so energy foundations have a higher heat transfer rate than boreholes [Brandl, 2006]. The

concrete also has a high thermal capacity so instead of just being a medium to suspend the pipes in it is a functional part of the thermal system. In particular for large diameter piles, the significant thermal mass of the concrete influences the heat exchange process, i.e. it takes a much longer time to reach a steady-state for the process, instead giving more importance to transient effects. These factors must be given carefully consideration during design and operation of the system [Brandl, 2006].

### 2.1.3. Heat pump

The heat that is extracted from the soil is not at the level where it can be used to heat a home. It comes out of the ground at around 15 °C and for the floor heating the temperature has to be between 25 °C and 35 °C [Brandl, 2006]. This difference needs to be bridged by a heat pump that uses electrical energy to compress the thermal fluid, raising its temperature. After the fluid has been pumped through the secondary system, giving off heat, it is decompressed by an expansion valve and pumped back into the primary system again. The process is visualised in figures 2.1 and 2.2. There is also electricity needed to pump the transfer fluid through the piles and through the secondary circuit. The ratio between energy output after heat pump and energy input is called the coefficient of operation, COP. The heat pump in 2.2 is 4, meaning a 75 % reduction in energy used for heating.

$$\text{COP} = \frac{\text{energy output after heat pump (kW)}}{\text{energy input for operation (kW)}} \tag{2.1}$$

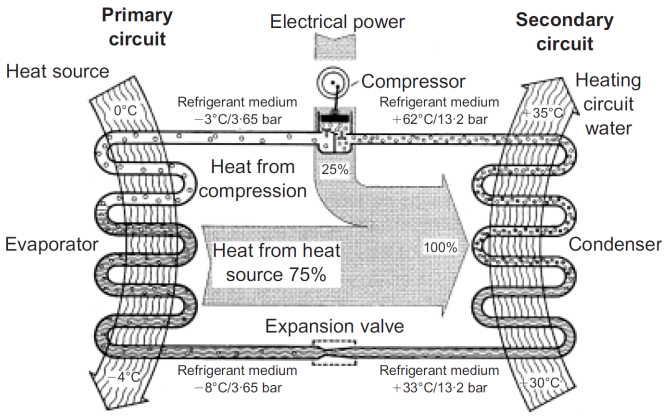



Figure 2.1: Heat pump schematic [Brandl, 2006]

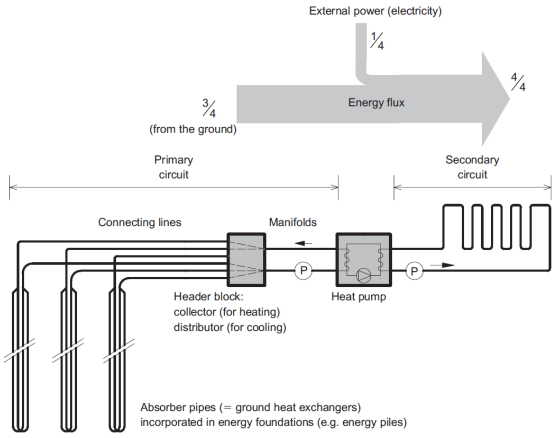



Figure 2.2: Ground sources heat pump system [Brandl, 2006]

## 2.2. Thermomechanics

To get an idea of how heat flows in the soil around the pile a little bit of background in thermodynamics is important. Capturing the thermomechanical behaviour of energy piles is a one-directional coupled problem - i.e. heat flow affects the mechanics of the problem, however mechanical loads do not affect heat transfer. This defines the need to understand the issues surrounding the reliable prediction of the temperature evolution in and around the pile.

### 2.2.1. Steady state heat flow

When a medium has a different temperature in different spots the heat will flow from the hot part to the cold part. The three modes of heat transfer are as follows:

I. Conduction

II. Convection

III. Radiation

Conduction is when the heat flows through the medium itself, convection is the relative motion between parts of the medium and radiation is the loss of heat through electromagnetic radiation. Heat flow in the soil is mostly conduction, the water inside the pores can convectively transfer heat, but that process is a lot slower than conduction. Radiation is a process that is even less significant in the soil.

One dimensional steady state heat flow through a slab will result in a linear difference between the temperature at one side of the slab to the other side of the slab. With equation 2.2 the temperature at a certain distance through the slab can be calculated and equation 2.3 shows the linear relationship between distance and temperature in the steady state where heat flux (heat transfer per unit area) is constant in time.

$$T(x) = T_1 + \left(\frac{T_2 - T_1}{L}\right) x \tag{2.2}$$

$$\dot{q} = -k\frac{dT}{dx} = -k\frac{(T_2 - T_1)}{L} = constant \tag{2.3}$$

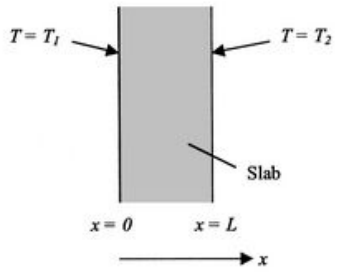



Figure 2.3: Heat flow through a slab [Spakovszky, 1993]

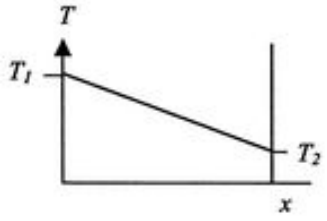



Figure 2.4: Steady state [Spakovszky, 1993]

Figure 2.4 is the steady state that will be reached when two bodies with a constant temperature influence each other. Figure 2.3 could be seen as a 2 dimensional soil body with a pile at $x = 0$ with temperature $T_1$, the temperature $T_2$ at distance $x = L$ at a large distance from the pile is the steady state soil temperature. In this simplified case the soil would keep heating as long as the source is active, not taking into account the fact that $T_2$ can change over time. In the case of a real energy pile, assuming constant temperature with depth (as stated in [Bourne-Webb et al., 2009]), there is heat flow in a radial direction. This changes the shape of the steady state temperature curve, see figure 2.5. This is the behaviour expected of the soil near the energy pile. The amount of influence the pile has on the soil diminishing rapidly with distance.

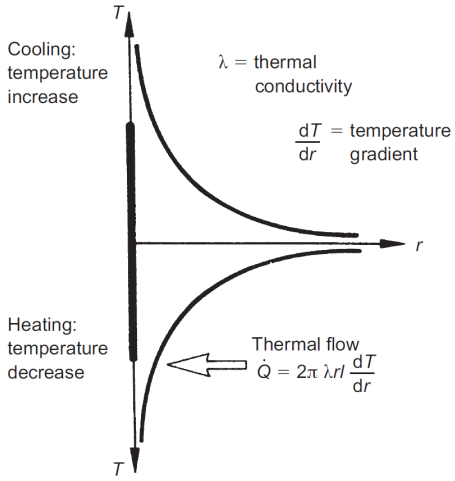



Figure 2.5: Radial heat flow [Brandl, 2006]

### 2.2.2. Infinite line source model

As stated in [Bourne-Webb et al., 2009], the flow of heat from an energy pile can be approximated by an infinitely long line source, radiating uniformly in all directions. The equation for heat flow originating from an infinite line source can be derived from the equation of heat conduction of an infinite cylinder, expressed by [Carslaw and Jaeger, 1959] as follows:

$$\frac{1}{r}\frac{\delta}{\delta r}\left(r\frac{v}{\delta r}\right)+\frac{1}{r^2}\frac{\delta^2 v}{\delta\theta^2}+\frac{\delta^2 v}{\delta z^2}=\frac{1}{\kappa}\frac{\delta v}{\delta t} \tag{2.4}$$

Where $r$ is the radius, $v$ is temperature. $\theta$ is the angle with respect to the axis, $z$ is depth, $\kappa$ $(m^2/s)$ is the thermal diffusivity and $t$ is time. In the axisymmetric case of an infinite line source, the terms for $\theta$ and $z$ will fall out. In more a contemporary notation this will take the following form [Ghasemi-Fare and Basu, 2013].

$$\frac{1}{\alpha}\frac{\delta T}{\delta t}=\frac{\delta^2 T}{\delta r^2}+\frac{1}{r}\frac{\delta T}{\delta r} \tag{2.5}$$

$$\alpha=\frac{\lambda}{\rho C_p} \tag{2.6}$$

Where $r$ is the radius, $T$ is temperature, $z$ is depth, $\alpha$ $(m^2/s)$ is the thermal diffusivity and $t$ is time. $\alpha$ is dependent on $\lambda$ $(W/mK)$, the thermal conductivity of the medium, $\rho$ $(kg/m^3)$, the mass density and $C_p$ $(J/kgK)$, the specific heat capacity.

The analytical solution to this problem can be found in Ingersoll et al. [1954]. With $\dot{q}_l$ as the heat flux per unit length $(W/m)$ and $Ei$ the exponential integral. This equation can be used to solve the infinite line source problem. Following elaboration is from Low et al. [2015].

$$T(r,t)=-\frac{\dot{q}_l}{4\pi\gamma}Ei\left(\frac{-r^2}{4\alpha t}\right) \tag{2.7}$$

$$Ei(x)=-\int_{-x}^{\infty}\frac{e^{-u}}{u}\mathrm{d}u \tag{2.8}$$

Equation 2.8 has the approximate solution:

$$Ei(x)\approx\gamma+\ln|x|+O(x^2) \tag{2.9}$$

Equation 2.9 is valid for small values of $x$, which means large values of $t$. The $O(x^2)$ term is insignificant for large $t$ And $\gamma$ is Euler's constant. This equation does not take into account heat loss through the bottom of the pile, as it models an infinitely long line source. The solution will become less accurate as the modelled domain becomes shorter.

### 2.2.3. Thermal conductivity

An important parameter in all of these calculations is thermal conductivity $\lambda$ ($W/mK$). Thermal conductivity along with specific heat capacity dictate the efficiency of a ground source heat pump. To design a system, a prediction of the thermal behaviour of the pile and the soil is important and the operating temperatures have to be adjusted to ensure optimal usage, but for all these calculations thermal conductivity is needed. The GSHP Association [2012] describes three methods for measuring this value and in Low et al. [2015] these three ways are described and compared, differentiating between in situ and laboratory tests.

**Needle probe**

Needle probes are thin needles of about 150 mm with a heating wire in the middle and it can be used in the field as well as in a laboratory. The heating wire can heat up to a certain temperature and then measure the speed at which the temperature dissipates. With this measurement the thermal conductivity can be calculated. The needle can be pushed into the ground manually, but that limits the depth of the measurements done in the field, or the needle can be fixed on a cone during a Cone Penetration Test (CPT) [Fugro, 2017]. Equation 2.7 and 2.9 can be adapted to calculate this recovery, with $t_1$ the time where the heater stopped heating.

$$T(r,t_1) \approx -\frac{\dot{q}_l}{4\pi\lambda}\left[\gamma + \ln\left(\frac{r^2}{4\alpha}\right) - \ln(t_1)\right] \tag{2.10}$$

$$T(r,t_1) \approx \frac{\dot{q}_l}{4\pi\lambda}\ln(t_1) - \frac{\dot{q}_l}{4\pi\lambda}\left[\gamma + \ln\left(\frac{r^2}{4\alpha}\right)\right] \tag{2.11}$$

With $\Delta T = T(t_1) - T(t_2)$, filling in equation 2.11,

$$\Delta T \approx \frac{\dot{q}_l}{4\pi\lambda}\ln\left(\frac{t_1}{t_2}\right) \tag{2.12}$$

$$\lambda \approx \frac{\dot{q}_l}{4\pi\Delta T}\ln\left(\frac{t_1}{t_2}\right) \tag{2.13}$$

With equations 2.12 and 2.13 thermal conductivity $\lambda$ can be calculated with two measured temperatures in the needle. First at $t_1$ when the heater just stops working and after a sufficiently long time after that at $t_2$.

**Thermal cell**

The thermal cell is a laboratory test, detailed in Clarke et al. [2008], it is an apparatus in which an undisturbed 100 mm diameter sample can be put, see figure 2.6. There are thermistors along the specimen to monitor the temperature, in order to calculate the thermal conductivity the specimen is insulated radially. The bottom heater can be turned on and at the top the resulting temperature change can be measured, when a steady state has been reached, the thermal conductivity $\gamma$ can be calculated with equation 2.14. With $Q$ power input, $A$ cross-sectional area of the specimen, $\Delta T$ the measured temperature difference and $L$ the length of the specimen [Low et al., 2015].

According to Low et al. [2017] thermal cells do not give accurate enough measurements of thermal conductivity due to radial heat losses of up to 50 %. When the soil has a higher thermal conductivity, the radial heat losses decrease, still transient measurements are considered to be more accurate.

$$Q = -\lambda A\frac{\Delta T}{L} \tag{2.14}$$

**Thermal response test**

The temperature response test (TRT) is a full scale field test where the energy pile itself is used as a needle in the same way as with the needle probe. A TRT is a transient test and it is therefore more accurate when measuring thermal conductivity than the previously mentioned tests [Low et al., 2017]. The thermal fluid in the u-pipes is heated with a constant power, so the maximum temperature of the fluid is not relevant. The power that has been used is needed to calculate the thermal conductivity in equation 2.12. The heat is stopped at a certain point, and the temperature decrease is measured over time.

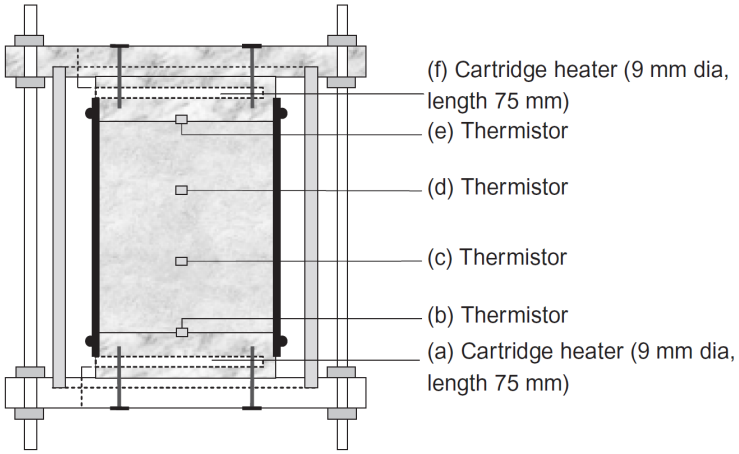



Figure 2.6: Thermal cell test [Clarke et al., 2008]

According to Low et al. [2015] and Clarke et al. [2008] the TRT is the most used test for measuring thermal conductivity for energy piles, because it is the easiest method at the moment. The test conducted by Low et al. [2015] shows that measurements done with the needle probe and the thermal cell show consistently lower values of thermal conductivity than the TRT. They attribute this to disturbing the sample, losing confining pressure and the sample drying out. The TRT tends to give the most accurate measurement, however the outcome is the average thermal conductivity of the entire soil body along the pile. When the soil varies a lot with depth this averaging can negatively influence detailed calculations such as in chapter 3. A solution would be to take extra care when extracting the samples and devising tests that do not influence the measurements, by controlling pressures and moisture content for example.

### 2.2.4. Mechanical effects

Thermomechanics is the coupling of temperature with mechanical behaviour, which is done through the expansion of materials as the temperature increases. The thermal expansion coefficient is the parameter that determines the amount of expansion per degree. In the case of an energy pile the different thermal expansion coefficients that are important are the concrete and the different soil types. To things that stick to each other, that want to expand at different rates will exert a force onto each other. One of the materials wants to expand more than the other and is inhibited to do so, then that thermally induced strain is turned into a mechanical stress in the more expansive material.

## 2.3. Experiments

This section contains previously done full scale energy pile experiments. From those tests a lot can be learned on the behaviour of energy piles as well as what a good way of conducting an energy pile experiment is. In the past two notable energy pile experiments have been conducted. The resulting paper from Ecole Polytechnique Fédérale de Lausanne (EPFL) in Switzerland was published in 2006 [Laloui et al., 2006] and the Lambeth College experiment published an article in 2008 [Amis et al., 2008]. The two experiments have been done in different soil conditions, so both are interesting.

### 2.3.1. EPFL experiment

At the university in Lausanne an experiment was conducted on a pile in a building that was planned to be built, so it was not a purpose built experiment. The goal was to study the increased loads in the pile due to the thermal effects. On the side of the building one pile with a diameter of 880 mm and a length of 25.8 m was fitted with one polyethylene pipe to pump thermal transfer fluid through. Instrumentation was added to measure all the effects of the thermal loading such as vibrating-wire extensometers for vertical strain and temperature. Fibre-optic extensometers for vertical strain as well as fibre-optics for radial strain. And a load cell at the bottom and some extensometers at the top to determine the axial load placed on the pile. The subsurface is layered alluvial soil on gravelly moraine and eventually a sedimentary rock. This is different from the London clay from the Lambeth College test as well as the soft soil conditions at the TU Delft site.

**Loading scheme**
The mechanical load was a static load placed on top of the pile, and the thermal load was controlled by a heat pump. The two types of load were applied separately and sequentially to decouple the pile response. Eight tests were conducted where the load on top of the pile was increased every time due to a new storey being constructed, up to a maximum of 1300 kN. And the thermal load was $\Delta T$ = 21 °C with respect to the mean temperature of the soil for the first test and $\Delta T$ = 15 °C for the remaining tests.

**Results**
The results include a numerical prediction that they have done in addition to the experiment. The most interesting thing however is the vertical stress induced in the pile as a result of the thermomechanical loading. Figure 2.7 shows that the measured vertical stresses within the pile can double when the pile is vertically fixed. When just loading mechanically the toe does not carry any significant load. Thermomechanical loading will use some of the end bearing capacity. This figure was the first showing the vertical stress induced by temperature, Bourne-Webb et al. [2009] cited this figure as a basis for their tests. Other results include small heat induced vertical strains in the soil 1 m from the pile. And that these vertical strains are too small to have any effect on the pore water pressure and thus the effective stress remains the same.

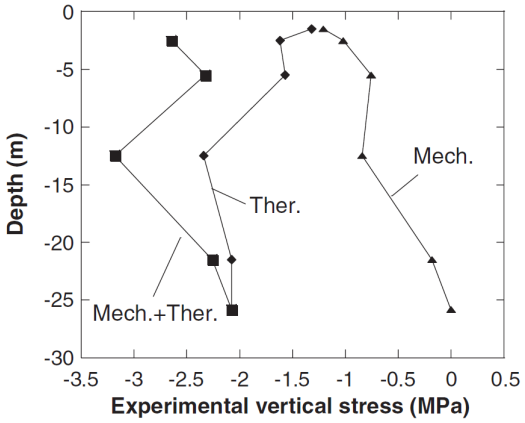



Figure 2.7: Vertical stress EPFL experiment [Laloui et al., 2006]

## 2.3.2. Lambeth College experiment
The goal of this test was to improve upon the knowledge of the thermal behaviour of the pile as well as heat propagation through the soil. This pile is a 550 mm diameter and it is 23 m, designed for a typical working load of 1200 kN. The biggest difference between this pile and the pile at EPFL are the soil conditions. The Lambeth College pile is built in London Clay formation, a very over-consolidated clay that is known for its stiff behaviour, so it was considered a floating pile where the bearing resistance was predominantly shaft friction. The EPFL experiment was an end bearing pile because it was based on a rock formation. The difference between load transfer modes affects the way the temperature influences the pile behaviour as well.

**Loading scheme**
Although this test is part of a building too, the pile was fitted with a loading frame attached to four anchor piles. This way the mechanical load was not bound by the staging of the building process, so there was more freedom to choose an independent testing programme. So they loaded the pile first at the calculated working load of 1200 kN. After that they increased the load to 1800 kN. Then removed that excess load again, and performed the thermal load tests at 1200 kN. They cooled with a thermal fluid of -6 °C for 4 weeks. And after that they heated the pile at 40 °C for 12 days. Then some 24 hour cycles of heating and cooling. During the last cooling cycle a maximum load test was performed to 3 times the working load. After that there was a recovery time where the soil returned to the state it was in before the tests started. They could not do any more tests after this because the planned building needed to be put on the pile.

**Results**

The initial paper by Amis et al. covered some of the results. But a year after this Bourne-Webb published a paper with a more comprehensive overview and interpretation of those results [Bourne-Webb et al., 2009]. In figure 2.8 the measured strains in the pile are shown. The cooling phase on the left shows a large reduction in strain in the pile, and even some negative strain near the pile tip. The heating phase, shown on the right side, causes a large increase, practically doubling the measured strain.

In figures 2.9 and 2.10, the strains have been converted into stresses. These stresses are carried by the shaft in the form of shaft resistance until the pile tip supports the rest. Equation 3.1 is the relationship between temperature used by Bourne-Webb et al. [2009], where $\alpha_c$ is the coefficient of thermal expansion of the concrete, $A$ is the cross-sectional area and $E$ is Young's modulus. Equation 2.16 shows how that can be converted into an axial load $P$. It should be noted that this approach ignores the effect that horizontal stress has on the strain in the vertical direction. This is the case when the pile is fully restrained in the axial direction, as it is the maximum amount generated by temperature. If the pile can move freely, then there is no build up of stress in the pile. When it is restricted, either by a building on top and the load bearing layer, or due to shaft friction, an increase of stress will be present in the pile.

$$\epsilon_T = \alpha_c \Delta T \tag{2.15}$$

$$P = \epsilon_T AE \tag{2.16}$$

The load in the pile can only be reduced by the friction on the pile. This means that the gradient of that reduction says something about the amount of friction. So the shaft resistance graphs in figure 2.9 and figure 2.10 are derivatives of the load in the pile. This is the only way shaft resistance can be quantified as it is not measurable. The shape of these graphs is better explained in section 2.4.

One of the biggest challenges of the energy pile experiment is to get a sense of the changes in shaft resistance as the pile goes through the thermal cycles. The amount that the pile-soil interface is influenced by radial expansion of the pile or changing soil parameters is interesting. With that knowledge the initial state of the soil before temperature loading could give a prediction of the axial fixity and consequently thermally induced stress in the pile.

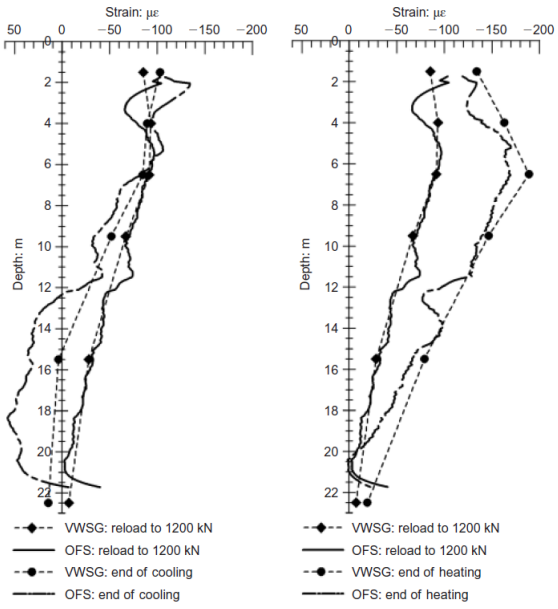



Figure 2.8: Vertical strain Lambeth College [Bourne-Webb et al., 2009]

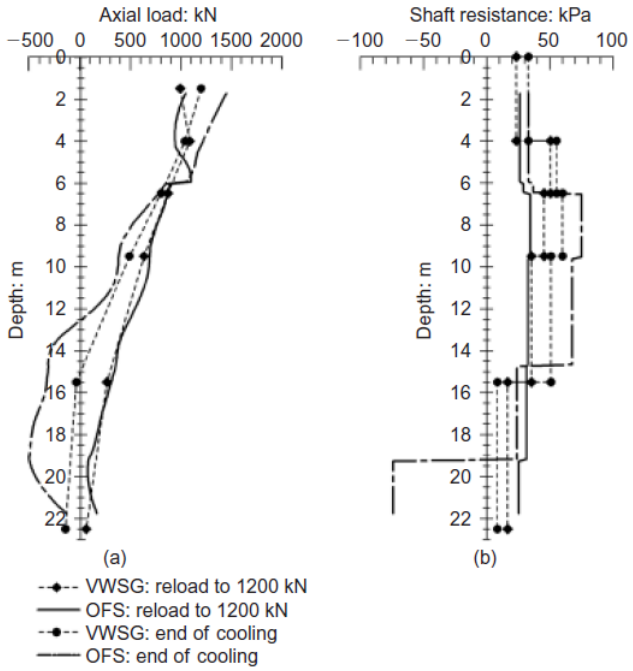



Figure 2.9: Axial load and shaft resistance when cooling [Bourne-Webb et al., 2009]

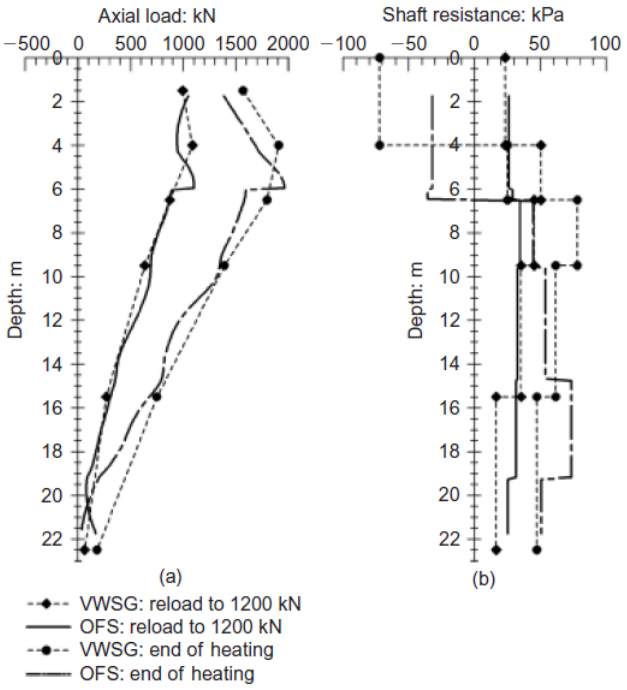



Figure 2.10: Axial load and shaft resistance when heating [Bourne-Webb et al., 2009]

## 2.4. Mechanisms

The behaviours observed in these experiments have been simplified into a few mechanisms, they are the effects of temperature and mechanical loads added to each other so that the thermomechanical behaviour can be seen. They have been better described in a 2012 paper [Amatya et al., 2012] and a 2013 paper [Bourne-Webb et al., 2013] then in the original papers [Amis et al., 2008, Bourne-Webb et al., 2009]. A necessary requirement for accurate modelling and back-calculation of field test results is a clear understanding of the mechanisms governing the soil response to mechanical and thermal loading.

Instead of equation 2.16 this paper makes a difference between the axial stress that is theoretically induced and the stress that is actually measured. The $\epsilon_{T-Free}$ term from equation 2.17 is the strain that would be induced if the pile were free moving. However equation 2.18 shows the relationship between the observed strain $\epsilon_{T-Obs}$ and the restrained strain $\epsilon_{T-Rstr}$. It is clear that the theoretical strain and the strain measured are different quantities. This restrained strain is the value with which to calculate the thermal stress induced in the pile. So equation 2.18 substituted into equation 2.19 gives equation 2.20, and that equation can be used to calculate the thermally induced axial load in the pile. It should be noted that this is a 1 dimensional interpretation of the stresses in and on the pile, only the vertical stress direction is taken into account. This method disregards the effect of the horizontal stresses, but the due to the aspect ratio of the pile (long and thin), the horizontal stresses are negligible. In chapter 4 a limit calculation is made to see the maximum effect of the horizontal stresses on the pile and check this assumption.

$$\epsilon_{T-Free} = \alpha \Delta T \tag{2.17}$$

$$\epsilon_{T-Rstr} = \epsilon_{T-Free} - \epsilon_{T-Obs} \tag{2.18}$$

$$P_T = EA\epsilon_{T-Rstr} \tag{2.19}$$

$$P_T = EA(\alpha_c \Delta T - \epsilon_{T-Obs}) \tag{2.20}$$

Figure 2.11 shows the pile response for purely mechanical loading. It is assumed that the load is resisted only by the friction at the interface, as is typical for the floating piles in London clay. The strain is highest at the top and it decreases with depth as the stress is reduced via shearing on the pile-soil interface. The load is downwards, as is the direction of the strain and the direction of the shear stress on the interface $q_s$, is in the opposite direction, as it is caused by the deformation and movement of the pile. The amount of shear stress is equal with depth as the soil is idealised as a homogeneous material that resists movement equally with depth.

Figures 2.12 and 2.13 show the behaviour of only cooling and the combined load and cooling case. The pile is shrinking along a null-point in the middle of the pile. The null-point is the location on the pile where there is no displacement, and the highest stress increase as a consequence. The interface shear direction is still downward in the top half, but at the bottom it has reversed, in figure 2.13 the two mechanisms are added together. The top part of the pile inducing more shear along the interface and so the stress in the pile is reduced faster than in the purely mechanical case. In the case of strong cooling, like in the schematic for instance, the bottom part of the pile might even be subjected to tensile forces. These mechanisms do not include soil behaviour, so the fact that the soil around the top half of the pile might fail and slip at a certain stress state is not included in the analysis. In that case the lower part of the soil will have to carry more, or it will come down to the pile tip.

The last two cases in figures 2.14 and 2.15 show heating, where the behaviour mirrors the cooling state. The pile now expands about a null-point at the centre of the pile, so the shear stress induced by heat in the top half will counter the shear stress induced by the mechanical load and vice versa in the lower half. The net result in figure 2.15 suggests that a doubling of axial load the centre is possible. In this case as well, the behaviour of the soil is not taken into account. If the pile-soil interface fails on account of the shear stress, the pile tip will have to carry the load.

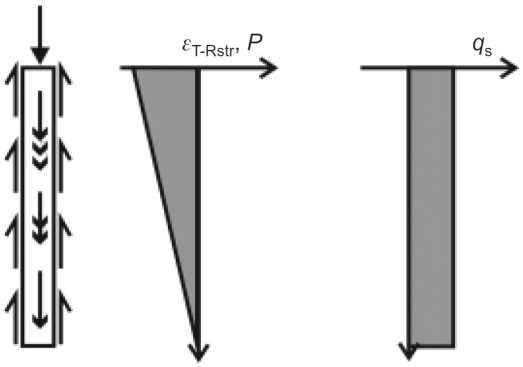



Figure 2.11: Response mechanism load only [Amatya et al., 2012]

Table 2.1: Mechanism parameters

| | |
|---|---|
| $\epsilon_{T-Rstr}$ | axial strain in pile |
| P | axial load in pile (=$\epsilon AE$) |
| $q_s$ | pile-soil interface shear stress |
| A | pile cross-sectional area |
| E | pile elastic modulus |

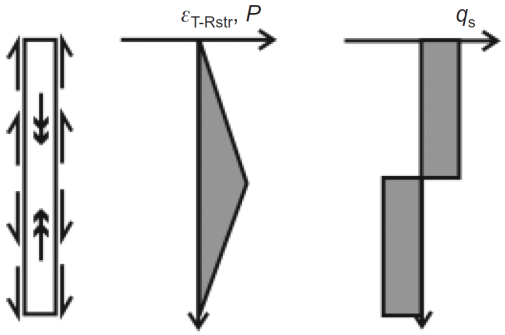



Figure 2.12: Response mechanism cooling only [Amatya et al., 2012]

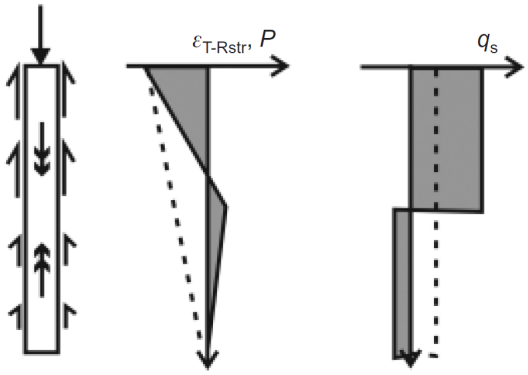



Figure 2.13: Response mechanism combined load and cooling

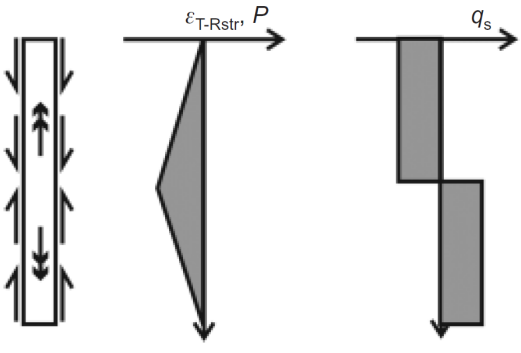



Figure 2.14: Response mechanism heating only [Amatya et al., 2012]

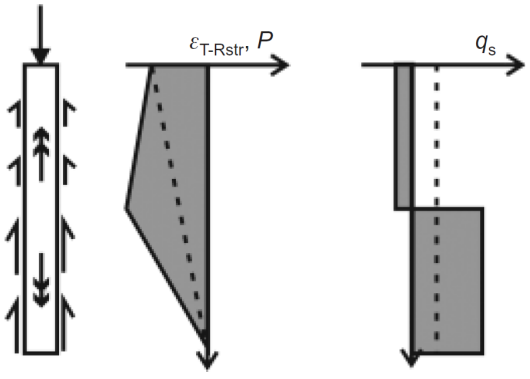



Figure 2.15: Response mechanism combined load and heating [Amatya et al., 2012]

## 2.5. Cyclic behaviours

The cyclic behaviour is expected to play a role in the pile's lifetime. The GSHPA only specifies that it is important but that further research is needed [GSHP Association, 2012].

### 2.5.1. Remoulding clay

Some effects are hard to study, for example the remoulding of clay on the pile-soil interface due to the continuous movement of the pile next to it. Remoulding clay will change the strength from what it was before, so if this effect takes place over a long period of time, it could affect the bearing capacity. During the experiment, if a continuous strain profile can be made, the shear stress profile on the interface can be extrapolated. Because the reduction of strain with depth is a measure of the amount of shear stress is on the interface, see section 2.3. Over time, this strain reduction might not be present in a certain layer after some cycles could indicate the soil is slipping due to remoulding.

### 2.5.2. Ratcheting

Another possible effect is ratcheting, in piles this means an accumulation of deformation due to cyclic loading. The pile contracts due to cold, making it come off the pile tip, then it can then settle due to the load that is still on top. When a heating cycle starts again, it will expand, but now the pile tip is already on the dense layer and the pile can only extend upwards. The bit of plastic deformation in the soil that has happened on account of the settlement of the cooled pile is not regained in heating. And with each passing cycle this might keep on accumulating.

Centrifuge modelling has been conducted on two energy piles by Ng et al. [2016]. One wished-in-place to design depth, this is done to model a bored pile (EP-R in figure 2.16. The other pile was wished-in-place up to 3 times the diameter above design depth and driven in for the rest (EP-D in figure 2.16). Ratcheting happened for the wished-in-place pile, but not for the driven pile, that even showed some heave. The crushing of sand particles during the pile installation and the densification of the sand, contributed to the dilation during thermal loading, as well as reducing contraction during cooling. All these effects cause the pile to move upwards.

Some remarks have to be made on this research. The modelling in a centrifuge changes quite a bit about the experiment. The piles that are concrete normally were modelled with aluminium, they were hollow to be able to apply the temperature and the bottom of the soil body was close to the bottom of the piles. All of these things could have changed the behaviour significantly, but despite these possible imitations showed a significant difference in behaviour was observed. So their findings about the crushing of sand particles can still be correct. The Delft pile will be a screwed pile and the expectation is that the pile will ratchet downward as seen in the EP-R line in figure 2.16.

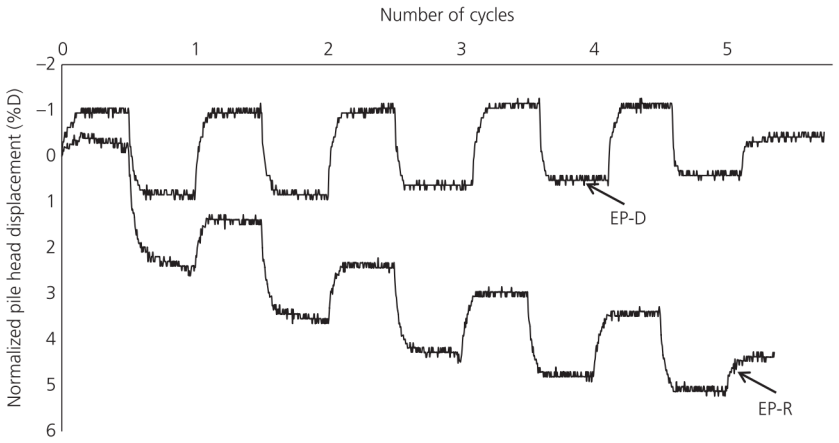



Figure 2.16: Ratcheting of energy piles in a centrifuge, EP-D is jacked-in and EP-R is whished-in-place [Ng et al., 2016]

# 2.6. Numerical modelling of energy piles

## 2.6.1. EPFL simulation

Laloui et al. [2006] simulated their experiment mentioned in section 2.3 with a Thermo-Hydro-Mechanical (THM) coupled finite element model. The geometry was axisymmetric and the pile-soil interface was perfectly rough. That means that the nodes of the soil and the nodes of the pile were directly connected without the possibility of relative movement. This approach has been adopted to eliminate unknowns associated with the effects of installation on the interface and forcing any plasticity/failure to occur within the soil. The soil was modelled with the Drucker–Prager thermo-elastoplastic model. Thermal boundaries allowed for heat flow through the edges of the mesh except for the symmetry line, where the heat flux was null and a constant temperature was imposed on the top of the model. On of their main results is shown in figure 2.17. It shows quite a good fit for vertical pile stress. More so for the mechanical load than the thermomechanical load case.

Although the results fit reasonably well, they made a few assumptions that can be improved upon. The pile-soil interface is not perfectly rough, if the pile fails at the interface, it will have the complete strength of the soil. Where the interface in reality will have a reduced strength when compared to the soil itself. The size of the model is only 7 m wide, a larger model will reduce the effect of the boundary conditions at that edge. Notably, the temperatures imposed are taken from the field measurements, and therefore they should be correct. Other ways of imposing this temperature requires calculating the heat flow through the concrete. Stating that the model then precisely copies an experiment is unverifiable. The downside for this thesis is that there are no data points in an already built pile to base the modelling on. Another way of imposing temperature must be sought.

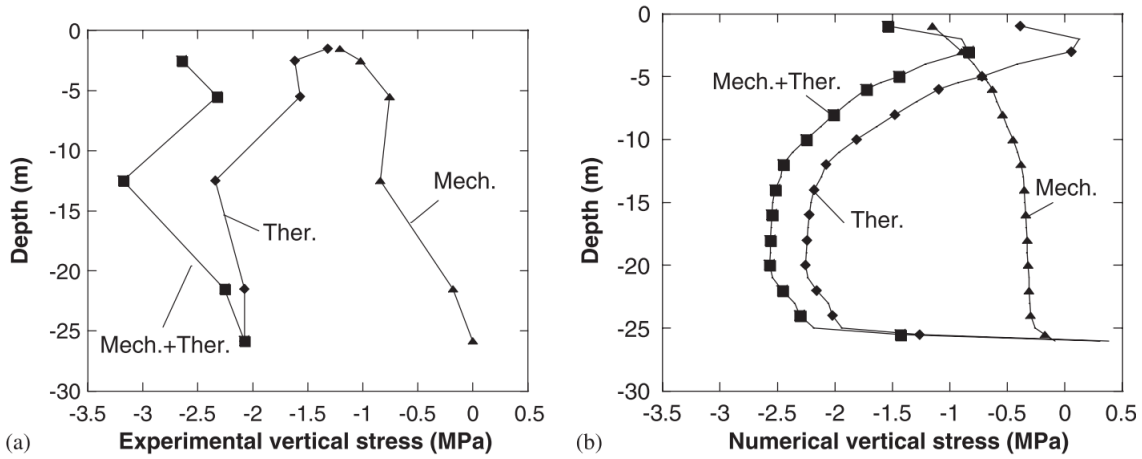



Figure 2.17: Thermomechanical vertical stresses in the pile at EPFL:(a) experimental results (b) numerical results [Laloui et al., 2006]

## 2.6.2. Lambeth College simulation

Gawecka et al. [2016] performed extensive modelling of the Lambeth college pile. The test included a back-analysis of the experiment and an explorative study afterwards. The study included changing modelling approach, the method of thermal load application and the effect of changing some parameters. This numerical simulation will be used in chapter 3 to verify the model intended for the Delft pile.

This analysis is done in the Imperial College Finite Element Program (ICFEP), with a fully coupled THM model. The pile-soil body was modelled axisymmetrically. The London clay was modelled with a undrained pore water pressure profile, small strain stiffness and pressure dependent permeability. This is the typical modelling approach when modelling geotechnical structures in London Clay. The pile-soil interface is not modelled with separate interface elements, hence no relative movement between the pile and soil is allowed. They did however make the first layer of elements next to the pile very thin so that the behaviour there was more realistic. It does mean that when it fails, it will fail in the soil and not at the interface. So slip is not something that they were able to pick up.

Their results of the back-calculation of the experiment are referenced in chapter 3, as well as the explorative study which is also approximated by the DIANA model. One of the most notable results is the vertical pile head displacement over time in figure 2.18 and the axial stress over time in figure 2.19. The numerical scheme for this analysis was to cool the pile at 4.5 °C for 5 months and then heated at 34.5 °C for 6 months. The last month the pile was brought back to 19.5 °C which was the mean soil temperature to start with. The temperature is applied at a rate of $\Delta T = 0.5$ °C. There were 3 different analyses. A is the full THM coupled model, B1 is the fully undrained analysis and B2 is fully undrained but without heat transfer to the soil. Figure 2.18 is the vertical displacement of the pile head over time. All three analyses are roughly equal until the point where the goal temperature of 4.5 °C is reached at around day 30, after that, A and B1 keep on increasing over time. This effect is due to the fact that the pile reaches the temperature first, with the corresponding thermal expansion. The soil has yet to reach the same temperature, at first the soil is holding on to the pile, inhibiting the full movement of the pile. This is explained in section 2.4, a free moving pile will expand more than a pile that is restricted, so when the soil slowly increases in temperature and thus expands as well, the pile will expand with it. For analysis B2 where there is no heat transfer to the soil the induced load goes to a maximum, but the other analyses decrease over time due to the soil expanding where B2 stays the same.

The restrained axial strain ($\epsilon_{T-Rstr}$) is responsible for the thermally induced stress in the pile. So when that restrained strain decreases the vertical stress in the pile decreases as well, as is seen in figure 2.19. The stress of analysis B1 decreases a bit faster than the analysis A, this is mirrored in the slightly faster pile head movement of that analysis as well.

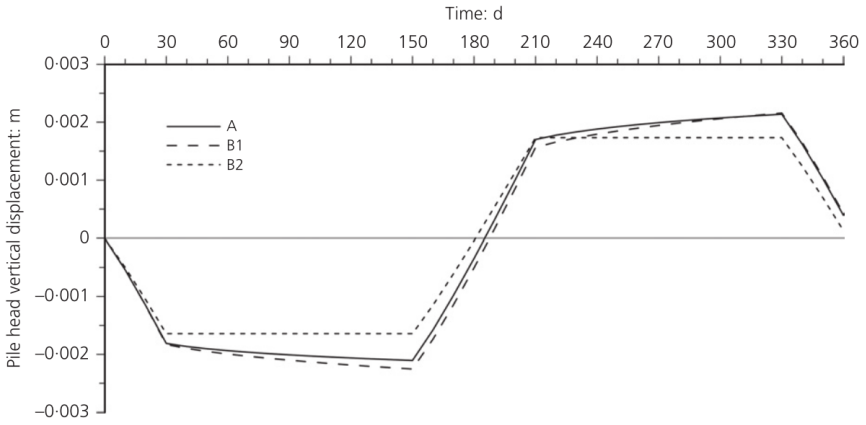



Figure 2.18: Vertical pile head displacement over time [Gawecka et al., 2016]

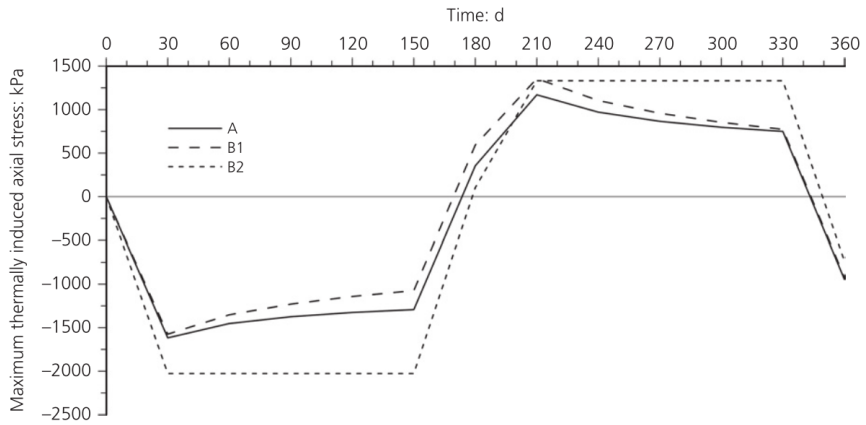



Figure 2.19: Axial stress over time in the pile [Gawecka et al., 2016]

## 2.7. Pile displacement calculations

Pile displacement calculations for a mechanical load can be done with the load-transfer method [Knellwolf et al., 2011, Suryatriyastuti et al., 2014], or finite difference or finite element calculations. The latter is what is done in this thesis, but the load transfer-method could be a good method to make quick calculations for energy piles. With the load transfer curves method a pile is divided into small rigid sections and they are connected to springs. The springs represent the pile stiffness, and they interact with the soil via soil springs that represent the pile-soil interface. The small sections ensure that different soil layers can be assigned different soil properties. Relative displacement at the pile-soil interface mobilizes shear stresses and this relationship is described by load-transfer curves, see figure 2.20. Here the $K_s$ is the slope for shaft load-transfer function and $K_b$ is the slope for the base. They are the spring stiffness for the shaft and base springs. Until the load reaches half of the capacity $q_s$, the behaviour is elastic, but after that there is plastic deformation development and the spring is 5 times less stiff. The unloading and reloading behaviour is still at the old stiffness, but the plastic deformations are not regained. If a pile is loaded to half its ultimate load it will have a factor of safety of 2, and the behaviour will be perfectly plastic.

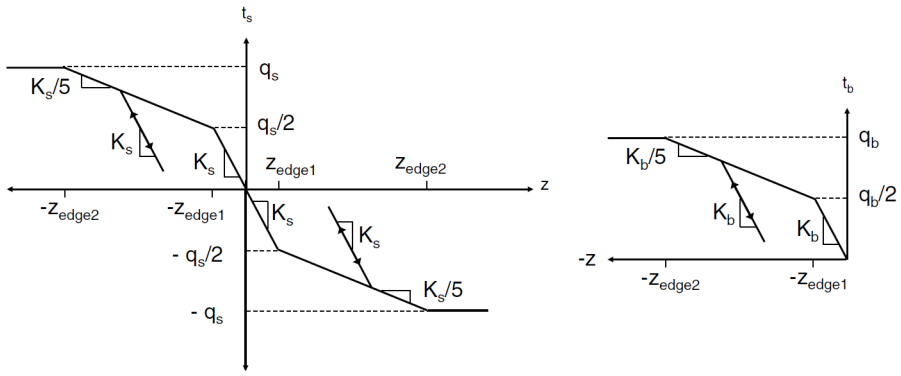



Figure 2.20: Load-transfer curves [Knellwolf et al., 2011]

The method is adapted to make it suitable for energy piles. It does not take into account a few important behaviours influenced by the change in temperature. Radial effects are not calculated, so the influence of a radially expanding pile on the interface will be neglected and the direct influence of temperature on the soil properties is not considered. Thermally induced soil deformations, and changes in properties can affect the interface and the bearing capacity. The spring constants needed to calculate thermomechanical behaviour correctly are non-physical parameters, and hard to calibrate. They can be found once the pile is constructed and tested, but then it needs to be built before it can be engineered. A project would require a test-pile where these parameters can be calibrated, but that takes a lot of time and might not be worth it for smaller projects.

### 2.7.1. GSHPA standard

The Ground Source Heat Pump Association located in the United Kingdom has written a standard for the design of energy piles [GSHP Association, 2012]. The standard incorporates guidelines and best practices, as well as setting out the different roles during the design, construction, operation and maintenance of the system. Design charts are proposed, generally suited for common soil profiles in the UK. They identify some considerations that should be taken into account when designing an energy pile that are not relevant in a normal pile design.

### 2.7.2. Design considerations

Both the effects of the thermal and mechanical loads must be accounted for in the design. The mechanical part is the same as for a non-energy pile, a non-energy pile standard is recommended. Figure 2.21 shows a summary of the additional considerations for thermoactive pile.

#### Thermal effects on soil parameters

The heating will not affect medium dense to dense non-cohesive soils. The increase of temperature will expand the water, increasing pore pressure. But the fact that this soil is porous means that the excess pressure

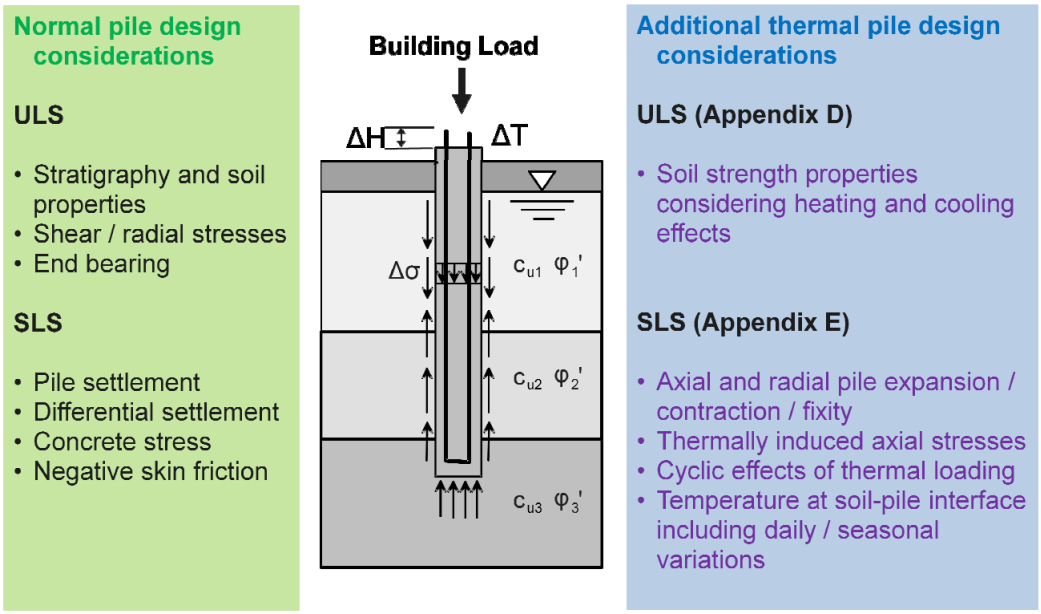



Figure 2.21: Additional considerations for geotechnical design of thermal piles [GSHP Association, 2012]

can dissipate before it has any negative effect. In fine-grained cohesive soils the effect is expected to be bigger. The excess pressure cannot dissipate fast enough and thus the preconsolidation pressure, stiffness and strength of the soil could be influenced, in the soil as well as at the pile-soil interface. Normally consolidated soft clays are expected to consolidate more over time applying negative skin friction to the pile. This effect can be increased and sped up by the thermal load.

**ULS design considerations**
According to the standard in the Ultimate Limit State (ULS) the entire shaft friction is mobilised as well as the base capacity as well. ULS is said to have been reached when settlement has occurred of 10 % of the pile diameter [GSHP Association, 2012]. The thermal strains are not large enough to affect this very much. However the possible decrease in soil strength must be taken into account when defining the ULS.

**SLS design considerations**
The Serviceability Limit State (SLS) is bound by different guidelines than the ULS. The SLS should be assessed for movements from the mechanical and thermal loading. An increase in temperature can initiate a further consolidation process, thereby leading to negative skin friction developing along the shaft [Abuel-Naga et al., 2005]. The increase in pile load as a consequence of heating combined with the mechanical load must not exceed the maximum allowable stress for the concrete.

The amount that this pile stress increases by is dictated by the axial fixity of the pile. A completely free-moving pile will expand without inducing any extra pile stresses. This unrestrained movement might become a problem for the structure on top. If it is completely fixed, the load will increase the most, because the thermal expansion is inhibited by the soil. It is possible that this increase will be more than is allowed for the concrete strength. So in order to predict this behaviour, it is important to analyse the axial fixity.

Another consideration that is mentioned is cyclic loading. The thermal loading is inherently cyclic, both seasonal and diurnal. In the standard it is stated to be important, however no indication was given on how this cyclic behaviour should be accounted for. In appendix E of the GSHPA standard [GSHP Association, 2012] shows a few graphs of cyclic live loads on piles. Although a thermal load on a pile does increase the stress in the pile as a change in load will do, the effect of temperature on the soil is not taken into account at all. The effect of radial expansion of the pile on the shaft friction is disregarded as well. The code also mentions the need for more research in this subject.

## 2.8. Conclusions

In the literature the expected behaviour of an energy pile under thermomechanical loading can be found. The basis in thermomechanics shows the expected temperature profile in the soil, so the distance that the heat travels can be estimated. The need for a thorough site investigation including lab testing to find all the relevant soil properties is clear. In order to predict the behaviour, not only are the strength parameters needed but also the thermal properties.

### 2.8.1. Applicability to the Delft experiment

There are some extra mechanisms to investigate in Delft, such as down-drag caused by thermally induced consolidation in the soft layers. Soft layers can dilate or compress depending on the stress history [Cekerevac and Laloui, 2004]; a normally consolidated clay can compress and an overconsolidated clay will dilate when thermally loaded. The temperature will also decrease the preconsolidation pressure, causing more settlement. The measurements in the experimental pile will include strains, but the measured strain will be less than the theoretical strains due to temperature. The difference between the two will be the restricted strain, which is the value needed to calculate the thermally induced axial stress.

In the numerical part, the changes of the Laloui et al. [2006] and Gawecka et al. [2016] models will be minor. An interface will be modelled, because the relative movement of the pile and the soil are of interest. It is to be expected that the pile will move along the soil in a certain part of the pile, e.g. in the region of the weaker peat and clay layers. The particular places need to be located and extra sensors can be placed there. Stress along the interface is not something that can be measured, it can however be calculated if a high resolution strain profile is measured in the pile. The decrease of strain, and thus stress, in the pile can only be accounted for by induced shear stress along the interface. In figure 2.17-a the amount of strain measurements is quite low, and from those measurements only a crude estimation of vertical stress and interface behaviour can be made. Ideally the strain measurements are done continuous so the calculation of stress is continuous as well, but at the very least strain gauges are required at the depth of each soil layer.

### 2.8.2. Comments on the experiments from literature

These two experiments (in Switzerland and London) have started to quantify the behaviour of energy piles. It is clear that the axial stress in the pile will increase with temperature based on its fixity. There are however some large differences between these experiments and the pile planned in Delft. The granular soil founded on hard bedrock in Switzerland and the London Clay formation at Lambeth College. In Delft the soil is the same as in large parts of the Netherlands, very soft clays and peat on deeper sand layers.

The EPFL pile is of interest because of the incremental loading scheme, the increasing load due to the building on top being incrementally finished. This also means that the pile has not been loaded to a significant portion of the bearing capacity during most of the test. The building was eventually finished, and the experiments duration was coupled with that, so it could be that the cyclic effect simply hadn't had enough time to develop. The conclusion to the article [Laloui et al., 2006] states that the strains in the pile are thermo-elastic and that the friction resistance is not affected by temperature. This might be different when the pile is loaded to a more extreme degree. This can be done by having a pile with a lower factor of safety, loading it to a higher degree of capacity.

The Lambeth college pile was designed to have a factor of safety of 2.5 at a working load of 1200 kN. In terms of the concrete stress ratio this is $\sigma_3 / f_c = 0.14$, with $\sigma_3$ the principle stress direction and $f_c$ the concrete strength. A smaller pile will have a lower bearing capacity but is can be loaded to a higher percentage of the concrete strength, which increases the chance that cyclic effects occur in the pile as well as in the soil. Another issue was that the test duration was too short to see any cyclic effects, as with the EPFL test. The measurements were done with vibrating wire strain gauges (VWSG) and optical fibre sensors (OFS). The measurements done with these two types of sensors show very different results. The strain in figure 2.8 shows a considerable difference between the VWSG and the OFS measurements, mainly in the cooling graph. The OFS measurements show a large amount of positive strain compared to the VWSG. A lot of effort needs to go into using the right sensors to get correct data. The differences in measurements in the same pile show that it is still not clear which measurements are correct and what the precise mechanisms are.

All of these insights should be carried forward to the Delft experiment. The measurements have to be planned carefully to get the most complete picture. Accurate pile head movement, surface settlement and a load cell in the toe of the pile will all contribute to an accurate relationship between the load and the shaft resistance. The soil conditions in Delft are such that the behaviour of the pile will be somewhere in-between the two previously mentioned experiments. It will not be a floating pile as the layers are too weak, but also not a completely end-bearing pile either, there is a shaft resistance comparable in magnitude to the pile toe resistance. The pile, having a hybrid mode of load bearing, gives a good opportunity to study the mechanisms proposed by Bourne-Webb et al. [2009] and Amatya et al. [2012] for characterising the behaviour of energy piles.

### 2.8.3. Numerical modelling

Research has shown that a ground source heat pump system can be modelled approximately as an infinitely long line source, radiating uniformly in all directions [Bourne-Webb et al., 2009]. It would be interesting to see if a very simple model like this would yield similar results in the varied soils of Delft. This research however was done in a mostly uniform London clay formation; the situation in the Green Village is much more variable. It contains more porous materials that will have more convective heat transfer as well as softer soils where a temperature difference will have a greater impact on soil stresses. During the numerical modelling portion of this thesis it is important to see if the different soil types have a significantly different thermal behaviour and different effects on the pile. The difference is likely to be large, as each of the soil types present here will interact differently with the pile at varying temperatures. The direct effect on the design of the experiment is that with a large vertical variance in soil behaviour a large amount of sensors are needed.

# 3

# Model building, verification and validation

## 3.1. Introduction

As a first step to designing the pile, a numerical approximation will be made with DIANA FEA. This chapter contains the initial modelling, the verification and validation of the method. The goal of this numerical model is to find out how big the thermal effects on the soil and the pile will be, as well as give an indication whether or not the proposed experiment scheme will lead to good results. These effects include internal pile stresses and changes in shaft resistance. But also displacements of the pile head over time. This gives an idea as to where the sensors must be placed to yield good results, and it's necessary to design a good experiment. In order to get representative results the model needs to be validated against experimental and numerical data from previous studies [Bourne-Webb et al., 2009, Gawecka et al., 2016].

## 3.2. Modelling strategy

The model is built up from a simple model and complexity is added step by step. This chapter contains the details the four distinct steps that were taken to model the complete energy pile. That model is used to analyse the proposed energy pile experiment, the steps taken to change the model to fit the situation and the analyses done are in chapter 4.


I. Model verification and validation. Page 23

- Heat flow analysis. Page 27
- Structural analysis. Page 28
- Coupled THM analysis. Page 29
- 3D modelling of cooling pipes. Page 36

II. Modelling proposed experimental pile. Page 39


Firstly just the heat flow is calculated, the pile is set at a steady temperature and the heat flow through the soil is the outcome. This analysis gives an idea of the influences of the convective boundary with the air, and the vast soil body around the pile. After that, a yearly temperature cycle was simulated for 6 years, this is a more likely thermal load on an energy pile. Secondly a purely mechanical load is simulated, this shows the behaviour of the pile under normal use without temperature changes. When the temperature is added, the outcome of this mechanical simulation have to be subtracted in order to identify the influence of the changing temperature. Next the thermal calculations will be superimposed onto the mechanical calculation and this thermomechanical model is the final iteration, on the basis of this the Delft pile will have to be built. DIANA offers two ways of coupling thermomechanical behaviour. One is a staggered analysis and the other is a full coupling, which is called mixed analysis. As the heat flow influences the mechanical behaviour but not the other way around, it is seen as a one-directional problem and these can be solved by using the staggered analysis. This means that first the temperature is calculated at all the timesteps and then that temperature field is superimposed onto the mechanical calculation. Lastly the various methods of applying the temperature to the pile have been investigated. The entire pile can be set to a certain temperature, that way the

thermal capacity and thermal conductivity of the concrete are completely neglected. Another way is to put a line on the axisymmetric model at the location where the u-pipes with thermal fluid would be in the pile. Due to the axial symmetry the line is effectively shell with a surface area and via that surface and the heat flux calculated in the model the amount of energy input into the soil can be calculated. The third way is to implement cooling pipes into the model, they simulate a thermal fluid flowing through the pipes in the pile. Cooling pipes work by setting an inflow temperature for the thermal fluid, and the outcome is the outflow temperature, that difference can be used to calculate the amount of energy that is taken up by the soil, as well as the amount of energy that needs to be supplied by the heat pump. Investigating the difference between these different types of thermal boundary is important, because cooling pipes take a lot longer to simulate, and if both types of boundary give similar answers then there is no need to further complicate the model.

After building the thermomechanical model it will have to be verified. This process entails checking to see if the program as it is, implements the math and physics behind it properly. The assumptions that are made about the expected behaviours can be qualitatively checked against the outcome of the model. If they are not as they should, then there is a fundamental problem with the math behind the FEA software and not with the implementation of it.

After verification the model and the assumptions will have to be validated. This is done by simulating the Lambeth college experiment in London(Amis et al. [2008] and Bourne-Webb et al. [2009]). This experiment was chosen to try and simulate because of the isotropic soil conditions and results that resemble the mechanisms detailed in section 2.4 very well. The simulation outcome will be put on top of the experimental outcome to see if reality is simulated precisely enough. This pile was modelled before by Gawecka et al. [2016], so besides replicating the experimental data, the data from this paper can be approximated as well. An interesting conclusion that can be drawn from this paper is that the effect of inducing stress in the pile as a result of the temperature difference reduces over time. The soil catches up to the pile with respect to expansion or contraction and it relaxes and lets go of the pile, reducing thermally induced stress. Replicating this effect in this model is important in understanding the behaviour the experimental pile will have.

### 3.2.1. Effects to investigate

A numerical model can be used to generate lots of data, but certainly not everything is important. The temperature has a lot of effects in the soil and on the soil pile interface and those effects can be expressed in many different parameters.

**Soil temperature**

This is the reason to build energy piles. The soil needs to be heated in the summer and that heat needs to be used in the winter. But how effective will this process be at the site of the Green Village. How far will the heat propagate, and how much heat is eventually stored. A prediction of this effect will dictate the heat pump needed to generate results in the energy pile experiment.

**Normal stress**

The normal stress in the pile will be affected by the heat. Heating the pile makes it expand, and if it is anything but free moving, extra stress will be induced. The reverse effect is seen when cooling. If the normal stress exceeds material strength it will fail. Or at least reduce the safety factor to such a degree where the structure is no longer deemed safe. A large cooling cycle could even cause tensile stresses in the pile. Which can cause cracking in the concrete. Knowing this effect will increase requirements for reinforcement steel.

**Shaft friction**

A shrinking and expanding pile will influence the shaft friction, if the pile shrinks more than the soil it will come loose and reduce the friction. An expanding pile will push against the soil increasing the vertical fixity. A reduction in effective soil stress will also cause the soil to push against the pile less than it was before, and induce less shaft friction.

**Pile movement**

When cooling, the pile will shrink about a null point. This point is in the middle of the pile, but moves up and down with heating and cooling. This means that the pile will be lifted from soil at the pile tip. If the pile is still

loaded, and some tip resistance is needed for support, the pile will settle. When it then expands in heating, it has nowhere to go but up, because the pile bearing layer is very stiff. Or the bearing layer is not stiff enough, and the pile will settle. This is a cyclic effect that might result in very large settlements over time. Those are dangerous when not all piles in the structure are energy piles. The effect that will occur will depend on the dominant load-carrying mechanism and on how extreme the temperature cycle is.

**Transient effects**
The transient effects are the pile behaviours depending on time. A pile heated at a certain temperature will move due to the thermal expansion. After that there is a time-dependent further pile head movement. Axial stress will decrease over time as well. To what degree do these effects change over time? And do these effects eventually reach a steady state?

**Cyclic effects**
Heating and cooling cycles change the direction of the thermal expansion every time it changes. With that change the direction of shear stress on the pile will change as well. This cyclic pile movement along the interface can reduce the strength of the soil at that point. The up and down movement of the pile tip can have an effect on the soil below it. Each cooling cycle the pile tip is lifted and the soil can relax, then in heating it will expand against the soil again. If during cooling it settled a little bit, the stress in heating is now larger than is was before. over time these cycles could increase the soil strength by densifying it, or it could settle more by this ratcheting effect.

**Pore water pressure**
Heating water in the soil will cause it to expand, causing the pore water pressure to go up. This rise in pressure will reduce the effective soil stress. In time the excess pressures will dissipate and this will cause soil settlements.

All of these effects must be investigated at the site of the Green Village of the university. To get the right input parameters for the model a site investigation must be undertaken. Thermal conductivity and capacity affect the propagation of heat, hydraulic conductivity will affect the build-up of pore pressures and shaft friction will affect pile fixity, an important factor in the generation of normal force. So if the model has to reflect the situation in the field a lot of information must be gathered. Only then can the design of the pile be optimised.

## 3.3. Domain and material parameters

### 3.3.1. Modelled domain

This model emulates the Lambeth college experiment [Bourne-Webb et al., 2009], so the pile geometry and soil layers are taken from that paper. In that paper, it also is stated that the heat flow through the soil can be simplified to an infinitely long cylinder radiating outwards. This means that the flow of heat can be modelled axisymmetrically as well as the structural analysis. The pile that was built has a diameter of 550 mm and a length of 23 m. The soil is a single layer of clay material, with sufficient depth as to minimise the influence of the bottom boundary.

**Boundary conditions**
At the far right side of the model lateral movement is inhibited and at the bottom it is the vertical movement. The left side is the axial symmetry line, and the energy pile is located there as well. The top of the model is a convective boundary with the air, where the outside temperature will be modelled, by means of a sinusoidal function of daily averages with a mean of 9.6 °C and an amplitude of 7.4 °C. This the actual daily mean temperature curve in Delft. At the bottom a prescribed temperature is present to emulate the steady soil temperature at depth. The far right edge is a no flux boundary, the same as the symmetry line, making sure there is no influence from an outside source. The soil pile interface is a frictional interface, with the Mohr Coulomb parameters cohesion, a friction angle and a dilatancy angle, as well as conduction coefficient to allow for heat flow. The temperature of the pile is a prescribed temperature on a heating line at the location where normally the u-pipe would be, making sure the concrete still has a cover of about 70 mm.

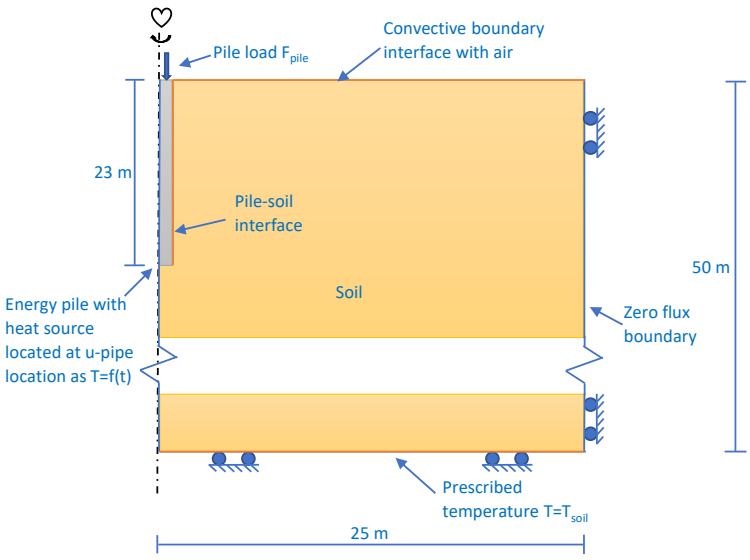



Figure 3.1: Modelled domain

### 3.3.2. Material parameters

At first the model was a linear elastic sand material show in table 3.1. Next to the mechanical parameters are thermal parameters conductivity and capacity. The energy pile experiment used for validation is set in uniform London clay, which is very stiff and overconsolidated. In the table 3.3 the soil parameters used in the model are listed. Two sets of clay parameters were used, the first set was an approximation based on a stiff clay. In the second test they were tuned to fit the situation of London clay better. The second set of parameters were taken from the GSHPA standard [GSHP Association, 2012], except the thermal properties, they are from the numerical approximation done by Gawecka et al. [2016].

Table 3.1: Material parameters initial simulation

| | Unit | Sand | Concrete |
|---|---|---|---|
| Youngs modulus | $N/m^2$ | 4.00E+07 | 3.00E+10 |
| Poisson's ratio | – | 0.2 | 0.2 |
| Mass density | $kg/m^3$ | 1900 | 2500 |
| Porosity | – | 0.3 | - |
| Thermal conductivity | $W/m°C$ | 2.100 | 2.674 |
| Thermal capacity | $J/m^3°C$ | 2.70E+07 | 1.58E+06 |

Table 3.2: Material parameters pile-soil interface

| | Unit | Interface |
|---|---|---|
| Normal stiffness | $N/m^3$ | 1.00E+10 |
| Shear stiffness | $N/m^3$ | 1.00E+09 |
| Cohesion | $N/m^2$ | 0 |
| Friction angle | ° | 20 |
| Dilatancy angle | ° | 0 |
| Conduction coefficient | $W/m^2°C$ | 10000 |

Table 3.3: Material parameters Lambeth pile

| | Unit | Clay, material 1 | Clay, material 2 | Concrete |
|---|---|---|---|---|
| Youngs modulus | $N/m^2$ | 1.10E+08 | $400c_u$ | 4.00E+10 |
| Poissons ratio | – | 0.2 | 0.2 | 0.2 |
| Saturated density | $kg/m^3$ | 2000 | 2000 | 2500 |
| Porosity | – | 0.2 | 0.2 | - |
| $k_0$ | – | 0.56 | 1.0 | - |
| Lin. thermal expansion | $m/m°C$ | 5.00E-07 | 5.00E-07 | 8.50E-06 |
| Shear strength $c_u$ | $N/m^2$ | 1.52E+05 | 6.00E+04+(8.00E+03)$z$ | - |
| Friction angle | ° | 26 | 26 | - |
| Dilatancy angle | ° | 12.5 | 12.5 | - |
| Thermal conductivity | $W/m°C$ | 1.79 | 1.79 | 2.33 |
| Thermal Capacity | $J/m^3°C$ | 1.82E+06 | 1.82E+06 | 1.92E+06 |
| Fluid bulk modulus | $N/m^2$ | 2.15E+09 | 2.15E+09 | - |

## 3.4. Heat flow analysis

These models are all with the first set of materials parameters, shown in table 3.1. The first model consists only of a pile that had an imposed temperature different from the soil. The soil was 12 °C as this is an approximation of the steady soil temperature. It is assumed to be constant with depth. The pile is set at 7.5 °C and a it was run for 2 years. The cold pipe will keep on cooling down the soil until it is stopped. The contour plots in figures 3.2 to 3.4 show the temperature distribution at different times. The temperature goes down in the soil up until about 5 metres. But that is only 0.5 °C difference from the mean temperature.

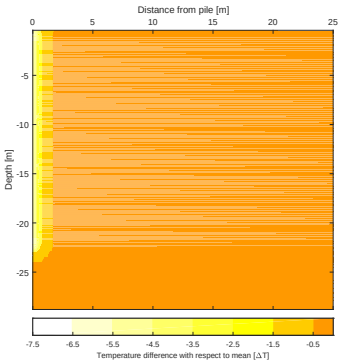



Figure 3.2: Temperature contour after 30 days

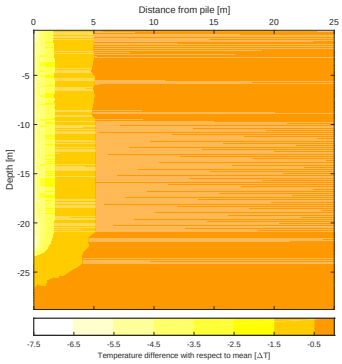



Figure 3.3: Temperature contour after 360 days

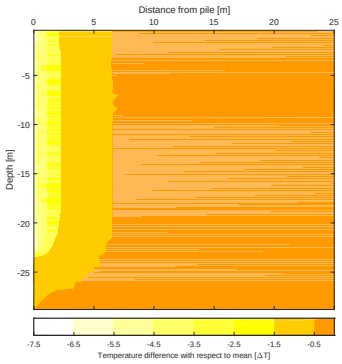



Figure 3.4: Temperature contour after 720 days

After that the pile was set to a different temperature at each day, as it would with actual use. This was to see how far the heat would propagate when the temperature changes over time. Figure 3.5 shows the curve that was used to model this, a sine wave with mean 7.5 °C and an amplitude of 7.5 °C. It starts at a time where the temperature outside is roughly the same as the initial temperature field in the soil. This is to prevent a first step that changes the stress state too much causing problems in the structural analysis. It represents two years of seasonal temperature variation. This is because when it is hot outside, the pile will be loaded with hot transfer fluid and the other way around for cold weather.

Figure 3.6 shows the temperature in a point at 1.4 m distance from the pile at a depth of 10 m. Here the difference between the initial cycles and later on is clear. During later cycles the behaviour is more realistic than during the first cycle. This is because the soil was still at the initial temperature in the first cycle, where in the second cycle the was already closer to the actual steady seasonal temperature condition. This is due to the temperature being rather low compared to the soil temperature, there is mostly cooling in the soil rather than heating. Later on when running the simulations to figure out the cycle needed for the experimental pile, running a few years of just surface temperature will give a good start point for the temperature distribution naturally present in the soil. Figures 3.7 to 3.9 show the same behaviour. At the first cold point the -0.5 °C line

is at 2.5 m from the pile and it is at 6 m at the same point in the second cycle. Figure 3.8 shows that the heating part of the cycle is too short to propagate throughout the entire soil body. So there is still cooling capacity left in this time of the year.

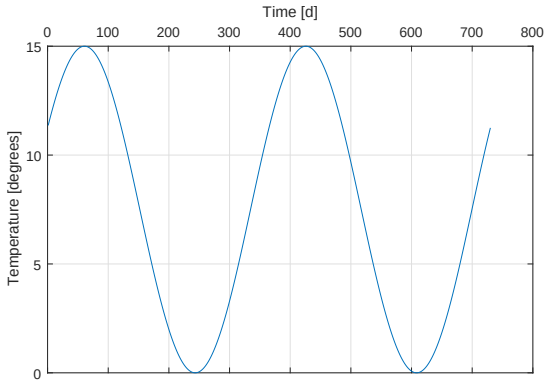



Figure 3.5: Two years of temperature cycles in the pile

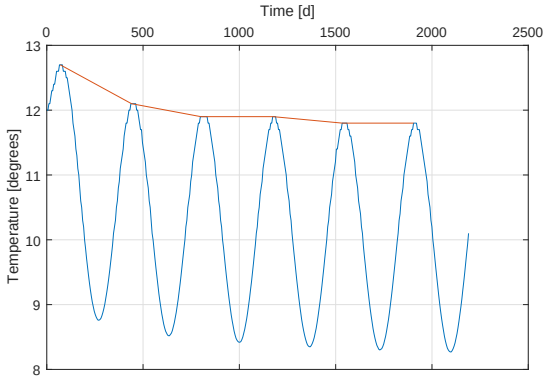



Figure 3.6: Temperature at set distance in time

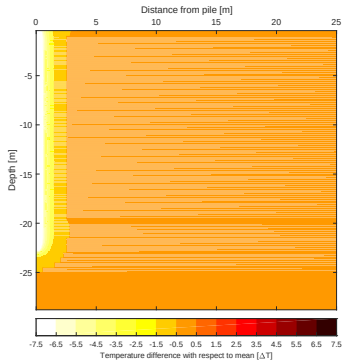



Figure 3.7: Temperature contour at cold point 243 days

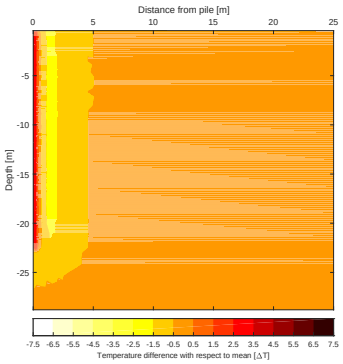



Figure 3.8: Temperature contour at hot point 426 days

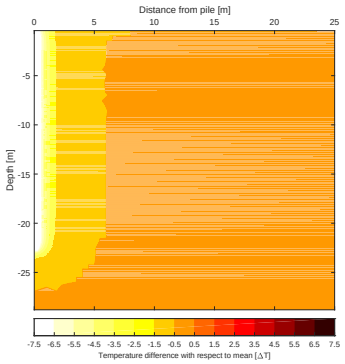



Figure 3.9: Temperature contour at cold point 608 days

## 3.5. Structural analysis

The structural non-linear analysis module available in DIANA was used to analyse the pile behaviour. This method first calculates the linear elastic field as a result of the pile, the soil self weight and the presence of a hydraulic head. In the second phase a load is applied to the pile. The load applied is a fraction of a calculated capacity of the pile using the $\beta$-method [Bowles, 2007]. This method discretises the pile into segments and with the shaft resistance of eacht of those segments the capacity of the shaft is calculated. The base resistance is calculated separately with the Brinch-Hansen method. That way the load will not exceed capacity, which would not lead to a stable calculation. The pile has a capacity of 780 kN without taking into account any safety factors, for the calculation half of that capacity was chosen, 390 kN.

When loading the pile with 390 kN the axial stress in the pile will be reduced by the shaft friction, and the residual load will be underneath the pile tip. In figure 3.10 the yellow line is the normal force in the pile according to the $\beta$-method, the blue and the red lines are from the numerical simulation. The numerical lines shows a much higher stress than the analytical one. On account of the initial condition a considerable stress is seen in the pile on top of the self weight. Figure 3.11 indicates that the pile is pushed out of the soil when the pile load is not yet applied. This means that there is a mistake in the initialisation of the model, which can be seen in the shear stress on the interface in figure 3.12. At the top the shear stress line is straight, because the interface is behaving plastically and no load is carried in this part. The soil is hanging on the pile instead of the the pile being supported by the soil. Only at a depth of around 12 m, where the direction of the shear stress on the interface reverses, is the normal stress is reduced.

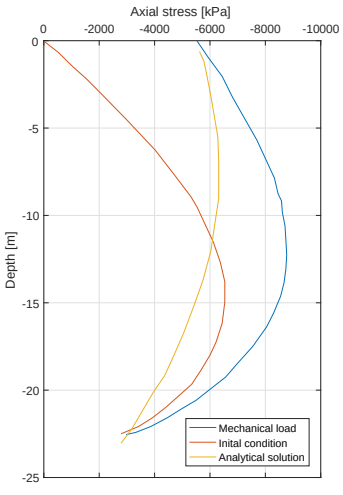



Figure 3.10: Axial stress, preliminary analysis

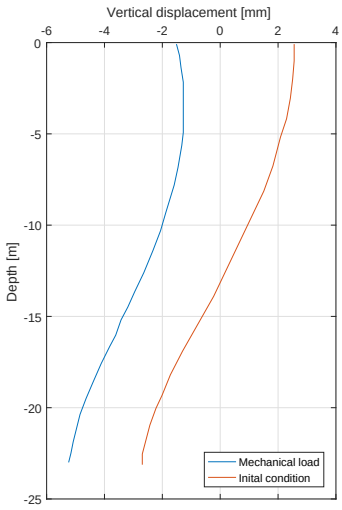



Figure 3.11: Vertical displacement, preliminary analysis

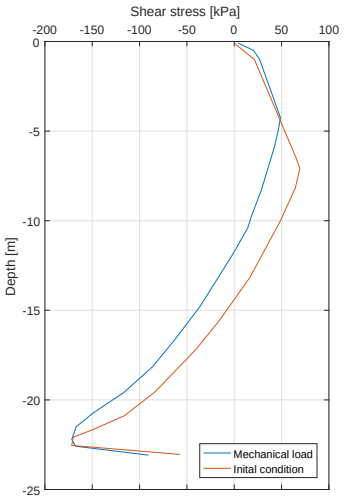



Figure 3.12: Shear stress, preliminary analysis

In numerical modelling of geotechnical structures it is important to get the initial soil conditions right. DIANA has a $k_0$ procedure. It takes the soil weight and the $k_0$ and it calculates the initial stresses in the soil. When that is done while the pile is in the model already the initial settlement of the soil will be more than the pile. Therefore the soil will hang on the pile. When constructing an actual pile, there is no hanging soil. The pile is heavier than the soil and that will induce some settlement of the pile. On the other hand, when the soil around a pile settles due to loads that are applied it can induce negative skin friction. But a displacement is needed for this. In the initial state of an installed pile this is not the case. To solve this a phased analysis is needed where the soil is initialised without the pile in it. In section 3.6 this has to be solved in order to get reliable results.

## 3.6. Coupled THM analysis

The material parameters used in DIANA for this model are listed in table 3.3, both clay material 1 and clay material 2 were modelled. The model was run a couple of times to simulate different situations. They were both done with the clay material 1 at first but then later updated to clay material 2. The changes entailed prescribing a different time sequence to the heating line in the pile. To reach the temperatures in the heating line and keep a stable numerical simulation the incremental temperature of the heating line was half a degree per day. Both cases are modelled fully undrained as that is probably the closest to the situation in London clay.

**Analysis specifics**

The experiment started out with a mechanical load test at 1800 kN, but after that the load is reduced to 1200 kN and the thermal load is applied. In this case they pumped a transfer fluid into the pile at -6 °C for 28 days. In order to model this, the heating line is a boundary condition temperature of -4 °C for 28 days. This value is chosen as the average between the temperature going in and an approximation of the temperature coming out at -2 °C. After the cooling phase they began heating at 40 °C for 12 days. This temperature is approximated as 35 °C at the location of the thermal boundary in the model, this is because the 40 °C thermal fluid is not 40 °C in the entire pile. The original paper measured the temperature on the outer perimeter of the pile to be 35 °C. There was a power outage in the actual experiment, but for the sake of simplicity this is not taken into account. It is not about exactly replicating the experiment, more about getting an insight in how the model works.

**Temperature distribution**
First result to check is the temperature distribution through the soil, if this is not correct, the stresses as a result of this will not be correct either. The paper from the Lambeth college pile contains contour diagram plots of temperature against distance made at the end of the first cooling period of 28 days. Figure 3.13 shows the calculated temperature curve against point taken from that contour diagram. Figure 3.14 shows the same thing but for heating. Both material sets showed the same result as no thermal properties were changed in-between. In figure 3.14 there is a dip in the numerical simulation, this is because the heating cycle was done after the cooling cycle. There is a part of the soil body that still has a lower temperature due to that previous cooling time. The volumetric heat capacity of the soil used in the model is probably higher than in the experimental data and the steady temperature field has not been reached yet, that is why the peak is still visible in the results from the numerical simulation.

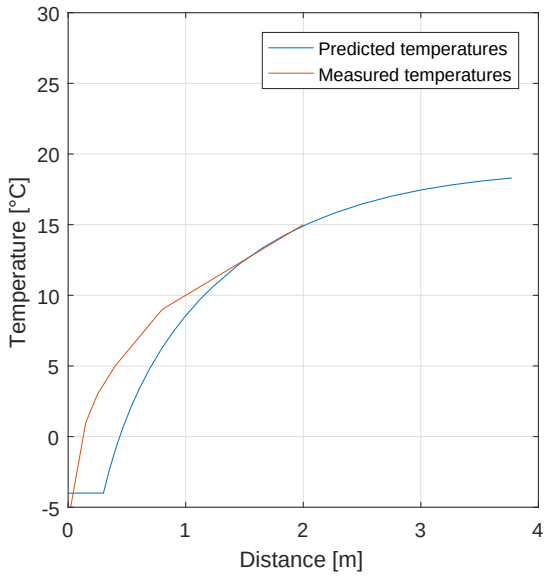



Figure 3.13: Temperature curve in cooling phase

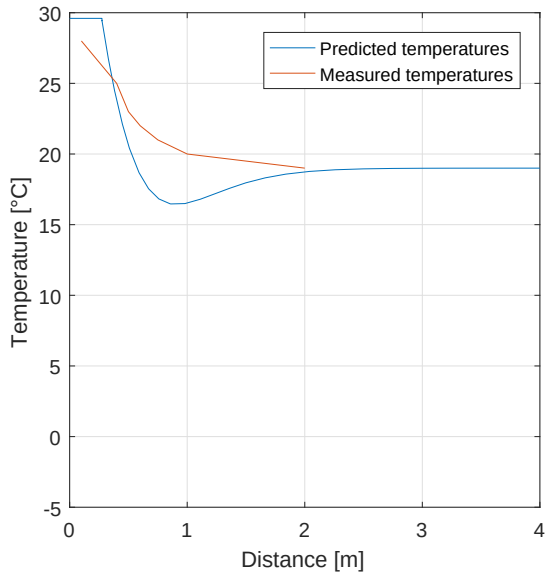



Figure 3.14: Temperature curve in heating phase

**Axial stress after cooling and heating**
The experiment results contain graphs with the stress in the pile [Bourne-Webb et al., 2009] and that stress can be taken from the numerical model as well. Figures 3.15 and 3.16 contain the numerical approximations of axial stress caused by the purely mechanical load, the thermomechanical load and the experimental data. These stresses are present in the pile after cooling for 28 days and figures 3.17 and 3.18 show the axial stress after the heating period of 12 days.

Both the simulations of material 1 and material 2 seem to approximate the measured values. Material 1 overestimates the normal force induced by heat, and underestimate the normal force reduced by cooling. This is because with material 1 the overall stiffness is much higher, where material 2 has a depth dependent stiffness. When heating the soil with material, it reacts very stiff to the expanding pile inducing more stress see figure 3.17. Material 2 on the other hand induces a bit less in the beginning but goes down slower at the lower end of the pile, see figure 3.18.

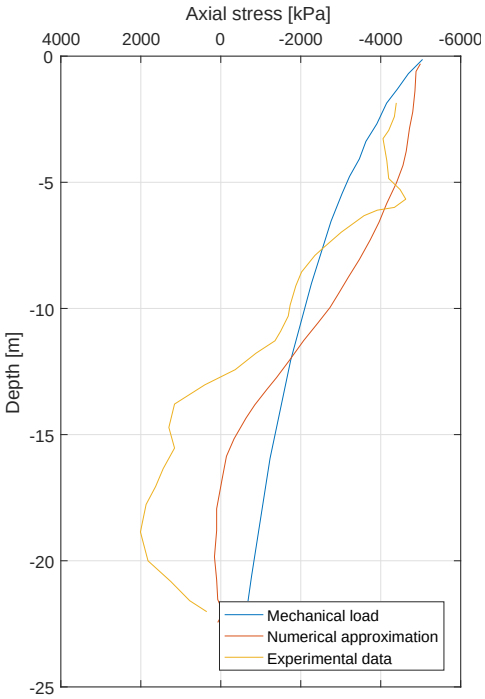



Figure 3.15: Axial stress with depth after cooling phase, material 1

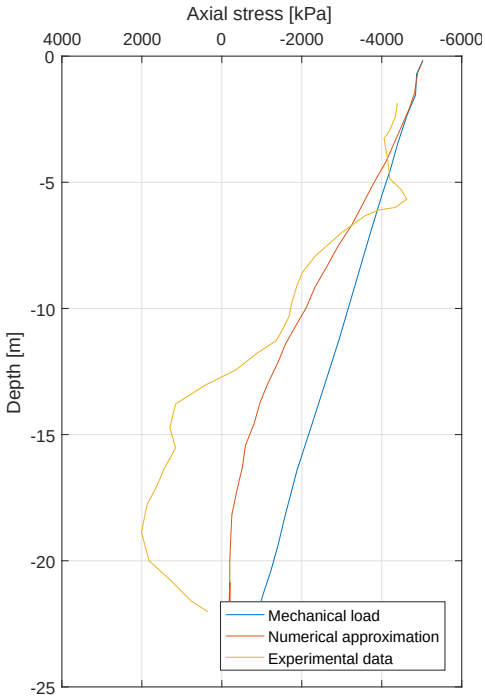



Figure 3.16: Axial stress with depth after cooling phase, material 2

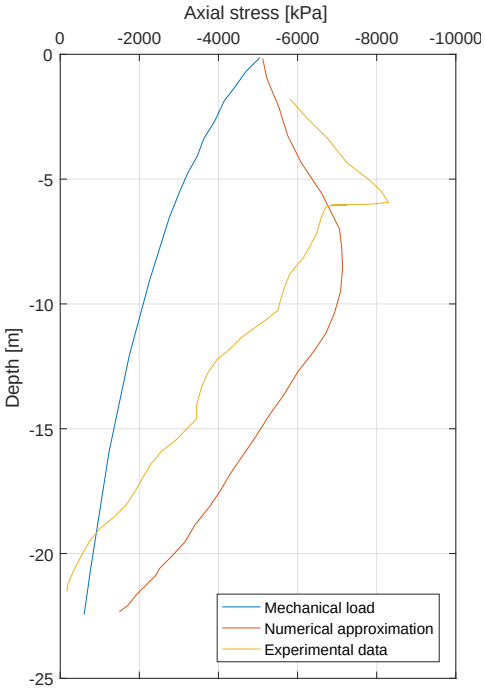



Figure 3.17: Axial stress with depth after heating phase, material 1

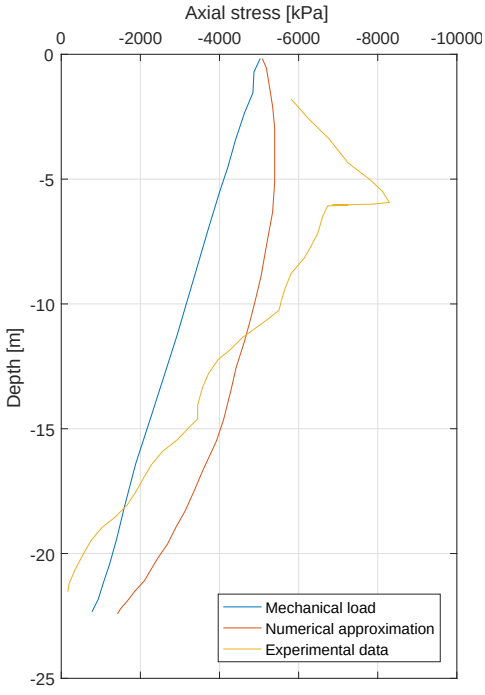



Figure 3.18: Axial stress with depth after heating phase, material 2

### 3.6.1. Replicating previous numerical study

Gawecka et al. [2016] first used numerical methods to model the Lambeth pile experiment results and after that, they did an explorative study to the effect of varying soil conditions. This is the approximation of their model using the different parameters were highlighted in the original paper. Each of the graphs contains three lines, after cooling, after heating and the purely mechanical load. The cooling period ended after 5 months of cooling at 4.5 °C and the heating period ended after 6 months of heating at 34.5 °C.


I. Vertical pile head displacement Page 32

II. Shear stress on the interface Page 33

III. Axial stress in the pile Page 34

IV. Radial stress on the interface Page 34

V. Transient effects Page 35


The graphs on the left side of eacht of the results are done with material model 1 and the middle is material model 2. The figures on the right side are what the graphs are trying to approximate from Gawecka et al. [2016]. The behaviour of the first material model can be explained by its high stiffness, but even though the London clay formation is very stiff, the second material model seems to come closer to both the experimental data and the numerical approximation from the papers.

**Vertical displacement**

The vertical displacement graphs resemble the Gawecka paper very well. Figure 3.20 is the best fit. In these graphs the null-point is visible. This is the place about which the pile expands and contracts and it sits at about -17 m, the same as in figure 3.21. The most notable change between material 1 in figure 3.19 and material 2 in figure 3.20 is the amount of upwards movement of the pile head during heating. This is most probably due to the phased analysis that was used for the second analysis. The soil hanging on the pile kept the pile from extending too much.

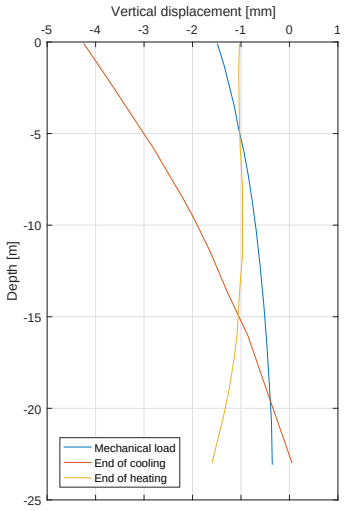



Figure 3.19: Vertical displacement, material 1

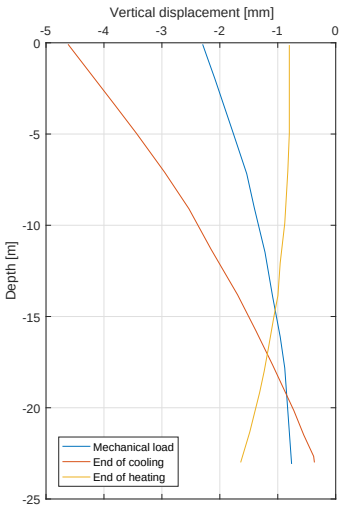



Figure 3.20: Vertical displacement, material 2

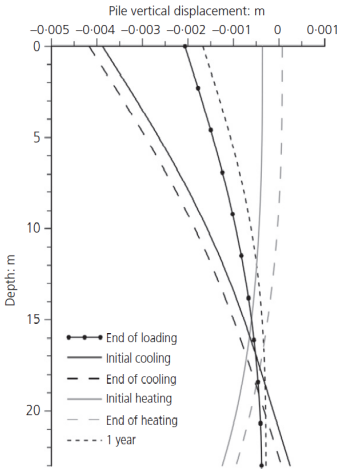



Figure 3.21: Vertical displacement from Gawecka et al. [2016]

**Shear stress**

Shear stress on the interface is an important outcome, it describes the way that the pile carries the load on top combined with the thermal load to the surrounding soil. Figure 3.24 shows the best comparison to figure 3.25. The null-point from the vertical displacement graphs is visible again. The direction of the thermally induced shear stress on the interface changes direction at that point. In the heating phase the top part above the null-point goes against the direction of the shear due to mechanical loading. And below the null-point it goes with that direction, increasing the total amount of shear stress on the interface. The cooling phenomenon is the same but opposite. This is in accordance with the mechanisms specified in section 2.4.

In figure 3.23, the soil is still hanging on the pile, yet they are of interest. The line for both the heating and the cooling phase are inclined with depth. The confining stresses are increasing with depth, the two quantities are linked. The shear has a maximum value, associated with the roughness of the pile and the strength of the soil. A shear stress graph against depth resembles Mohr's circle on its side, as shown in figure 3.22. The Y-axis is now depth and from that the principle stresses can be calculated. The maximum shear stress on the interface can be derived from its depth. Those straight lines mean that the pile-soil interface at that location is at failure.

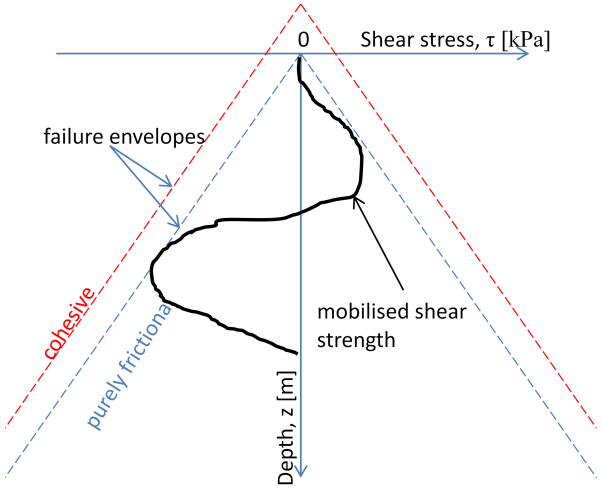



Figure 3.22: Shear stress envelope [I.A. Pantev]

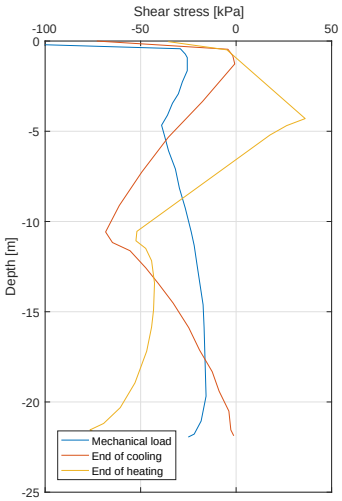



Figure 3.23: Shear stress on the interface, material 1

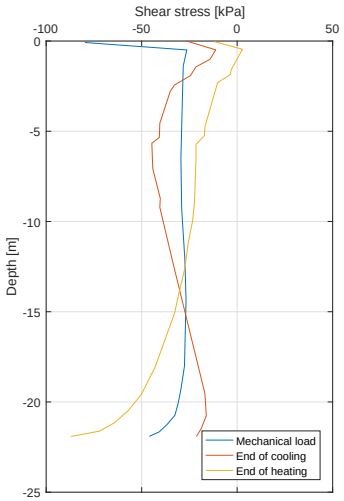



Figure 3.24: Shear stress on the interface, material 2

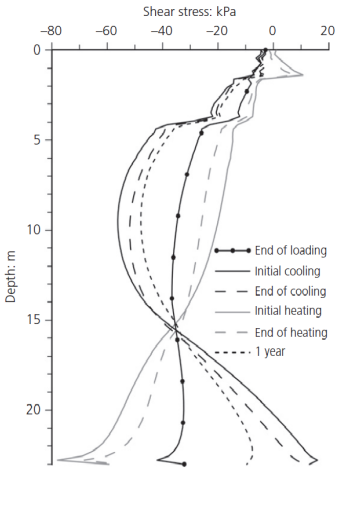



Figure 3.25: Shear stress on the interface from Gawecka et al. [2016]

### Axial stress

Here material 1 in figure 3.27 shows the best approximation of 3.28 again. The heating phase induces some more axial stress at the top because here the pile is moving against the direction of shear. So the pile is not carrying any load at that point. When cooling, the bottom part of the pile goes against the direction of shear and as a result that part of the pile is not carrying a lot of load any more. Extreme cases of cooling might even get some tensile forces in the bottom part. As time goes by the amount of axial stress in the pile will decrease as the soil is expanding and releasing the pile as it heats up or cools down as well, figure 3.32 will explain this behaviour better.

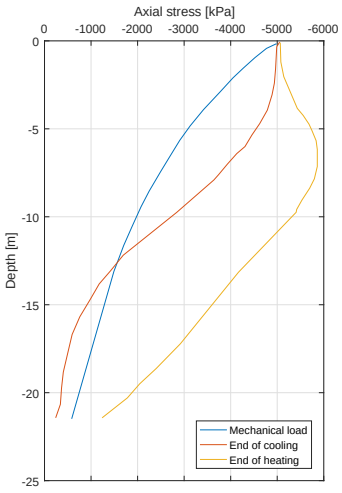



Figure 3.26: Axial stress with depth, material 1

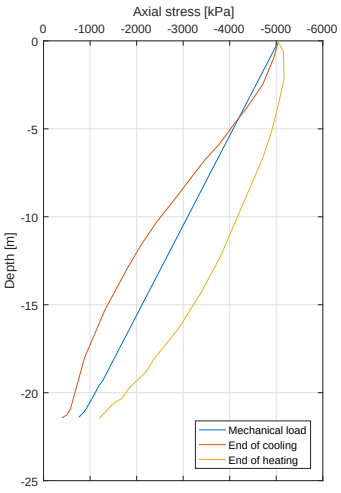



Figure 3.27: Axial load with depth, material 2

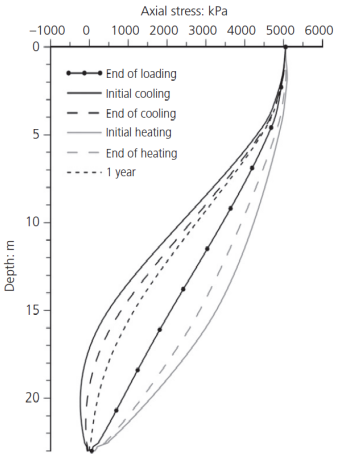



Figure 3.28: Axial stress from Gawecka et al. [2016]

### Radial stress

The radial stress on the interface is the pile pushing against the soil as it expands. Normally the radial stress is about $k_0$ times the vertical soil stress as the pile and soil are in equilibrium. As the pile heats up it expands and induces some radial stress, in cooling this is reversed and the pile will leave a gap where the soil will push against it in return. Figures 3.29 to 3.31 contain the thermally induced radial stress, so the effect of the initial condition is subtracted. The soil becomes stiffer with depth so the value of radial stress increases as well. Figure 3.30 does resemble the shape of figure 3.31 but not the amount of stress induced. This is because the soil $k_0$ profile of the soil in the Gawecka et al. [2016] is significantly higher than the one used in this model. The $k_0$ profile starts at 1.5 and linearly decreases to 1 at around the bottom of the pile. These numbers are to be expected in the high London clay, but the changing $k_0$ profile is not accounted for in this model.

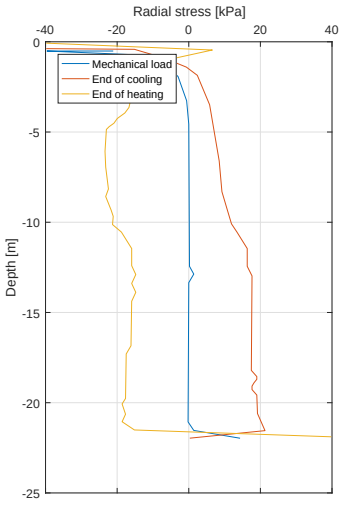



Figure 3.29: Thermally induced radial stress with depth, material 1

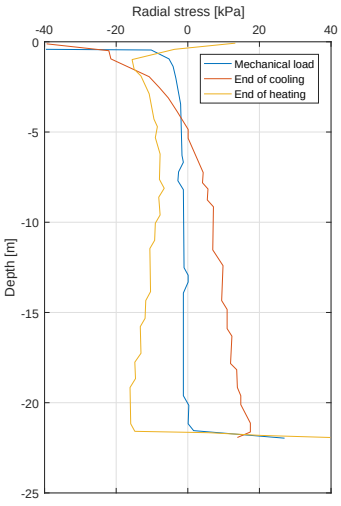



Figure 3.30: Thermally induced radial stress with depth, material 2

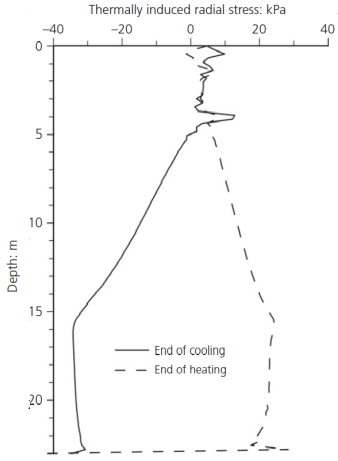



Figure 3.31: Therally induced radial stress from Gawecka et al. [2016]

**Transient effects**
Two transient effects shown in figures 2.18 and 2.19 are simulated. As time passes the axial stress in the pile decreases as the soil expands or contracts with the soil. This expansion of soil happens later because the heat takes time to transfer into the soil. That is a time dependent effect that is interesting for the experiment.

In figure 3.32 the difference between the modelled thermally induced stress is with the stresses taken from Gawecka et al. [2016]. As stated before, the magnitude of the stresses might not be correct. But that is not the point of this model. Qualitatively the behaviours are the same. A maximum is reached as the cooling or heating reach the peak. It is then kept at that temperature letting the soil catch up to the pile. The reduction then flattens out over a longer period of time. Not back to zero, because the soil still exerts force on the pile as it is still displaced from the original position.

Figure 3.33 shows the vertical movement of the pile head. it moves down during the cooling phase. Still being held in place by the soil. As the soil shrinks with cooling as well, the pile is released and able to shrink more. The soil inhibiting pile movement and then releasing it is shown in figure 3.32.

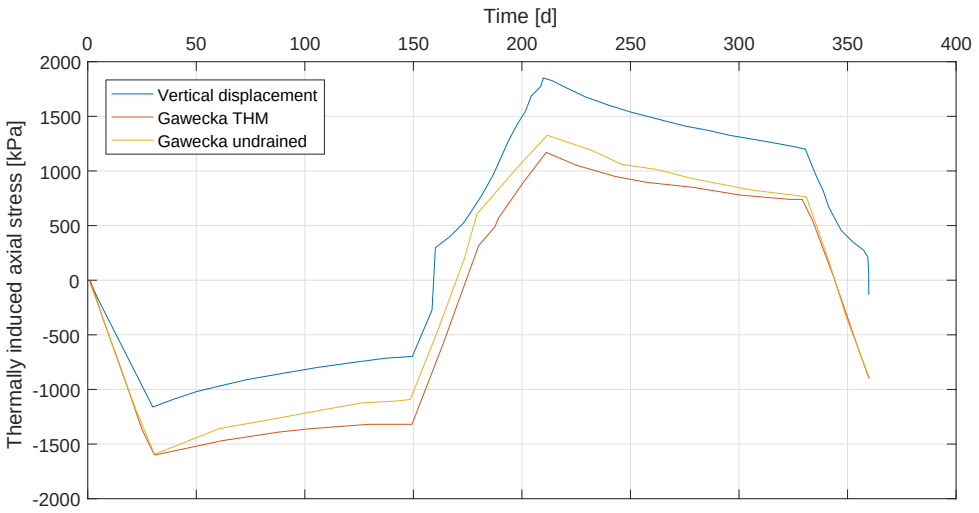



Figure 3.32: Thermally induced normal stresses

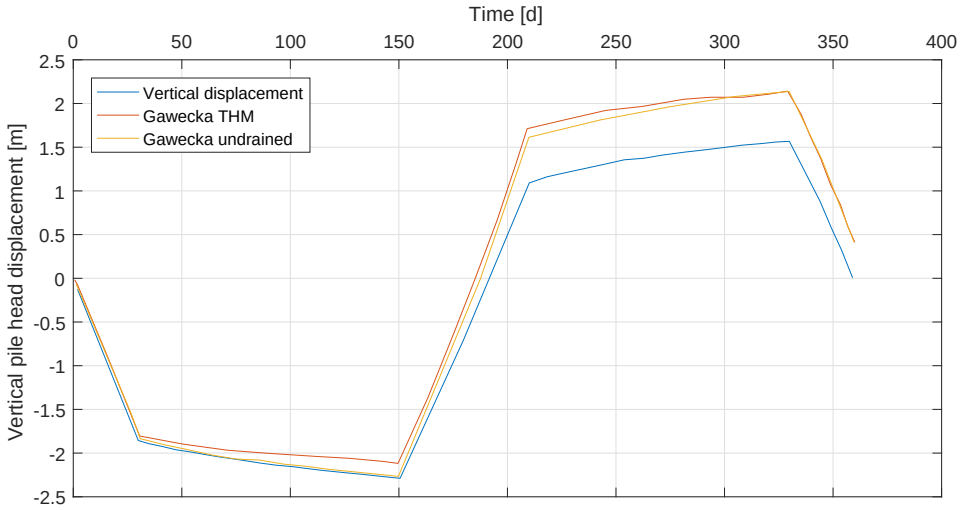



Figure 3.33: Pile head vertical displacement

**Parameter changes**
The model went through a number of changes going from the first material model to the second one. The changes and the reasoning behind them are listed here.

I. Depth dependent stiffness and shear strength. Although London clay is very stiff, it is unlikely that it is as stiff as material model 1 say it is throughout the entire depth. So changing the stiffness to be depth dependent leads to a more realistic behaviour.

II. Increase in $k_0$. The Gawecka paper calculates everything with a $k_0$ of 1.5 in the top part down to a value of 1 after 21 metres. Although this seems quite unrealistic, it did yield much better results. Where at first there was hardly any thermally induced stress, the increase in $k_0$ changed that. This made clear that when the soil in Delft will be modelled, factors like $k_0$ and stiffness are very important. They govern the pile fixity and thus the amount of stress that is induced.

III. Phased analysis. In order to fix the pile hanging on the soil. The analysis had to become phased. This meant that the in an initial step there was no pile at all, and that the soil could settle into a normal state. The nodes of the pile were tied to the nodes of the soil, so that the pile, when installed, was still in the same place. The installing of the pile after that meant that the pile would settle a little bit into the soil instead of the other way around.

## 3.7. 3D modelling of cooling pipes

Although literature suggests that an energy pile can be approximated with an infinitely long line source [Bourne-Webb et al., 2009], the heating line method used in the modelling is still an approximation of a u-pipe in a concrete pile. Cooling pipes in DIANA are line elements where an entry temperature can be given, the thermal fluid in the cooling pipe will give off heat as the soil warms up and lead to a reduced temperature of the fluid coming out. This difference in temperature can be expressed in terms of energy that is taken up by the soil and what is to be supplied by a heat pump in order to run the experiment, see equation 3.1. An energy pile with pipes in it is no longer axisymmetric, so the model will have to be made in 3D.

$$Q_T = \Delta T * Q_w * c_p * \rho \tag{3.1}$$

With $Q_T$, Energy input in $J/s$, $\Delta T$ change in temperature, $Q_w$ the flow rate, $c_p$ the specific heat and $\rho$ the water density. The downside of using cooling pipes is that the model is no longer axisymmetric. It will have to be done in 3D and that takes a lot more time to run. If there is a difference in accuracy that time investment might be worth it, but if the results are comparable it does not add anything to the results. To check how these two methods compare both have been modelled. Figure 3.34 shows the temperature distribution throughout the soil for both the 3D model with the cooling pipes and the axisymmetric model with the heating line. The temperature profiles are taken at two depths after 25 days of cooling at 5 °C. The thermal fluid might lose some of its heat on its way through the cooling pipe, so if there is a difference it will be at the deeper location, but it is also shown that at 9.5 m depth the profiles match. The fact that the results are so similar leads to the conclusion that if the goal is an accurate thermomechanical model of an energy pile, an axysimmetric approach is good enough. The temperature calculation can be done after that to get an idea of what the output temperature of the thermal fluid will be. Because the temperature distribution is the same for cooling pipes and the heating line, it will affect the pile more than the soil. In order to know the effect on the internal stresses of the pile itself, the cooling pipe method will be beneficial.

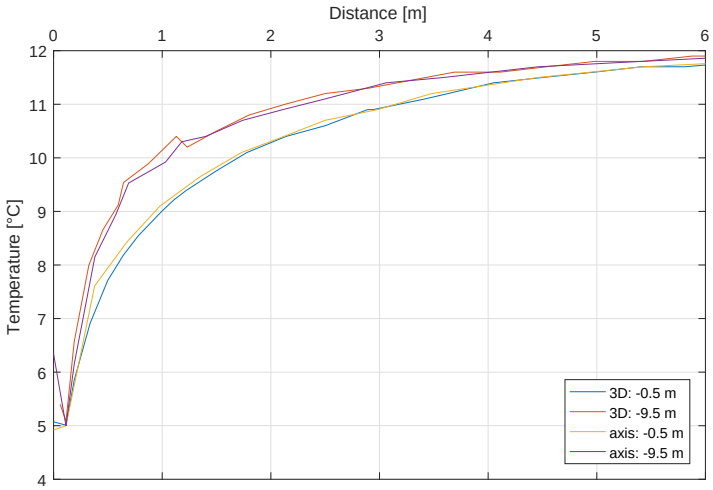



Figure 3.34: Soil temperature at 1.5 m distance for cooling pipes and heating line

## 3.8. Discussion

The modelling of the experiment in London and the comparison to the numerical model by Gawecka et al. [2016] was very helpful. All the steps from the start of the modelling to the full staggered analysis of the experiments are in this chapter and the changes made to the model in order to make the results more realistic are listed. All these changes contribute both to a better fit for the experimental data as well as a better understanding of how the pile will behave in the field. The mechanisms need to be clearly understood in order to model the Delft pile. The varied soil layers will change the clear graphs from the homogeneous London clay into much more varied graphs where it becomes less clear what the results mean.

One of the most important steps in the modelling of the energy pile was the phased analysis. In order to get the correct initial stresses in the soil the stresses needed to be calculated without the pile installed first. DIANA 10.1 does not have a built-in feature to do this yet, so in order to have a phased analysis some tweaking of the input data file ($.dat$) needed to be done. In a phased analysis the initial soil state is calculated without the pile in the soil, but to prevent the hole where the pile would be to collapse there needs to be soil in its place. The tweaking of the $.dat$-file entails linking the nodes of the soil to the nodes of the pile with tyings, mimicking a soil body, because the nodes of the pile will settle at the same rate as the soil. In the second phase the tyings are turned off and the pile is put in. The only extra stress that is added in this phase is the self weight of the concrete.

The thermomechanical behaviours and mechanisms predicted from the literature study are seen in the modelling. The largest difference between previous modelling and the model in this chapter is the use of a pile-soil interface. This is a difficult element to model because most of the parameters associated with it are not measurable. They can be approximated from field measurements, for example the relationship between axial stress and depth tells something about way the interface distributes the load. It should be noted that no parameter optimisation was done after THM analysis, before which the material properties were changed from material model 1 to material model 2.

The application of the temperature on the pile is done in steps of 0.5 °C per day. This is done for numerical stability as the pile can not expand more than that in a single time step, as was taken from the original paper [Gawecka et al., 2016]. In the tests done in section 3.7 the temperature is applied at 2 degrees per day, which was stable for the DIANA model. Ideally the temperature can be set in a single step, where the pile does not need to expand completely in that same step. This is the case for cooling pipes, the fluid will flow through the concrete and the temperature flows gradually. The results of the different temperature application modes lined up in figure 3.34 and show that they are interchangeable.

The numerical results from both the paper by Gawecka et al. [2016] and the DIANA model do not model the experiment exactly. There are differences, mainly in the strain and stress graphs, but the mechanisms associated with those graphs are seen in the numerical results. There is still a large challenge in modelling the pile-soil interface as well.

A few things that are not modelled:

I. **Pore water pressure.** This is not accounted for in this stage of the modelling, as Gawecka et al. [2016] show that the pore pressure development due to the thermal loading is small when compared to the other stresses in both the pile and the soil. Gawecka et al. [2016] also show that the thermally induced vertical stress reduces slightly quicker when it is fully undrained compared to fully coupled. In chapter 4 it is discussed if that assumption was correct.

II. **Cooling pipes.** It has been shown that there is no difference between the heating line and the cooling pipe with regards to the temperature distribution throughout the soil. The added benefit of the cooling pipe is that the difference between the input and the output temperature can be used to calculate the amount of energy that is input into the soil. This aspect can be used to design the heat pump for the experiment. This requires the model to be turned into a 3D model, so the time it takes to run the model increases a considerably. The thermomechanical calculations can be done axisymmetrically and the temperature calculation with cooling pipes can be done to investigate the outflow temperature of the energy pile.

III. **Cyclic behaviour.** The cyclic effects on the pile and the soil are not yet modelled and the experiments and later subsequent modelling both have not incorporated a lot of cycles. This is done in chapter 4 but checking this against experimental data is difficult and this will only be possible once the Delft experiment is running. The prediction of those cyclic behaviours can be based on the fact that the model itself has been validated with an experiment.

Changing the model to fit the situation in Delft will require site investigation to model the soil materials correctly. The main differences will be the diverse soft soil layers present in Delft compared to the homogeneous stiff layer of London clay. The graphs from the replicated Lambeth college approximation all show clear behaviours with continuous lines. The null-point is visible in the vertical displacement graphs and in the shear stress on the interface, exactly at the locations where they are to be expected according to the mechanisms. These data are more difficult to interpret in the Delft situation as there are soft layers that might not carry any load from the pile and will not do so under any thermal load. Difference in stiffness between layers will affect the shear stress on the pile and thus the reduction in axial stress with depth. The stiffest layer is probably the one where the pile will be founded on, so the prediction is that most of the changes due to temperature will happen as well.

## 3.9. Conclusion

After the work described in this chapter the model is considered to be verified. This means that DIANA is the right program to do the modelling with. The heat flow is correct, the mechanics are correct and the one-way coupling is good enough to simulate energy piles. So there is no need to do the full coupling. All the effects are seen, both the steady state and the transient effects.

The model has been validated with both an experiment and another numerical model of the same experiment, except for the cyclic effects. These are not yet modelled, or measured in an experiment and this is one of the goals of the energy pile project. In chapter 4 these cyclic effects of temperature on the pile and the soil will be modelled. This is not a verified part of the model, it can however be verified with the data that will be measured in the experiment at the Green Village.

# 4

# Modelling the experimental energy pile

## 4.1. Introduction

In this chapter the model built in chapter 3 is adapted to the situation in Delft. The field-scale pile experiment will characterise the macroscopic response of the structure and the effects of heating/cooling on the soil-structure interaction. From the literature study, the thermal effects and mechanisms are known, so the goal of the numerical study is to find out how these effects will manifest in the experimental pile in Delft. A prediction of those effects and their magnitudes will help to design the pile in such a way that the experiment is effective and efficient. It will also help to design the measurement plan such that the thermal effects will be recorded. In this chapter, both measurements and results will be discussed. Measurements refer to what the sensors will be registering during the proposed experiment and the results refer to the numerical analysis.

The first step is a structural design of the pile. This is not done numerically, but analytically with the same $\beta$-method as in chapter 3 [Bowles, 2007]. An older site investigation supplied in a report [MWH B.V., 2015] is compared to CPT's done at the exact location of the pile and they are used for material parameters in the Mohr-Coulomb material model. Additional field tests are conducted to find the thermal properties of the different soil types and these will be included in the material model as well. Information about the soil and site conditions is required when designing an actual or test installation, this allows the behaviour under thermomechanical loading to be approximated prior to construction.

In the second step a thermal cycle is described, such that all the different effects can be measured, both transient and cyclic. First the length of the thermal cycle was investigated, such that the predicted effects can be measured, but still limiting the amount of time one cycle takes. The model was then run for about 6 years with the calculated cycle and in the results all the effects seen in previous analyses could be found here as well. These results are then used to make predictions on the behaviour of the Delft energy pile experiment, both the expected needed range ans sensitivity of the sensors as well as time dependent effects.

## 4.2. Structural pile design

The geometry of the pile will be small enough so that the measurements are acute and accurate for the thermal tests, but without losing the primary function of a pile, which is a load bearing structural element. The two aspects are contradicting, so a good balance must be found. The parameter that might change the most when making a smaller pile is the radial thermal expansion, this expansion is a large contributor to the change in shaft resistance. This effect might be reduced too much when making the pile too small and that might lead to the measurements less clear. Increasing the pile size, both diameter and length, will increase the bearing capacity. A criticism of the previous EPFL experiment [Laloui et al., 2006], is that the pile that was used had a very large factor of safety due to its large size. Since a smaller pile has a smaller thermal mass, reducing the diameter will result in a decrease in time required for the thermal loading steps. It will also decrease the amount of dead load that has to be put on top of the pile on site, there are spatial restrictions at the site and less load will use up less space. A smaller pile can also be loaded to a higher percentage of the capacity.

The structural design of the pile used in the modelling was based on finding a practical solution. The goal of having a small diameter pile made it harder to have the pile based on the Pleistocene sand layer and a cage for a 300 mm pile would not be structurally sound for a 20 m pile. The next option for a smaller pile was dictated by the stratigraphy, the medium dense sand layer starting at 8.7 m depth is at the right depth for a 10 m pile. The boring company intended to do the work has only a few suitable drill bit sizes and so a 380 mm diameter pile of 10 m length was chosen. This will be a relatively small and thus weaker pile than it would normally be as a foundation pile. Thermo-mechanical loading will take the pile to a greater proportion of the design shaft resistance, this is as Bourne-Webb et al. [2009] suggested for future research. For the numerical model a load must be chosen to be put on top, an analytical calculation has been made as in chapter 3 according to the $\beta$-method [Bowles, 2007]. The load chosen for the pile is 195 kN, which is half of the calculated capacity, giving the pile an overall factor of safety of 2 before thermal loading. This method does not take into account any partial factors that should be there in normal pile design such as material factors and general safety factors.

## 4.3. Site investigation and material parameters

The Green Village is located at a site where a high-rise faculty building used to be before a fire destroyed it, so there were large foundations in place. After that fire, the basement floors and foundations were removed and the piles were cut and the site was filled again up to the current level of 1 m -NAP. The chosen site for the energy pile is at the edge of the site, away from the area with the largest pile density, there are still some piles in the area, but they can be largely avoided. The Green Village provided a complete geotechnical survey of the site [MWH B.V., 2015] in which the locations of all the old piles are shown. A number of old CPT's from a bit further away from the projected site are included, as well as an interpretation of the soil layering, see table 4.1.

In January of 2017 site investigations were done to map the layering of the subsurface on the exact spot of the energy pile. Aside from 4 CPT's a couple of boring's were attempted. An initial sampling campaign was carried out with a continuous Begemann sampler. This failed as the site investigation crew was not able to retrieve undisturbed soil, this poor sampling recovery was attributed to concrete debris in the top layers. Later in the year a hydraulic piston sampler was used to take samples from different layers. Laboratory testing of these samples is scheduled for a later date and thus outside the scope of this thesis. The tests can be used to improve upon the model for future research. The CPT's are shown in appendix A, and the interpretation is listed in table 4.2. The old and new datasets were collected in different locations, where the main difference is that a clay layer is still present in the new locations, because this layer was removed for the architecture building in the old location. The energy pile will be located at the edge of the green village site where the clay layer was not removed. The favourable conditions mentioned in 4.1, refer to the missing clay layer and are only present right underneath the demolished building. Other differences are small and to be expected with horizontal variability.

Because of the thermal aspects of this project an investigation of the thermal properties of the soil is needed as well. The samples that were taken during the site investigation can be used to find values for thermal conductivity $\lambda$, and thermal capacity $\alpha$. To get some preliminary results, a Thermal Response Test (TRT) was carried out in the different layers. From this a thermal conductivity value can be calculated in the same way it is done with the needle probe from section 2.2.3.

Typically CPT data can be used for pile design via direct methods such as Koppejan, or they can be estimated via correlations. The Dutch norm for geotechnical design has all of these correlations in table 2.b "characteristic values for soil properties"[NEN, 2016]. The table has relationships between a $q_c$ value form the CPT and all relevant soil parameters for the Mohr-Coulomb material model. The soil parameters derived from that table are listed in table 4.3.

The finite element mesh for this model is shown in figure 4.1, the different soil layers are in table 4.4. A saturated and dry backfill material were defined for below and above the water table respectively. The pile is on the left side of the mesh and the first 2.5 m close to the pile are finer than the rest. DIANA version 10.1 lacks adaptive mesh refinement, so the mesh was refined in steps approaching the pile. Optimisation of the mesh was not necessary, because the axisymmetric model is very fast in calculating the time steps. There is no need to make the mesh coarser because of a small increase in efficiency.

Table 4.1: Soil layers based on Dinoloket CPT's. [MWH B.V., 2015]

| Unfavourable conditions [m -NAP] | Favourable conditions [m -NAP] | Soil type |
|---|---|---|
| -1.0 to -2.5 | -1.0 to 5.0 | Sand |
| -2.5 to -5.0 | | Clay |
| -5.0 to -6.0 | -5.0 to -6.0 | Peat |
| -6.0 to -8.0 | -6.0 to -8.0 | Intermediate sand |
| -8.0 to -10.0 | -8.0 to -10.0 | Clay |
| -10.0 to -14.5 | -10.0 to -14.5 | Intermediate sand |
| -14.5 to -17.5 | -14.5 to -17.5 | Clay |
| -17.5 and on | -17.5 and on | Pleistocene sand |

Table 4.2: Soil layers based on 2017 CPT's

| Layer depth [m -NAP] | Absolute depth [m] | Thickness [m] | Soil type |
|---|---|---|---|
| -1.0 to -3.0 | 0 to -2.0 | 2.0 | Backfill / made ground |
| -3.0 to -5.1 | -2.0 to -4.1 | 2.1 | Peat |
| -5.1 to -8.6 | -4.1 to -7.6 | 3.5 | Silty sand |
| -8.6 to -9.7 | -7.6 to -8.7 | 1.1 | Clay |
| -9.7 to -14.3 | -8.7 to -13.3 | 4.6 | Sand (medium dense) |
| -14.3 to -15.7 | -13.3 to -14.57 | 1.4 | Clay |
| -15.7 and on | -14.7 and on | 14.3 (proven) | Sand (dense) |

Table 4.3: Material parameters for the Delft model

| Material | $E$ | $\nu$ | $\gamma$ | $\alpha_v$ | $C_u$ | $\phi$ | $\psi$ | $k_0$ | $\lambda$ | $C_p$ |
|---|---|---|---|---|---|---|---|---|---|---|
| | $N/m^2$ | – | $kg/m^3$ | $m/m°C$ | $N/m^2$ | ° | ° | – | $W/m°C$ | $J/m^3°C$ |
| Backfill dry | 1.50E+07 | 0.2 | 1800 | 1.70E-05 | 0 | 32.5 | 2.5 | 0.46 | 2.40 | 1.82E+06 |
| Backfill wet | 1.50E+07 | 0.2 | 2000 | 1.70E-05 | 0 | 32.5 | 2.5 | 0.46 | 2.40 | 1.82E+06 |
| Peat | 5.00E+07 | 0.2 | 1200 | 1.70E-05 | 3.00E+04 | 15.0 | 0 | 0.74 | 2.40 | 1.82E+06 |
| Silty sand | 1.50E+07 | 0.2 | 2000 | 1.70E-05 | 0 | 25.0 | 0 | 0.58 | 2.80 | 1.82E+06 |
| Clay 1 | 1.00E+06 | 0.2 | 1400 | 1.70E-05 | 3.00E+04 | 17.5 | 0 | 0.70 | 2.40 | 1.82E+06 |
| Sand 1 | 1.50E+07 | 0.2 | 1900 | 1.70E-05 | 0 | 30.00 | 0 | 0.50 | 2.80 | 1.82E+06 |
| Clay 2 | 2.00E+06 | 0.2 | 1700 | 1.70E-05 | 5.00E+04 | 17.5 | 0 | 0.70 | 2.40 | 1.82E+06 |
| Sand 2 | 3.00E+07 | 0.2 | 1950 | 1.70E-05 | 0 | 32.5 | 2.5 | 0.46 | 2.80 | 1.82E+06 |

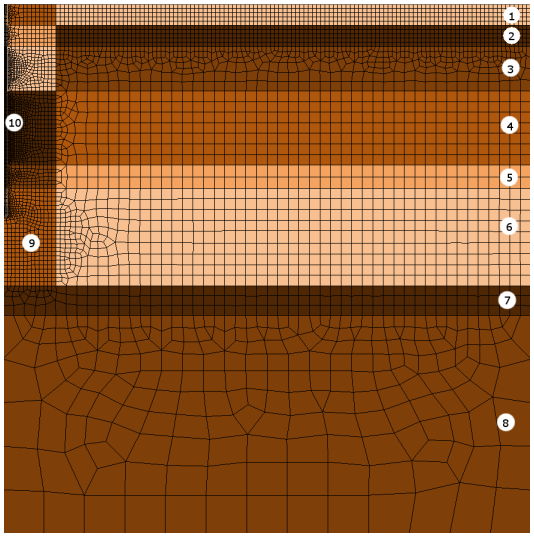



Figure 4.1: Meshed model with soil layers

Table 4.4: Annotations to figure 4.1

| # | Material | Mesh size |
|---|---|---|
| 1) | Backfill dry | 0.2 m |
| 2) | Backfill wet | 0.2 m |
| 3) | Peat | 0.5 m |
| 4) | Silty sand | 0.5 m |
| 5) | Clay 1 | 0.5 m |
| 6) | Sand 1 | 0.5 m |
| 7) | Clay 2 | 0.5 m |
| 8) | Sand 2 | 2.0 m |
| 9) | Shear zones | 0.2 m |
| 10) | Pile | 0.05 m |

## 4.4. Thermal cycle

Before the pile can be designed the thermal cycle that the pile will be put through must be evaluated. In this section the thermal cycle used for the numerical model will be investigated and chosen. Some preliminary results will be investigated to assess the pile reaction for each temperature increment. There are a few possible conditions that can be considered when deciding the timing of changing from heating to cooling and vice versa.

I. Known amount of heat energy applied.

II. Pile heated to a certain temperature.

III. Soil at some distance reaches a certain temperature.

The first option is probably the most practical because this is not dependent on the reaction of the soil, it is just an amount of heat that is applied and the reaction can be monitored. The second and third option require the pile or soil to heat up or cool down by a given temperature increment, this however will not be the most realistic approach. An actual energy pile will heat up until the source (the sun or waste energy) stops providing heat. The end temperature is never set, instead it would be limited by boundary conditions and heat pump capacity.

For the purpose of finding the thermal cycle for the numerical modelling the temperature of the pile will be set to a certain value. To see if the pile and the soil are affected to a significant degree the model is run at a set temperature for 360 days. This time is long enough that all of the initial transient effects on the pile are finished. The model is run at 20 °C, 35 °C and 50 °C, the reaction in axial stress seen in figure 4.2 and the model is run at -5 °C, 0 °C and 5 °C, pile reaction seen in figure 4.3.

With equation 2.16 the theoretical thermally induced axial stress can be calculated, this is then a maximum value assuming that the pile is fully restrained. The concrete parameters are listed in table 3.3, the calculated theoretical stresses due to just the temperature are listed in table 4.5. The numerical results are significantly higher than the analytical ones, even though the pile is in fact not completely restrained as it is assumed in the calculation. The higher then expected axial stress can be explained by the movement of the pile in the soil and induced friction along the pile shaft. This will increase the amount of stress in the pile, the same way mobilised shaft friction will carry load when the direction of shear is opposite to the pile load.

Table 4.5: Theoretical versus numerical axial stress

| Pile temperature [°] | $\Delta T$ [°] | Theoretical stress [kPa] | Numerical stress [kPa] |
|---|---|---|---|
| -5 | -17 | -656 | -995 |
| 0 | -12 | -463 | -655 |
| 5 | -7 | -270 | -420 |
| 20 | +8 | 308 | 616 |
| 35 | +23 | 886 | 1445 |
| 50 | +38 | 1465 | 2262 |

In order to see if a significant amount of soil is influenced, the temperature of the soil 1.5 m from the pile is investigated. This distance is chosen because at the site of the proposed experiment there is a pipe already installed about 1.5 m from the future location of the pile. Figures 4.4 and 4.5 show the infiltration of heat 1.5 m from the pile at a depth of 5 m, after 3 weeks the temperature difference is measurable for each of the pile temperatures. But when looking for a representative heating and cooling effect, it seems best to heat and cool with the same $\Delta T$, so that the heating and cooling effects are of similar magnitude. When cooling to 0 °C, the predicted $\Delta T$ =2 °C is almost reached. The upside of 0 °C is that the soil will not yet freeze, as with normal use the soil will not be frozen as suggested by the GSHPA standard [GSHP Association, 2012]. Previous field tests show that the soil can be frozen, but no detailed exploration of how this will affect the pile-soil system [Bourne-Webb et al., 2009]. If the mean is 12 °C, the heating must be at 24 °C, at that temperature the measured thermal response of the soil at 1.5 m from the pile after three weeks lies between the 20 °C line and the 35 °C line, at around $\Delta T$ =2 °C.

Option II for how to choose the thermal cycle in the numerical modelling is chosen, the pile will be heated and cooled with a $\Delta T$ of $\pm 12$ °C. Option I and III can be used as a way to check the soil response, the known amount of heat supplied is still an outcome of the operation of the heat pump and it will change throughout the thermal cycle. If the soil is already hotter, the heat pump will have to do less work to keep the inflow temperature of the thermal fluid at a certain level. The temperature at a certain distance from the pile can be used to back-calculate the average thermal conductivity of the soil. That is also a check of whether the system influencing the amount of soil that is needed.

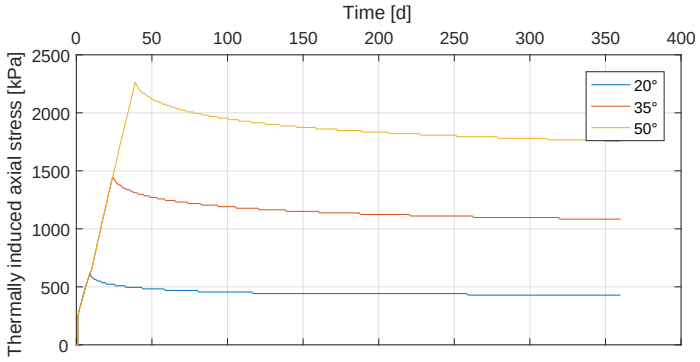



Figure 4.2: Maximum thermally induced axial stress in heating

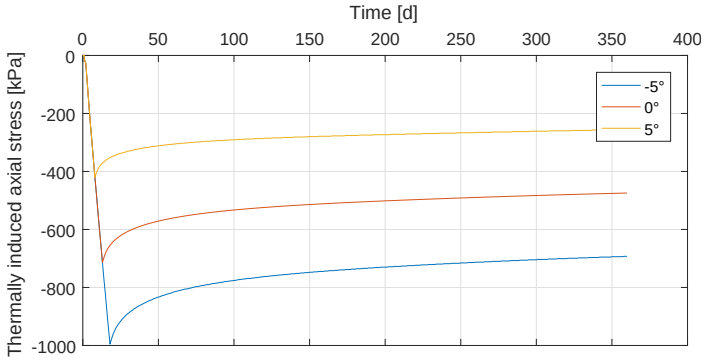



Figure 4.3: Maximum thermally induced axial stress in coolinge

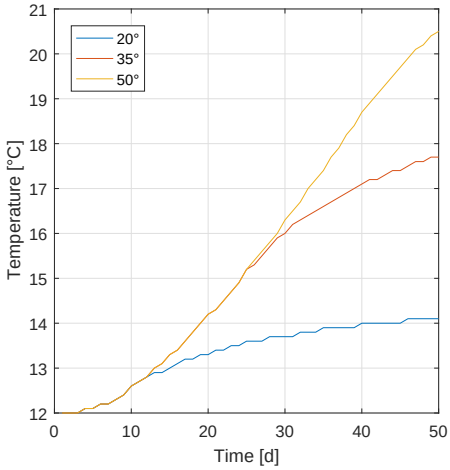



Figure 4.4: Temperature in the soil at 1.5 m from the pile, halfway down the pile in heating

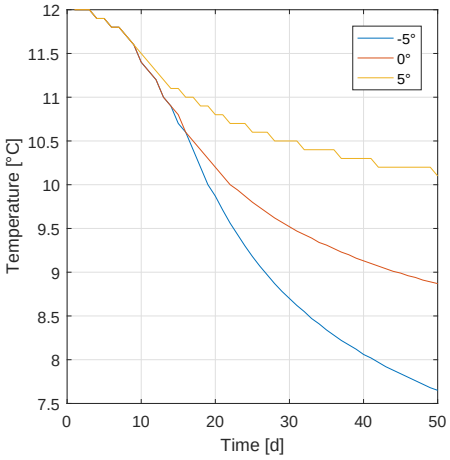



Figure 4.5: Temperature in the soil at 1.5 m from the pile, halfway down the pile in cooling

## 4.5. Results

The model was run for 67 cycles of three weeks, cooling at 0 °C and heating at 24 °C. Added to that is the time it takes to change from cooling to heating with the 2 °C per day temperature change in the thermal boundary. The total number of days was 2192, or slightly over 6 years. This is long enough to see some cyclic effects, and the cycles are long enough to see the transient effects and produce measurable results

The results in this chapter:

I. Temperature distribution during cycles. Page 44

II. Stresses and strains in the pile. Page 44

III. Pile movement and null-point. Page 49

IV. Transient and cyclic effects. Page 51

V. Measurement ranges. Page 52

VI. 3D modelling; cooling pipes. Page 53

### 4.5.1. Temperatures

Figures 4.6 and 4.7 show the pile cooling the soil at the start and the end of the cooling cycle respectively. Figures 4.8 and 4.9 show the start and end of the first heating cycle and represent the most amount of soil that is influenced by the pile.

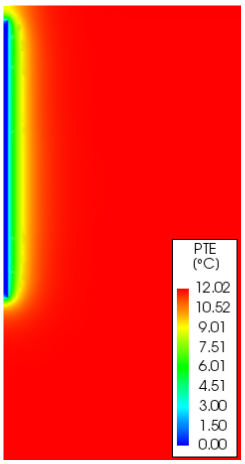



Figure 4.6: Temperature distribution of the pile and soil on day 7 of the cooling cycle

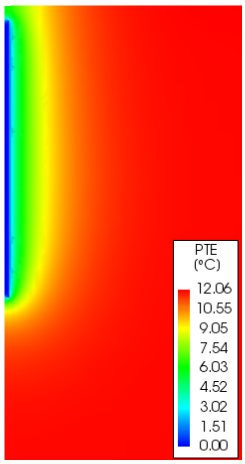



Figure 4.7: Temperature distribution of the pile and soil on day 28, the end of the cooling cycle

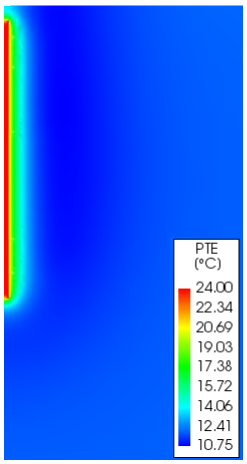



Figure 4.8: Temperature distribution of the pile and soil on day 40, start of the heating cycle

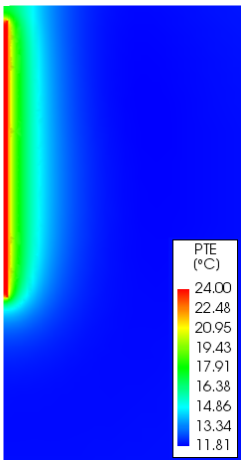



Figure 4.9: Temperature distribution of the pile and soil on day 61, end of the heating cycle

### 4.5.2. Axial strain, stress and shear stress

Strain in the pile is the measurement that will be done in the experiment, so the numerical approximation of strain is an interesting model outcome, from these strains the vertical stress in the pile can be calculated. Figures 4.10 through 4.12 show the strain in the pile at different times and figures 4.13 through 4.15 show the axial stress in the pile, the pile in the figures is widened for visibility. It is taken from the axisymmetric model, the left side of these contour plots is the symmetry axis.

Figures 4.10 and 4.13 are the axial strain and stress at the moment where only the load is applied, not yet any thermal load. The strain and stress are highest at the top and decreases almost linearly with depth, as is generally the case with non-energy piles. Piles that rely more on end bearing will see a less of a decrease in stress throughout the pile than floating piles in a homogeneous soil will. Figures 4.11 and 4.12 show the strain

at the peak of the cooling and heating cycles. The peak is the moment where the prescribed temperature has just been reached and the soil has not yet reached that same temperature, therefore the largest stresses are to be expected. In cooling the strain increases rapidly over the first metre, then stays relatively the same for largest portion of the pile and at the bottom there is another sharp decrease. A free-moving pile would have a continuous strain profile with depth, from this it can be seen that the pile is being held in place by the stiffer top and bottom layers. The heating profile shows the opposite behaviour in that the strain is first decreased in the first metre and changing from a contracting strain into an expanding strain, and at the bottom there is a sharp decrease back to 0.

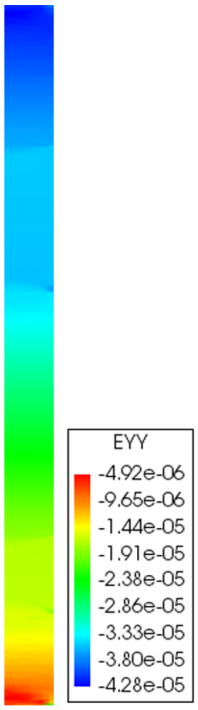



Figure 4.10: Axial strain in the pile, mechanical load

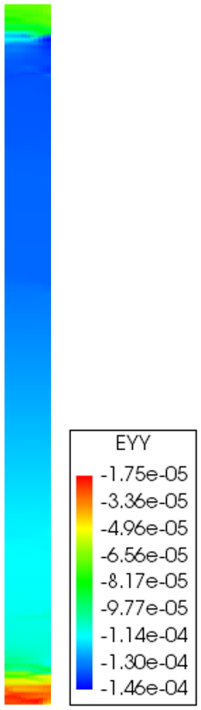



Figure 4.11: Axial strain in the pile, cooling cycle

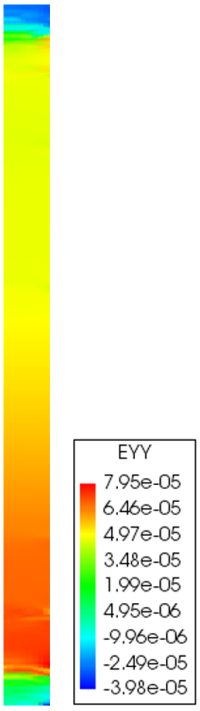



Figure 4.12: Axial strain in the pile, heating cycle

Figures 4.14 and 4.15 mirror the strain graphs, a large amount of strain means a smaller amount of stress at that point and vice versa, this is because the pile is restrained less when there is more observed strain. The stress in the cooling cycle shows a decrease of stress at the top, more rapidly than with the mechanical case and a spot of tension near the bottom of the pile. The heating case shows that there is more stress in the pile than for the normal mechanical case. Interesting about these plots is the influence of the interface is visible in the stress profile. The concrete near the interface is affected less by the increase of temperature and it resembles the mechanical stress profile more. The oscillations near the pile toe come from the influence of the interface on the pile. The graphs of shear stress on the interface in figures 4.18 and 4.21 show the source of these oscillations at 8.7 m depth. The spikes in shear stress come from the two soil layers with different stiffness on top of each other without any interface between them.

The axial strain and stress at the centre of the pile, the symmetry axis, are put into graphs to see the effects of the different soil types better. Added to that is the shear stress on the interface. The measurements during the experiments will be strains, the axial stress and interface shear stress will be calculated from that. Figures 4.16 through 4.18 are on day 7, the peak of the firsts cooling cycle, and figures 4.19 through 4.21 are at day 40, the peak of the first heating cycle. Each of these graphs have the total value, the mechanical value and the difference between the two, that difference is the part the thermal load is responsible for.

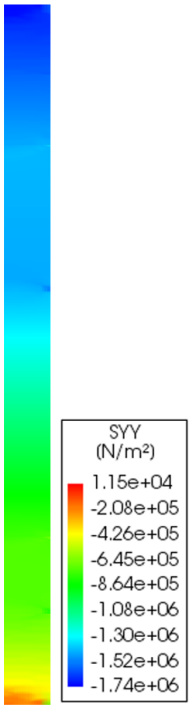



Figure 4.13: Axial stress in the pile, mechanical load

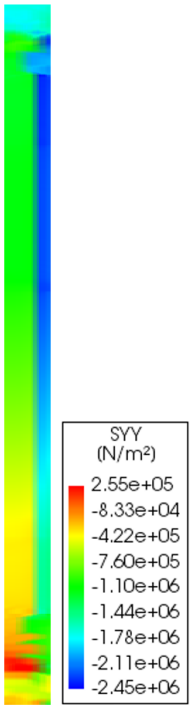



Figure 4.14: Axial stress in the pile, cooling cycle

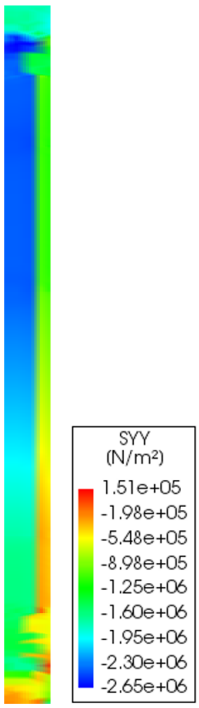



Figure 4.15: Axial stress in the pile, heating cycle

In the strain graphs (figures 4.16 and 4.19) the difference is shown between the strain from the mechanical load and the strain due to temperature for both heating and cooling. The temperature difference for both cases is the same ($\Delta T = 12°C$), but the amount of strain caused by that difference in temperature is smaller for the heating than for the cooling. This could be due to the fact that the cooling cause is in compressive strain and the heating case causes tensile strain. A smaller amount of strain during the heating phase means that the thermally induced stress is higher during heating. The soil around the pile is resisting the movement of the heating pile more than the cooling pile, even though the $\Delta T$ is the same for both cases, and that resisted strain is responsible for the stress in the pile.

Axial stress in the pile behaves as expected from the mechanisms detailed in section 2.4, the cooling cycle reduces the compressive stress towards the tensile stress near the toe and the heating cycle increases the compression. This is due to the pile either moving with, or against the direction of the mechanical load, increasing or decreasing the shear stress on the pile accordingly. As with the strain, it can be seen that the effect of heating is greater than the effect of cooling even though the $\Delta T$ is equally large. The shear stress graphs show the absolute amount, as well as the extra shear stress that is generated by the temperature. If the yellow line in 4.18 or 4.21 is at 0 that means that that particular layer in the soil is not resisting the pile any extra during thermal loading. A layer of interest here is the silty sand layer between 4.1 m and 7.6 m depth, apart from the sand layer where the pile is based on, this silty sand is the strongest layer. It contributes most to carrying of the load via shear stress on the interface, it does not however carry any extra load during thermal loading. This can be explained by the location of the null-point about which the pile expands and contracts. At the first cycle the pile moves about a null-point at 5.0 m depth, which is just above the middle of the silty sand layer. As the pile will only move a small amount just above and below the null-point, the shear stress also will not increase there. If the pile were for example 20.0 m long, the null-point would be much lower and then the layer would resist the movement of the pile a lot more. The positive of this is that the pile will reduce the load more during cooling, but the negative is that during heating the increase of stress would also be higher.

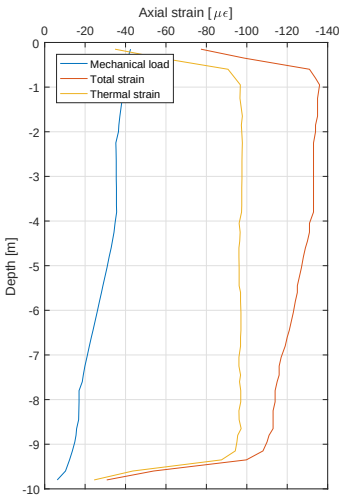



Figure 4.16: Axial strain, and strain increment, cooling cycle

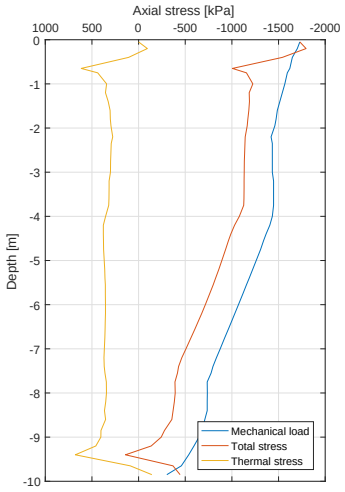



Figure 4.17: Axial stress, and stress increment, cooling cycle

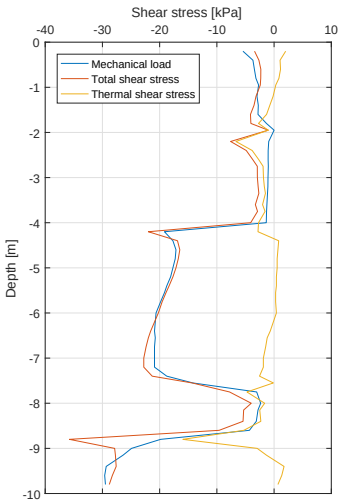



Figure 4.18: Shear stress, and shear stress increment, cooling cycle

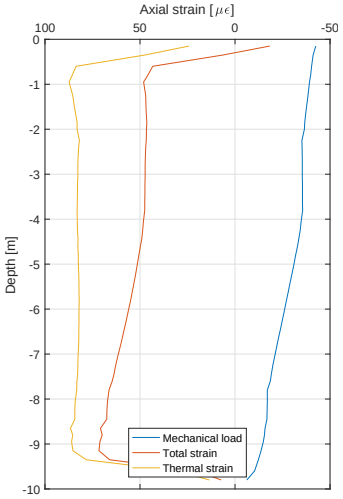



Figure 4.19: Axial strain, and strain increment, heating cycle

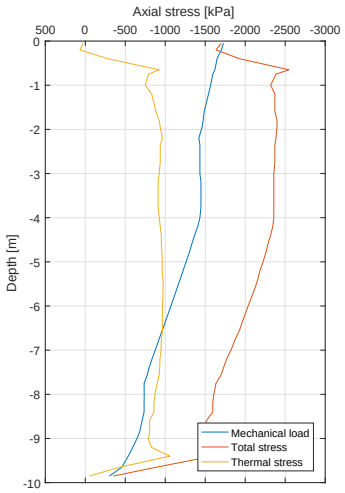



Figure 4.20: Axial stress, and stress increment, heating cycle

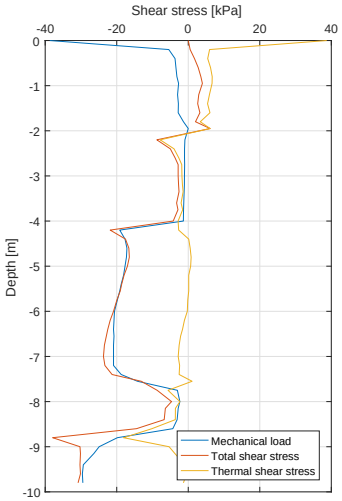



Figure 4.21: Shear stress, and shear stress increment, heating cycle

**Calculating theoretical stress from measured strain**

The theoretical thermal strain can be calculated and the observed strain can be subtracted from that to get the restrained strain. This is the strain responsible for the thermally induced axial stress, because an unrestrained pile will expand without any additional stress. The calculations are in equations 2.17 through 2.20. The thermal strain from figure 4.16 is a possible measurement of the experimental pile. The strains in the pile have to be measured when a load is applied, and again under thermal loading, in that way the different strains can be separated. The theoretical thermal strain can be calculated with the thermal expansion coefficient of concrete and the change in temperature, the restricted thermal strain can be calculated with that free strain (equation 2.18) and the restrained thermal strain and the pile stiffness can be used to calculate the thermal stress (equation 2.19). All of these calculations are done for the first heating and cooling cycle of the Delft pile, results are in table 4.6.

Table 4.6: Theoretical versus numerical axial stress Delft pile

| | Unit | Cooling | Heating |
|---|---|---|---|
| | [$\mu\epsilon$] | Strain | |
| Average total strain | | -119.8 | 50.7 |
| Average mechanical strain | | -28.0 | -28.0 |
| Average thermal strain | | -91.8 | 78.7 |
| Free moving thermal strain ($\Delta T \alpha_c$) | | -102.0 | 102.0 |
| Restricted thermal strain ($\epsilon_{Rstr}$) | | -10.2 | 23.3 |
| | [$kPa$] | Stress | |
| Thermal stress caused by $\epsilon_{Rstr}$ | | -408.0 | 932.0 |
| Average numerical thermal stress (figs:4.17 and 4.20) | | -326.0 | 853.4 |
| Difference in stress | | -82.0 | 96.2 |

There is a difference between the calculated thermal stress and the stress based on the measured strain during heating, this difference is the sum of the change in shear stress and the change in base resistance. When the base resistance is measured, the effect on the interface shear stress can be calculated. Finding the influence of temperature on the pile-soil interface is one of the main goals of the experiment, and via this path it will be possible to calculate that.

All of the calculations in table 4.6, including similar calculations in Amis et al. [2008],Bourne-Webb et al. [2009] and Amatya et al. [2012] are done under the assumption that the stress in the pile can be calculated with the strain in 1 direction, without taking into account the other directions. To reiterate the formula used in those aforementioned papers see equation 4.1. Strain in the vertical direction is also influenced by stress in the horizontal directions, the limit of this effect is stated in equation 4.2. With $k_p$ the passive earth pressure coefficient that governs the horizontal pressure when the pile is expanding and pushing against the soil (equation 4.4 . $k_0$ (equation 4.3) will be subtracted to only account for the influence of temperature, not the neutral earth pressure.

Calculating this at 5.0 m depth to see if it has any influence on the strain in vertical direction. The concrete parameters $E$ and $\nu$ are taken from table 3.3, and $\sigma'_v$ is the effective soil stress at that depth. The calculation is written in equation 4.5 and the conclusion that the vertical stress on the pile is not significant is valid.

$$P = \epsilon_T AE \tag{4.1}$$

$$\epsilon_{v,\sigma_h}\Big|^{lim} = \frac{(k_p - k_0)\sigma'_v \nu}{E} \tag{4.2}$$

$$k_0 = 1 - sin\phi = 1 - sin25 = 0.577 \tag{4.3}$$

$$k_p = \frac{1 + sin\phi}{1 - sin\phi} = \frac{1 + sin25}{1 - sin25} = 2.464 \tag{4.4}$$

$$\epsilon_{v,\sigma_h}\Big|^{lim} = \frac{(2.464 - 0.577)51200 \cdot 0.3}{4.0E + 10} = 0.72\mu\epsilon \tag{4.5}$$

### 4.5.3. Vertical displacement

The figures in this section show the vertical displacement of the soil and the pile. Figure 4.22 is the displacement contour from just the mechanical load. Figures 4.23 and 4.24 are the cooling cycle and heating cycle respectively. From the mechanical case to the cooling cycle the shrinking of the pile can be seen, the top part displacing down more than before. The pile is moving along the top soil layer, the soil next to the pile at that height is displacing less then before, this is due to the pile slipping and not pulling the soil down any more. In the heating cycle the pile still moves down as a whole, but less so than in the cooling cycle.

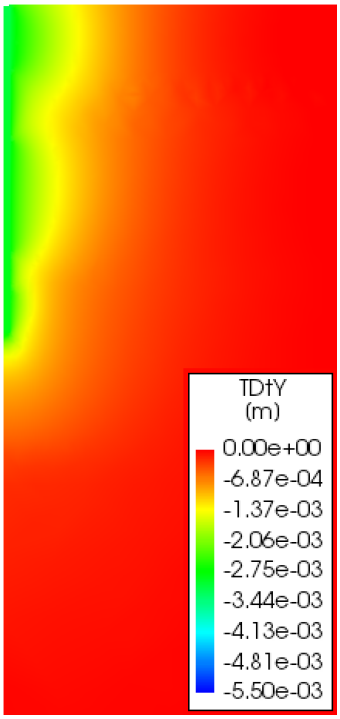



Figure 4.22: Vertical movement, pile and soil, only mechanical load

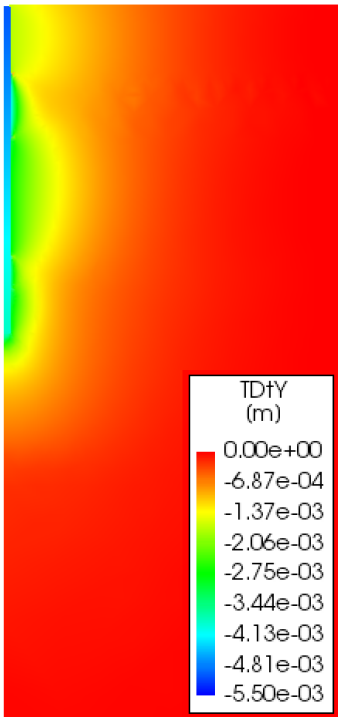



Figure 4.23: Vertical movement, pile and soil, cooling cycle

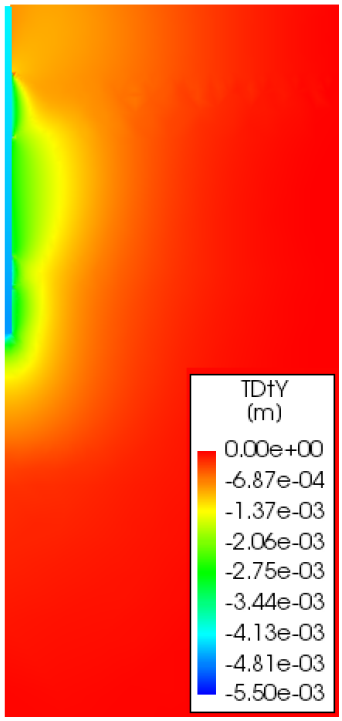



Figure 4.24: Vertical movement, pile and soil, heating cycle

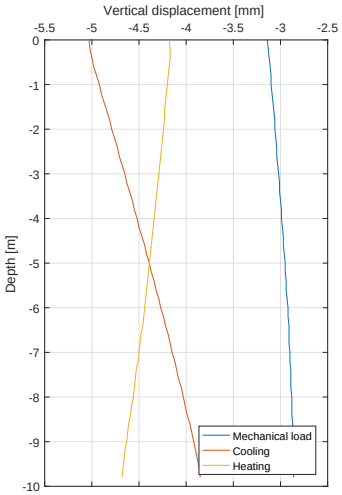



Figure 4.25: Vertical pile displacement, 1st cycle

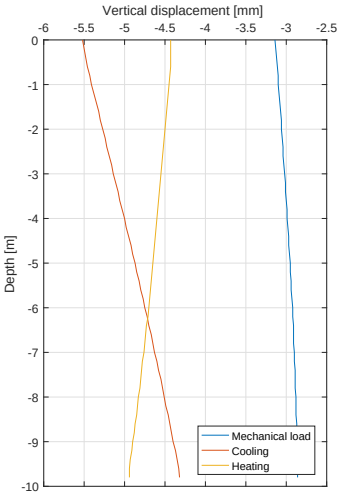



Figure 4.26: Vertical pile displacement, 10th cycle

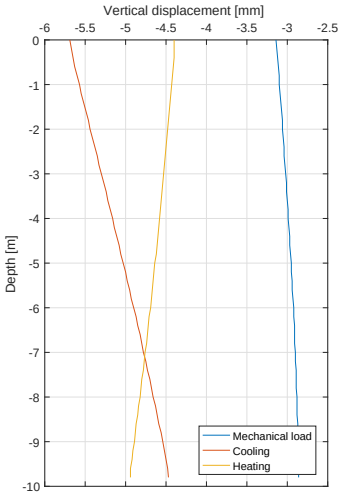



Figure 4.27: Vertical pile displacement, 60th cycle

### 4.5.4. Null-point

The point along the pile that does not move with temperature is called the null-point, the location of the null-point is expected to change due to weaker layers slipping along the interface. The strong layers draw more load to them and the null-point will move down the pile towards the tip. Figures 4.25 to 4.27 show the vertical displacement for the 1st, 10th and 60th cycle. The cooling and heating lines are subsequent thermal loads and the location where they cross is called the null-point. That point does not move throughout the entire cycle, so there will be no shear stress development in that location. As the pile goes through more cycles the null-point moves down, the progression can be seen in figure 4.28. This is due to the fact that the weaker layers will fail first and the stronger layers will contribute more, so the pile will be held in place better in those layers. The strongest layer is the sand layer on which the pile is based and the null-point is seen moving towards the sand layer. The movement of the null-point can be seen in the behaviour of the intermittent soil layers, figure 4.29 shows the shear stress on the interface on day 40 and day 2020. Although they look similar, the behaviour of the silty sand layer between 4.1 m and 7.6 m depth shows the effect of a moving null-point. During the first few cycles the null point is around -5.0 m depth, so there is almost no shear stress development on day 40 due to the applied temperature at that depth. Above and below the null-point the shear stress develops in opposite directions, increasing and decreasing respectively. On day 2020 the null-point has dropped to around -7.0 m depth and so did the point of no shear stress development. The fact that the layers have less of a grip on the pile can be seen in the reduced axial stress during heating in figure 4.30. The same point in the cycle during a heating phase induces 260 kPa less stress because of this effect.

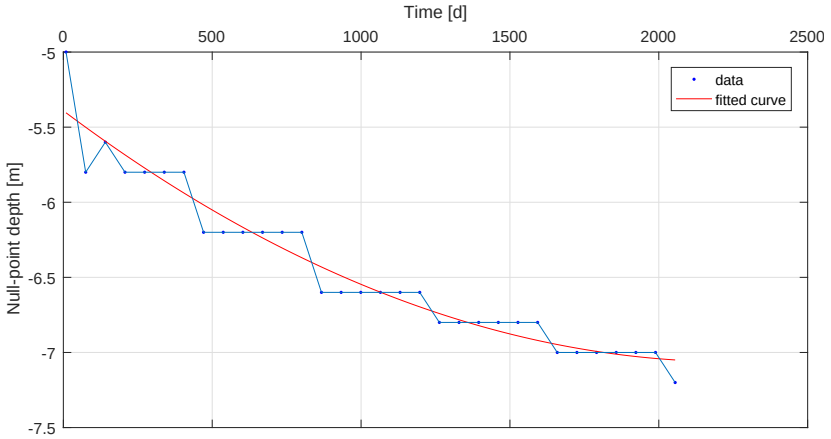



Figure 4.28: Null-point location over time

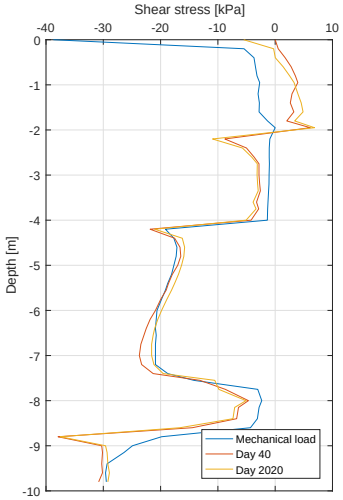



Figure 4.29: Shear stress on the interface on day 40 and day 2020

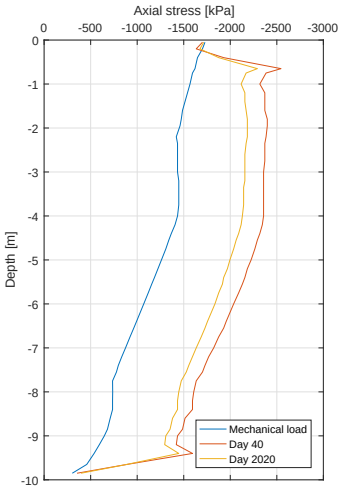



Figure 4.30: Axial stress on day 40 and day 2020

### 4.5.5. Transient and cyclic effects

Figure 4.31 shows the maximum thermally induced stress over time. The tensile side is during the cooling cycle and the compressive side is during heating. The same transient effect of reduction in thermal stress over time as the temperature remains stable is seen as in figure 2.19, it mirrors the increase in pile movement in figure 4.32. The maxima and minima of the thermal stresses do not vary a lot within this time. However it should be noted that when this value decreases more, something has happened at the pile-soil interface. Over time, due to cyclic shearing, a remoulding of the softer layers can occur. Cyclic degradation of the interface shear strength will lead to redistribution of the load carrying. In this case, the top layer and the bottom layer have the most strength and are not yet at capacity, so they will carry more load after thermal loading then before.

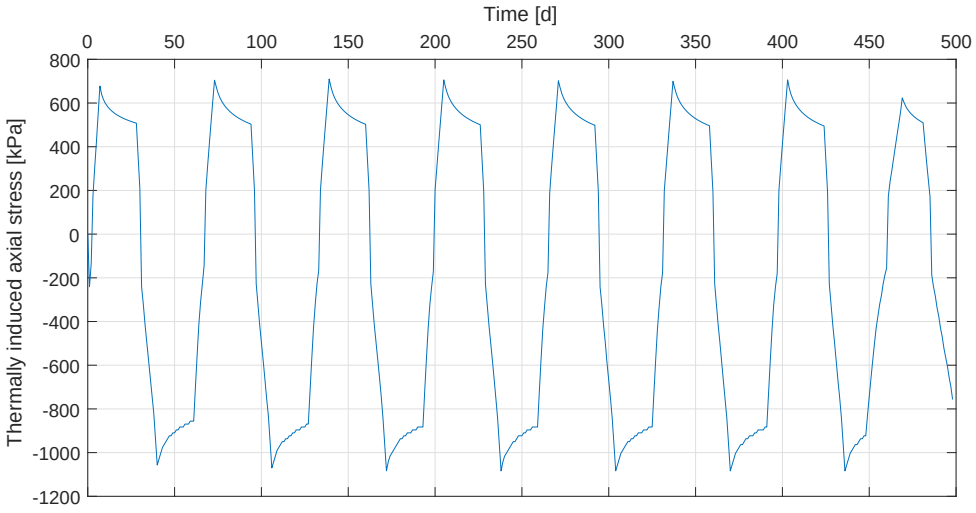



Figure 4.31: Maximum thermally induced axial stress, first 500 days

In figure 4.32 the vertical pile head movement has both a transient and a cyclic effect. The transient effect is the same as in figure 2.18, only in a shorter timespan. The pile head reaches a maximum at the point where the pile has reached its steady temperature. After that the pile slowly keeps moving in that direction as the soil releases the pile as it expands or contracts. The cyclic effect is the ratcheting similar to figure 2.16 from literature. Over time as the number of cycles increases the pile displaces downwards, this downward trend stabilises after a couple of cycles indicating that the pile has reached a new equilibrium.

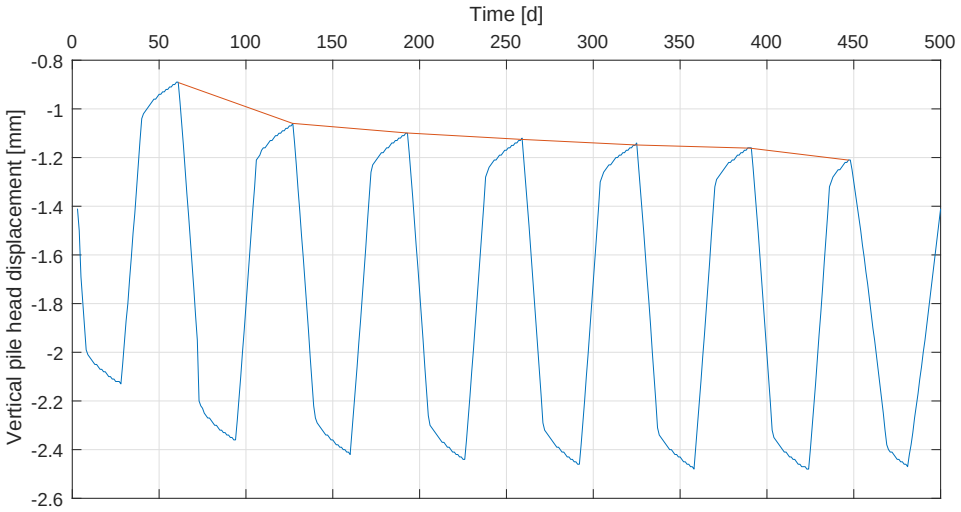



Figure 4.32: Vertical pile head displacement, first 500 days

The soil is affected as well, figure 4.33 shows that the soil will heave over time under thermal loading. The effect decreases over time because the soil moves in the same manner as the pile. First steadily increasing or decreasing until the temperature reaches a steady state, then increasing or decreasing at a slower rate. The thermal expansion coefficient of the soil is larger than that of the concrete. But the soil is farther away from the heat source so it reacts slower, and less pronounced. This effect will be difficult to measure in the experiment as the scale is small and there are other effects such as thermal consolidation and settlement due to the loading set-up.

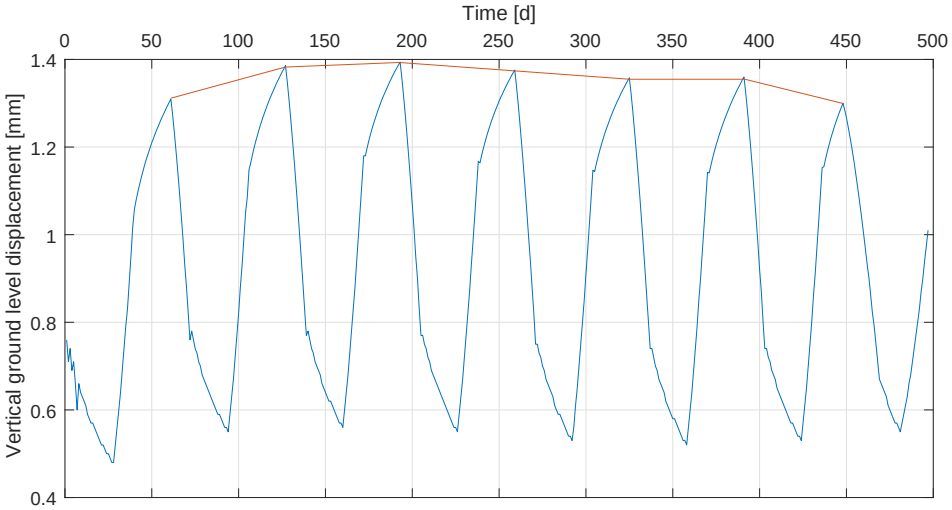



Figure 4.33: Ground level displacement 1.0 m from the pile

### 4.5.6. Measurement ranges

During the experiments the measurements are done with sensors and getting a good idea of the range of the measurements that come in through the sensors is helpful. Table 4.7 shows the expected measurements for various metrics at different temperature changes. All of the measurements are after 3 weeks of cooling or heating at a steady temperature.

It contains the expected temperatures at 1.5 m from the pile, as well as the total strains and thermal strains separately. The 1.5 m is chosen because at the site of the proposed experiment a tube is installed at that distance, the measurements can be compared to the results of the modelling. Maximum thermal strain is the calculated maximum amount of strain if the pile were to move freely. The free thermal strain will be the worst that would be measured that is why this is the upper limit of strain at these temperature differences. The thermal strains could be used when the strain gauges are set to zero after the load is applied, this means that only the thermal strain will be picked up. Knowing the strain due to the mechanical load is enough to calculate the total strain at that moment. The expected pile head movement is listed as well, however this will be difficult to measure.

Table 4.7: Expected measurements of various parameters

| $\Delta T$ [°] | Soil $\Delta T$ [°] | Total strain [$\mu\epsilon$] | Free thermal strain [$\mu\epsilon$] | Max thermal strain ($\Delta T \alpha_c$) [$\mu\epsilon$] | Pile head movement [$mm$] |
|---|---|---|---|---|---|
| -17 | -4.0 | -178.0 | -140.8 | -144.0 | -1.4 |
| -12 | -2.8 | -138.0 | -100.8 | -102.0 | -1.0 |
| -7 | -1.6 | -98.0 | -58.3 | -59.5 | -0.8 |
| +12 | +1.8 | 47.8 | 61.7 | 102.0 | 0.1 |
| +23 | +5.6 | 166.0 | 181.5 | 195.5 | 1.0 |
| +38 | +9.8 | 285.0 | 301.0 | 323.0 | 2.0 |

## 4.6. 3D modelling

The axisymmetric model is fine for the measurements discussed until now, it cannot however be used to calculate the energy usage of a heat pump. For that cooling pipes are needed in a 3D model, cooling pipes are u-pipes that go through the pile transporting thermal fluid. The temperature of the thermal fluid going in to the pile is higher than the temperature of the thermal fluid coming out during heating. The goal of this 3D modelling is to calculate the energy costs of the energy pile, running it with a constant temperature and in cycles. The 3D model is the same as the axisymmetric model in the sense that the boundary conditions, the soil layers, pile-soil interface and all the forces are the same. The biggest difference is the mesh, because of the large amount of elements that are used to get the 3D model the mesh had to be made less fine, otherwise the computational time would increase dramatically.

The input for the cooling pipes in DIANA are in table 4.8, the pipe has a diameter of 32 mm, or a perimeter of 0.1 m. The heat transfer coefficient is the resistance between the cooling pipe and the concrete, that is set at a very high value indicating that this is the upper limit of the heat loss thermal fluid. Fluid discharge is set at 0.25 $l/s$ or 900 $l/h$, and the volumetric heat capacity of the thermal fluid is also given, but in DIANA the product of these two has to be put in. With the cooling pipe temperature and equation 4.6, the amount of energy supplied by the heat pump can be calculated.

Table 4.8: Cooling pipe and thermal fluid parameters

| Parameter | Unit | |
|---|---|---|
| Pipe perimeter | $m$ | 0.1 |
| Heat transfer coefficient | $W/m^2°C$ | 10000 |
| Fluid discharge $Q_w$ | $m^3/s$ | 2.5E-04 |
| Volumetric heat capacity | $J/m^3°C$ | 3.06E+06 |
| Specific heat capacity $c_p$ | $J/kg°C$ | 2430 |
| Specific weight $\rho$ | $kg/m^3$ | 1260 |

$$Q_T = \Delta T * Q_w * c_p * \rho \tag{4.6}$$

The results in figures 4.34 and 4.35 show the temperature of the output temperature of a cooling pile kept at a temperature for an extended period of time. In the cooling case the inlet temperature of 0 °C is heated by the soil to 0.82 °C on the first day. This change in temperature becomes less as time goes by as the concrete and the soil around the pile cool as well. The energy that is costs for the heat pump to function is also in table 4.9, this energy cost decreases over time as well.

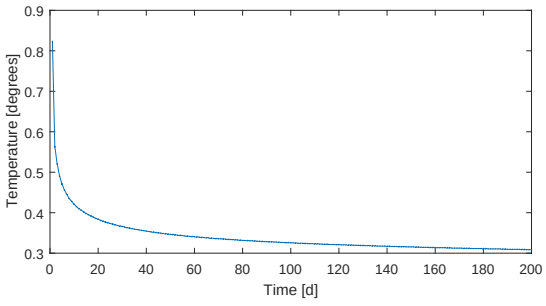



Figure 4.34: Output temperature cooling pipe for 0 °C input

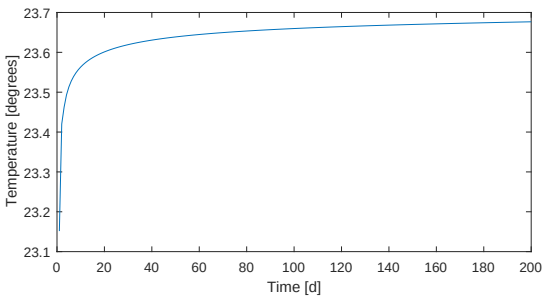



Figure 4.35: Output temperature cooling pipe for 24 °C input

The second set of results is the output temperature of the cooling pipe when the pile running thermal cycles. First the temperature is 0 °C for 30 days and then it is set to 24 °C for 30 days. This is roughly the same as the thermal cycle used in the axisymmetric modelling. It cannot be exactly the same because the heating line could not stably calculate larger changes in temperature than $\Delta T = 2°C$, the cycle for the 3D model is slightly longer to account for this time.

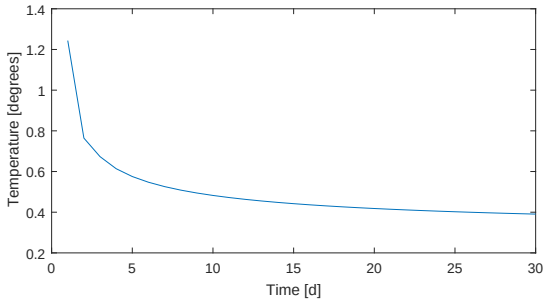



Figure 4.36: Output temperature cooling pipe for 0 °C input in cycle

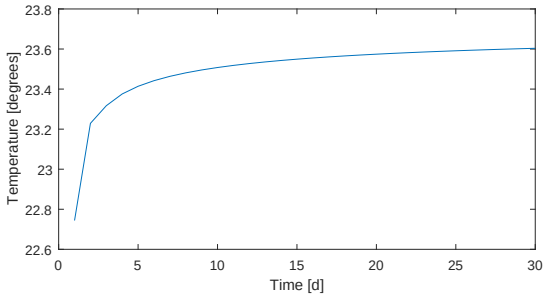



Figure 4.37: Output temperature cooling pipe for 24 °C input in cycle

The difference between inflow and outflow temperature for both the heating and cooling cycles goes up significantly when the pile-soil body is colder or hotter at the start. The experiment will be run like this, the thermal fluid flowing through the pile will always be flowing through a medium with a significantly different temperature. This means that the energy cost for running the model that way is a lot higher, at around 950 Watt at the start of the cycles. This extra temperature during cooling has to be lost for the sake of the experiment, probably via a heat exchanger with the air. The amount of energy added to the thermal fluid in the cooling phase is the amount of energy that will be used to heat the building on an energy pile in practice. A note to add to this is that in the calculation of the energy consumption there is no mention of the energy it costs to get the thermal fluid to the right inflow temperature. Only the amount of energy that is taken up by the soil.

Table 4.9: Output temperatures of cooling pipes in DIANA

| Steady state | Unit | Day 1 | Day 30 | Day 200 |
|---|---|---|---|---|
| Output temperature cooling | $\Delta T$ | 0.82 | 0.37 | 0.30 |
| Power output cooling | $J/s$ | 627.7 | 283.2 | 229.6 |
| Output temperature heating | $\Delta T$ | 0.84 | 0.38 | 0.32 |
| Power demand heating | $J/s$ | 643.0 | 291.4 | 244.9 |

| Phased | Unit | Day 1 | Day 30 | |
|---|---|---|---|---|
| Output temperature cooling phased | $\Delta T$ | 1.24 | 0.39 | - |
| Power output cooling | $J/s$ | 949.2 | 298.5 | - |
| Output temperature heating phased | $\Delta T$ | 1.26 | 0.40 | - |
| Power input heating | $J/s$ | 961.5 | 303.3 | - |

## 4.7. Conclusion

In this chapter the behaviour of the proposed energy pile experiment has been investigated. After changing the soil parameters from the model in chapter 3 to fit the situation in Delft the model was run to find a suitable thermal cycle. The cycle that was chosen is 3 weeks of heating/cooling at $\Delta T \pm 12°C$, the reason was that within this time a significant portion of the soil can be affected by the temperature, while still being short enough that a large amount of cycles can be done.

As the pile wants to expand but is held in place a restrained strain can be identified, this is the difference between the theoretical thermal strain and the observed strain. This restrained strain is the part responsible for the increased axial stress. The total thermal strain during cooling is -91.8 $\mu\epsilon$ and -10.2 $\mu\epsilon$ is the restricted strain, these tensile strains cause a maximum decrease in axial stress of 600 kPa. During heating the total thermal strain is -78.7 $\mu\epsilon$ and 23.3 $\mu\epsilon$ is the restricted strain, causing a maximum increase in axial stress of 1000 kPa. The difference between the calculated change in axial stress (calculated with $\epsilon_{Rstr} \times E$) and numerical change in axial stress can be attributed to the increase in shear stress at the interface and an increase stress at the pile tip. The interface shear stress is seen to increase during heating where a soil layer has to resist the pile more, i.e. the extremities of the pile, the same locations where the axial stress graph has the highest gradient.

The thermal expansion is the cause of pile movement as well, as the pile expands half of the pile moves up, and the other half moves down, reversing with cooling. This is seen in the direction of the shear stress as well. Where the pile does not move is called the null-point and that is the point that stays still during the entire heating/cooling cycle. A side effect of this is that at that location there is no extra shear stress development on the interface and no change in axial stress due to temperature change. It is shown that the null-point is at 5 m depth at the first cycle and gradually moves down to about 7 m depth after 60 cycles. This shows that there is a reduction in the strength of the soil holding the pile, but an increase in shear stress from the bottom layer and the pile tip resistance. It is also seen that the maximum amount of axial stress induced by the pile moving along the soil reduces over time due to this reduction in interface resistance. The reduction in shear stress is attributed to plastic deformations along that interface, and as a result the pile is seen moving down as the cycles progress. The amount of energy that it takes to heat up the thermal fluid from the pile so that the input temperature is constant has been calculated, this can be used to calculate the amount of energy that needs to be provided by a heat pump in order to run the system.

# 5

# Discussion

In this chapter the research questions are answered, using the results of the numerical modelling.

## 5.1. Thermomechanical effects

This section deals with the thermomechanical effects on an energy pile and the first 4 research questions will be discussed here. The questions are about the thermomechanical effects, the soil-structure interaction, the scale of these effects and the pile's bearing capacity.

### 5.1.1. Vertical pile displacement

When the pile heats up or cools down, the pile will expand and contract and the amount is governed by the thermal expansion coefficients. Each material expands at its own rate and the difference between expansion of two materials leads to stresses at their contact points. Thermal expansion is the main cause of pile movement after the displacement caused by the mechanical load. In the numerical results the amount of vertical movement was small, but the modelled experimental pile is smaller than a standard foundation pile. A regular pile used as a foundation in practice in the Netherlands will most likely reach the second sand layer starting at 14.7 m depth. The experimental pile saw vertical pile head displacements up to 2.4 mm added to the movement caused by the mechanical load (figure 4.31). A building built on longer piles can experience at least double that amount and if a more extreme thermal load is applied it will be even more. If not all piles underneath that building are energy piles and the energy pile is contracting, the building could be lifted off the pile. The load will have to be redistributed to the surrounding piles and settlement will occur. Differential settlement can cause problems in the building such as cracking of the foundation or subsidence. Vertical pile head movement is an important factor to measure well in the experiment as it governs the usability of the pile in practice.

The pile contracts and expands around a null-point, the location of that point is dictated by the location of the load carrying layers. The strongest layers hold on to an expanding/contracting pile the most, thus keeping it in place at that location. An unrestrained pile will expand about its centre, expanding equally in all directions. The null-point of an embedded pile will be lower than the centre assuming that the deeper layers are stronger. A floating pile will have this problem less as the load is distributed more equally along the shaft. The pile in Delft will be more end-bearing and so the null-point will be lower. In time as the weaker layers lose strength through constant shearing along the pile, the layer in which the pile is embedded will carry more and more load drawing down the null-point. That increases the amount of load in the toe, which needs to be measured in the experiment. It also increases the movement of the pile head, as a larger portion of the movement is generated above the null-point. The null-point was at -7.0 m after 60 cycles (figure 4.32), so 70 % of the pile moves in the same direction increasing the pile head movement. Add to that the possible negative skin friction due to thermally induced consolidation and the settlements will be even larger.

### 5.1.2. Axial strain

The axial strain in the pile is a result of both the mechanical and the thermal load. From the measured total strain the strain caused by the mechanical load needs to be subtracted, the result is the thermal strain. The theoretical thermal strain is the strain that can be calculated with the difference in temperature and the linear thermal expansion coefficient. From that theoretical strain the measured strain can be subtracted, that is the restricted strain responsible for the increase in axial stress. Before the thermal loading portion of the experiment starts, the temperature profile, strains due to mechanical load and pile head displacement must be known, otherwise differentiating the different types of strain is impossible.

### 5.1.3. Axial stress

From the axial strain profile the axial stress can be calculated, the calculation requires only the strain and the Young's modulus of the pile. The problem is that it is hard to determine the combined stiffness of a reinforced concrete pile and the validity of the results is tied to that calculation. It should be noted that the calculation of the energy pile stresses can be calculated in 1 direction, the influence of horizontal stresses and strains on the pile is negligible in this case. In the experiment, during a heating cycle, a doubling of axial stress could be observed, so for the concrete strength that has to be taken into account. During cooling cycles it could be that tension develops in the bottom part of the pile. When that happens the tensile strength of the pile needs to be checked.

Both the stress and the strain will increase as the difference of temperature in the pile with the temperature in the soil increases. This difference of temperature means a difference in thermal expansion/contraction, and so stresses will develop on the interface. As time passes and the soil close to the pile reaches the same temperature as the pile, the differential movement becomes less. The soil's hold on the pile becomes less and the stress in the pile will reduce. This effect will be noticeable as time passes, so during measurements a peak can be seen and after that the stress will only reduce.

### 5.1.4. Shear stress

If a pile tries to move in the soil it generates shear stresses along the pile-soil interface, it is one of the modes of load carrying for foundation piles. The movement in an energy pile however is more than it would normally be with just mechanical loading and the cyclic movement will negatively affect the strength of the interface with weaker layers. The development of the interface strength in time is one of the things that govern the bearing capacity. If the shear stress reduces in the weaker layers, the null-point will migrate towards the stronger layers. The load on the layer on which the pile is founded will increase in the case of the experimental pile. The difference in axial stress with the cycles can be accounted for by the increase in shear stress and an increase in pile toe stress. It is important that a loading plate is installed near the toe so that the stress at the tip can be measured. With vertical equilibrium of the stress in and on the pile, for a specific section, the change in strength of the interface for that section can be calculated. Measurements of stress are ideally continuous, but at the least measurements should be done at the top and bottom of each layer so that the change in shear stress over that layer can be calculated.

### 5.1.5. Cyclic effects

With cycles the pile-soil interface could restrict the pile less due to continuous movement of the pile along the soil. This loss of strength will lead to the overall settlement of the pile, even through the heating cycles. It will also lead to less stress generated in the pile because there is less restricted strain. The more the pile as a whole moves in the soil, the more the pile head will move, and with it the building on top. The reduction in strength in time is an important factor in investigating the safety of structures built on thermoactive foundations.

With the expanding and contracting concrete there is a chance that it might crack. This has not been modelled in this thesis, but should be taken into account in the experiment, especially because there could be tension near the pile toe in a cooling phase. The chance of cracking will increase with cycles, and bigger temperature differences. After the experimental pile has been through all of the cycles and sufficient results have been gathered, the pile can be subjected to more extreme temperatures. Seeing the effect when the thermal fluid has a very high temperature can lead to a better understanding of when the interface starts slipping. Temperatures below 0 °C will probably freeze the soil, and the behaviour of the interface with frozen soil can be investigated as well. If, during the cycles, a crack has formed and some ground water has seeped in and that freezes there is a chance that the crack becomes worse and becomes a problem for the bearing capacity.

### 5.1.6. Other effects

Thermally induced consolidation is an effect that has not been modelled in DIANA. An increase in temperature decreases the pre-consolidation pressure and increases the pore-pressures. Both these effects speed up consolidation of the soil and that means more negative skin friction on the pile. Even though the direction of the friction on the pile changes with the cycles, the direction of the consolidation remains the same. It could increase the stress in the pile during heating even more and decrease it during cooling, depending on where along the pile the consolidation happens. Monitoring this effect will be important as it is one of the things where building a pile in soft soils differs from building in harder soil. The problem with measuring this is that the soil also expands/contracts with the temperature cycles and this coincides with the thermally induced consolidation, differentiating between the two will be difficult. A way to find out if the soil has been consolidating due to temperature is to do more CPT's after the experiment has finished.

### 5.1.7. Scales of the effects

The scales of the thermal effects on the soil are given for $\Delta T \pm 12°C$ and for $\Delta T \pm 24°C$. Both the total stresses and strains are listed, as well as the thermal strain. This gives an estimation of both the range of the expected measurements as well as a desired sensitivity. The second temperature difference is not the advised value for the experimental cycle, but it gives an idea for the scalability of the expected measurements, the graphs of the results are given in appendix B.

Table 5.1: Expected measurements of various parameters

| | | $\Delta T \pm 12°C$ | | $\Delta T \pm 24°C$ | |
|---|---|---|---|---|---|
| | Unit | heating | cooling | heating | cooling |
| Axial strain | $\mu\epsilon$ | 50 | -135 | 140 | -220 |
| Axial stress | $kPa$ | 2500 | -125 | 3400 | -1000 |
| Pile head displacement | $mm$ | -4 | -5 | -4 | -5.8 |
| Thermal axial strain | $\mu\epsilon$ | 87 | -97 | 178 | -182 |
| Thermal axial stress | $kPa$ | 1000 | -600 | 1800 | -1200 |
| Thermal pile head displacement | $mm$ | -0.9 | -1.9 | -0.9 | -2.7 |

**Axial strain**

The strain in the pile will be between -135 $\mu\epsilon$ and 50 $\mu\epsilon$ for cooling and heating respectively at a temperature difference of 12 °C, compressive strain when cooling tensile strain when heating. The thermal strain is responsible for the ± 100 $\mu\epsilon$ difference from the mechanical strain. The thermal strain increases almost linearly with temperature, so if the experiment requires more extreme temperatures the expected strains can be extrapolated.

**Axial stress**

The scale of axial stress differs a lot between heating and cooling. The soil lets the pile contract more easily than expand, inducing a tensile axial stress of 600 kPa during cooling where the heating cycle induces an extra 1000 kPa in compression for a temperature difference of 12 °C. The 24 °C temperature difference shows an almost doubling of the stress and during heating the increase of 1800 kPa is an almost tripling of the original stress from mechanical loading and problems could arise with the concrete strength. The expansion of the pile has a linear relationship with temperature ($\epsilon_T = \alpha \Delta T$), however the interaction between the soil and the pile is non-linear. That is why when imposing a more extreme temperature difference, the increase in stress is non-linear. The soil could redistribute load and induce more or less shear stress along the interface, causing the stress reaction in the pile to be more or less than expected when considering the lower $\Delta T$.

**Vertical pile displacement**

The amount of vertical pile displacement, if the pile experiment is similar to the numerical model, will be between 3.0 mm and 5.5 mm between the heating/cooling cycles at 12 °C temperature difference. Vertical pile head displacement is roughly the same, however, the rest of the pile seems to move more overall see figure B.4 in appendix B.

## 5.2. Experiment design

This section deals with the experimental design, including pile geometry, length of the thermal cycle, energy consumption of the heat pump and sensor placement.

### 5.2.1. Pile geometry

The design of the proposed experimental pile is based on the soil conditions at the site and the nature of the experiment. Parts of the proposed experimental pile set it apart from what has been done before. These are the number of cycles, loading the pile to a higher percentage of its capacity and the soft soil conditions. Translating this to a pile design means that the pile must have a small diameter, this diameter then requires the pile to be shorter as well, because of structural problems that can occur when lowering the reinforcement cage into the pile. A pile in the Netherlands requires a sand layer to carry most of the weight and that was found at 8.7 m depth, so a pile length of 10 metres was chosen.

### 5.2.2. Thermal cycle

The proposed thermal cycle consists of 3 weeks cooling and 3 weeks heating and repeating this until enough measurements have been done. Three weeks is enough to see the time-dependent reduction in axial stress due to the soil releasing the pile, yet it is long enough to influence a significant portion of the soil. During heating, the stress builds up to roughly twice the mechanical stress, and in cooling some tensile stress is seen near the pile tip without freezing the soil. The more extreme case of $\Delta T \pm 24°C$ leads to unacceptably high stresses in the pile, however the vertical pile head movement would be easier to measure as it displaces more. Especially the tensile stress in the pile tip during cooling which is nearly 1000 kPa, see figure B.2 in appendix B. If, in the experiment, the measurements do not seem to be as expected, for example after an initial Thermal Response Test, the cycle can be adjusted.

### 5.2.3. Heat pump

In order to get the thermal fluid to the correct temperature a heat pump is needed. The pump has to cool or heat the fluid to the desired temperature and then pump it through the pile. When the fluid comes returns, the temperature is either higher or lower than the inflow temperature. If the fluid has cooled then the heat pump needs to use energy to heat it back up, if the fluid has heated then the excess energy needs to be dissipated. With a thermal fluid with a volumetric heat capacity of 3.06E+06 $J/m^3°C$ and a fluid discharge of 2.5E-04 $m^3/s$ the energy that is lost or gained by the fluid is 765.45 $J/s$ (or Watt) per °C. With two u-pipes with a total length of 40 m and a pile diameter of 32 mm, the amount of fluid that fills the pile is 320 $l$ ($0.016^2\pi \cdot 40$). First getting the temperature to $\Delta T = 12$ will cost (3.06E+06 $\cdot$ 0.032) 97.9 $kJ$, and then 765.45 $J/s$ per degree lost in the pile.

### 5.2.4. Sensor measurements and placement

The problem with taking measurements in the field compared to a numerical model, is that a lot of effects can not be measured. The stress in the pile and the shear stress on the interface are not measurable but of great importance to evaluating the bearing capacity of the pile. Apart from a loading plate near the toe of the pile, strains are the only quantity that can be measured, the rest need to be calculated. The pile is relatively small and so are the thermal effects, the sensors must have a high sensitivity. The piles size also means that there is limited space of where to put the sensors and choices need to be made as not everything can be measured. Influences from surroundings could be significant, such as settlement due to the loading rig and additional thermally induced consolidation. Because of the size of the pile, the micro strains developed due to temperature will not lead to a lot of pile head movement, in larger piles more commonly used for building foundations, the effect will increase greatly. Apart from sensitive sensors a solution could be to use more extreme temperatures, the effects of weather and soil will be less, relative to the pile temperature.

The effects of the temperature difference with the surrounding soil is listed in tables 4.7 and 5.1, an increase in $\Delta T$ shows a large increase in measured strains and temperatures. The downside to more extreme temperatures is the extra time it takes to reverse the cycle. This can be optimised during the experiment when measurements turn out to be unclear.

Figure 5.1 shows an example of the cross-section of the pile, the u-pipes are scaled correctly but the other sensors are slightly larger for visibility. There will be 2 u-pipes through which a thermal fluid is flowing, this means that there will be a hot side an a cold side to each of those. The hot and cold sides alternate so the the pile does not deform asymmetrically. The u-pipes will be affixed to the reinforcement cage as well as Optical Fibre Sensors (OFS) and strain gauges. Strain gauges are less ideal because they only measure strain at specific heights where OFS are capable of measuring a continuous profile and temperature at the same time. The OFS next to the u-pipes follow the entire pipe through the pile and the OFS on the reinforcement bars measure strain in-between the pipes. Having a measurement of strain in the hot and cold sides and in the middle enables the back-calculation of shear strains in the vertical direction.

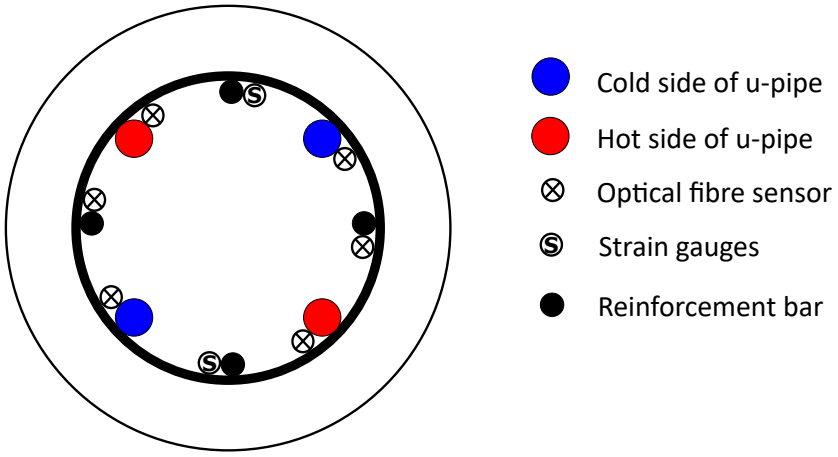



Figure 5.1: Sensor layout within a pile cross-section

There are strain gauges in the vertical direction at the top and the bottom of each layer, with those strains a stress profile can be calculated. As the measurements change over time the change in stress over the thickness of the layer is a measure of how the interface between the pile and that particular layer is influenced. The more measurements are done, the better the behaviour can be investigated. There will be horizontal strain gauges at three depths in the pile, see figure 5.2, so that the shear strain in the cross-section can be calculated. The locations are in the peat to see how the strain develops in a weak layer, in the silty sand to see the strains near the null-point and in the stiff bottom sand layer.They are fixed to the reinforcement cage, so every 250 mm a horizontal strain gauge can be installed. Having them in more layers at more depths will be beneficial to the amount of measurements that can be taken, however the practical issues of cost and installation difficulties have to be taken into account.

Some additional sensors are needed, a loading plate is inserted at the bottom to measure the load on the toe that was not taken up by the shaft friction, the change of this load in time will give information about the strength of the pile-soil interface as well. About 1.5 m distance from the pile there is a tube inserted in the soil through a hole made for a sample boring during the site investigation and in that hole an additional temperature sensor can be placed to measure the heat flow through the soil and check to what extent soil is being influenced. The boring was made for the site investigation, but the hole is still there and can be used to put sensors in, that is why extra measurement can be made at that distance.

The main problem with the energy pile experiment is figuring out how the different measurements and their causes can be specified. There will be strain in the pile due to mechanical load and the thermal load, the soil will settle due to the loading frame and other equipment on top as well as the thermal expansion/contraction. Getting good starting measurements where the influences of the pile load and equipment are known is very important, otherwise it will be very hard to tell the influence that the temperature has on the soil apart from

other effects. All of these sensors are placed within the pile, not on the pile-soil interface. This is because the pile is cast in place and installing sensors on the interface after the pile has been cast is impossible. Measurements of pore pressures in the soil would require more drilling in the area. The expectation is that the pore pressures do not influence the pile behaviour too much, but measuring them could be good to check the assumptions.

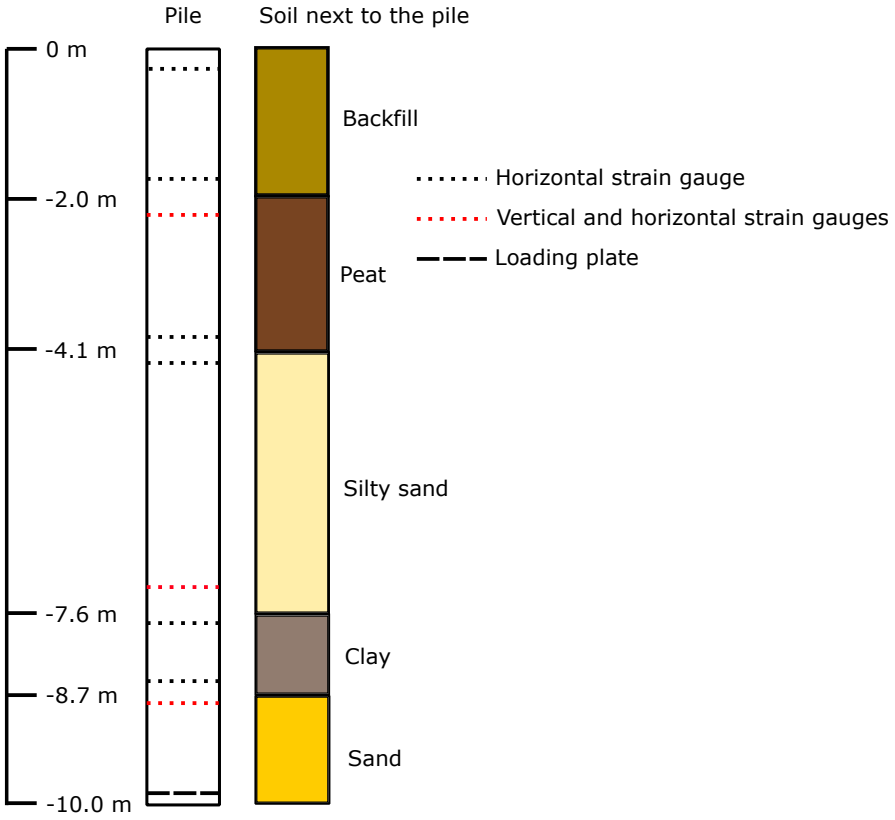



Figure 5.2: Sensor layout in a longitudinal cross-section of the pile

## 5.3. Numerical modelling

The model serves as an estimation of the pile and soil behaviour prior to installation. It provides confidence in the design and highlights areas where extra investigation is required. This section contains a discussion on the numerical model that was made, the assumptions that were made in the building of the model and the limitations of the numerical method.

### 5.3.1. Material models

All of the modelling in this thesis have been done with a Mohr-Coulomb material model, there are however more options to model the soil. Apart from a build up of plasticity no cyclic behaviours have been taken into account like small strain stiffness or hardening soil. DIANA does update the material parameters every time-step, but there are no specific parameters put in to govern that behaviour. Most of the behaviour modelled is from within the pile, which is linear elastic. In order to use these more complicated models, more laboratory testing needs to be done on the soil to determine the correct parameters. The goal of the numerical modelling in this thesis is to predict the behaviour of the proposed energy pile and for that the Mohr-Coulomb material model is complete enough. If in future research the experiment in Delft is back-calculated and the results from this model do not resemble the measured data, then other material models can be used to see which works best for an energy pile.

**Parameter determination**
Parameter determination was done with limited soil investigation. The table in the Dutch norm with characteristic soil properties based on a $q_c$ is a good starting point, but ideally there are some laboratory tests to verify the numbers. Important for the temperature distribution are the thermal properties, but they are based on only a few tests and some assumptions.

**Temperature application**
In this thesis the assumption that an energy pile temperature distribution can be approximated by an infinitely long line source has been verified. A heating line at the location of a u-pipe serves as a line source. The rate at which the temperature can change is dependent on numerical stability. If a big temperature change is imposed in a single time-step, the expansion/contraction of the pile will happen in the same instant. That forces the pile to move, where the soil has not yet been influenced by the temperature and the sudden jump from the pile will be too much for the model to calculate. Therefore imposing the temperature difference in 1 step is numerically impossible, but that is the way the field experiment is run. Thermal fluid will have a certain temperature and the pile will react, however it will take some time for the heat to flow through the pile. The more accurate way of heating the pile is with the cooling pipes in DIANA, but as it was shown, the difference in temperature distribution is not very large and therefore not worth the time investment to do a 3D model.

A consequence of this gradual temperature application is seen figures 4.31 and 4.32. The lines in these graphs will have less straight lines and increase more gradual as the temperature will flow according to figure2.5, and the increase in strain over time will have the same shape.

**Pile-soil interface**
The pile-soil interface is a difficult thing to model. The other numerical models made of energy piles discussed in chapter 2 had left it out and fixed the pile to the soil elastically as if the pile had perfect roughness. Which is not the case in reality, where the pile can slip and the temperature could have an influence on the interface in the soft soil layers. The interface used in DIANA has a few parameters based on some rules of thumb, ideally these will be calibrated on the basis of a tests on an actual pile. But that will have to come later as the experiment is not yet in that stage. There is debate on what the best way to model pile-soil interaction is. In a way, the parameters used in the interface control the behaviour without being based on measurements. The experimental energy pile is mainly an experiment to better understand the behaviour of the pile, but the behaviour of the pile-soil interface could be investigated as well, both the physical and the numerical interfaces.

**Stress calculation**
The calculation of strain, to stress, to shear stress of chapter 4 works because it is a numerical model. When using experimental measurements the data will not be as nicely distributed as the graphs from the model. The reason that the calculations of strain to stress is correct is that parameters such as thermal expansion coefficient and pile stiffness are completely correct because they were defined in the model. In the actual experiment it will be harder to get accurate values for those two quantities. Calculation of the stiffness of a concrete pile with a reinforcement cage is not straightforward as it needs to be found in laboratory testing, or a 3D numerical simulation with DIANA. The stiffness of the steel is known better, but the total stiffness of the pile needs to be calculated with the relationship between the amount of steel in the pile and the stiffnesses of both the steel and the concrete. If the determination of those parameters is off, then the calculations of the stresses in the pile will be off.

### 5.3.2. Hydraulic behaviour
All of the modelling of the energy pile have been done with undrained behaviour, whereas in previous research [Gawecka et al., 2016, Laloui et al., 2006] in London a full thermo-hydro-mechanical coupling has been done. In Gawecka et al. [2016] the build-up of pore pressures was insignificant and the effect it had on the pile as well. The homogeneous clay layer that the London pile experiment was built in can be considered to be completely undrained, the varied soil layers in Delft however are closer to fully drained. The clay layers are thin and can drain excess pore water to the adjacent porous sand layers. So in order to find the upper limit of the influence of pore water pressure, the model was made to be undrained. In the actual experiment it will be interesting to measure the pore water pressure close to the pile, to see if it really is insignificant.

# 6

# Conclusions

The proposed energy pile experiment was modelled in this thesis. The researched questions were based on investigating the thermal effects on the pile and soil and then design an experiment to measure those effects. First the known behaviour of energy piles was investigated in literature in chapter 2. Previous experiments that were done are investigated and the reason why more research is needed becomes clear. The flow of temperature through soil is known well, but the effect it has on the soil, and the pile-soil interface is still largely unknown. Previous experiments were done in different soil types [Amis et al., 2008, Laloui et al., 2006], that have different modes of bearing mechanical load. The Laloui et al. [2006] pile was an end-bearing pile based on rock and the Amis et al. [2008] pile was set in London clay and is a floating pile without much load on the pile tip. The situation for the Delft experiment is somewhere in-between, a stiffer bearing layer but also shaft resistance. Not only are the behaviours of the various layers interesting, also the change of those behaviours as temperature changes through cycles. So now the question was: what are the effects on the varied and weaker soil layers in Delft, and how do they change over time?

To answer that, the model was first made in DIANA and then validated and verified by comparing it to previous projects. The pile was designed to fit the conditions of the experiment, so small enough so that a lot of cycles can be done quickly and big enough to still be considered a foundation pile. A pile with a diameter of 380 mm and a length of 10 m is smaller than a normal foundation pile, but that does ensure that the pile can be loaded to a bigger percentage of its capacity and that thermal cycles are relatively short. A cycle of heating and cooling with $\Delta T \pm 12°C$ for three weeks was chosen to load the pile. The results showed that all the desired effects are seen within that time, without increasing stresses beyond the pile's capacity.

The modelling proved that all of the mechanisms from literature (see chapter 2) are found in the Delft soil as well, but they are more hidden than with the homogeneous soil conditions in London for example. Strain occurs as a pile heats up or cools down, the pile is not free to expand as the soil does not expand at the same rate. From the amount of strain measured and the amount of strain that should be there considering the temperature difference, a restrained strain can be calculated. Axial stress increases when the pile wants to expand, not only because the soil is holding on to the pile causing restrained strain, but also as the pile moves along the soil generating negative skin friction. The model will output the shear stresses on the interface, but in the experiment they cannot be measured. The change in axial stress with depth can only be accounted for by the shear stress on the interface, that is how the shear stresses must be calculated in the experiment. Vertical pile movement is a result of both the thermal strains that were not restrained, the pile will expand when heated and contract when cooled and the mechanical load on top.

Piles that are free to expand/contract will do so about a null-point in the centre of the pile. The pile in Delft will not be unrestrained and the layers that exert the most shear stress will affect the location of that null-point. The more shear stress generated at a point along the pile the less the pile will move. In Delft the null-point is at around -5 m in the first cycle, right in the centre. This means that the parts of the pile above and below the centre restrain the pile equally. However, as cycles of heating/cooling pass the weaker layers will no longer be able to resist the increased movement and fail. That means that the bottom layer draws more load and in doing so pulling the null-point down as well. This effect means that the load on the toe of the pile

will increase over time. In terms of bearing capacity calculation this means that over time the shaft resistance becomes less important as the pile becomes more end-bearing. In order to be safe a solution could be that shaft resistance is not taken into account at all and that only the pile tip resistance is used for the capacity. This could be the safest solution but not the most economical, it is unlikely that the entire pile-soil interface loses all of its strength. A middle ground where only a percentage of the shaft resistance can be used for the calculation would be beneficial for safety and cost of the design. This can be put into a standard for energy piles as a measure of the cyclic effects on the pile-soil interface.

Cyclic behaviour in literature suggest that the pile might accumulate strains with each heating/cooling cycle and the modelling sees that as well. Without using a cyclic model, within the first 10 cycles, the pile settles an additional couple of millimetres. In practice, that effect might be bigger as there are more time-dependent processes that change the balance of the forces on the pile. Temperature dependent consolidation will cause extra settlements in the weaker layers inducing more down-drag on the pile. A repeated lifting of the pile tip from the load bearing layer and then dropping it again might cause plastic deformations and subsequent settlement as well.

All of these effects will be measured by sensors in and around the pile. In chapter 5 the layout of those sensors is proposed as well as expected ranges of the measurements that are expected during certain temperature loads. There are still different configurations that can work as well, but for this pile, the main challenge is to measure with precision. The effects are small and there are different causes for strain that have to be specified as well as different causes for pile movement. Getting good starting measurements so that the influences of the pile load and loading equipment are know are very important, otherwise it will be very hard to tell the influence that the temperature has on the soil apart from other effects.

# 7

# Recommendations

In this chapter some recommendations are made for further the research on the topic of this thesis.

**Calibration**
Obviously the research on the energy pile will continue with the construction of the experimental pile proposed in this thesis. The measurements done in that experiment can serve as a way to further validate the model and calibrate the parameters used. Form initial thermal response testing the thermal conductivity of the soil can be checked, and the samples that were taken have to be examined in the lab to determine the rest of the soil properties. If the measurements are detailed enough and the strain and stress graphs resemble the ones in chapter 4 then the influence of thermal cycles on the interface can be calculated. From that the interface could be calibrated and the model can be rerun to better understand the influence of interfaces.

**Cracking of concrete**
The concrete is under a lot of stress, and the changing of the direction of the strain with each cycle is not good for the concrete. The pile tip will experience tension when cooling to a more extreme degree. If water seeps into a crack and then it freezes the crack will widen and weaken the pile. A numerical investigation to this effect will be beneficial and at the end of the experiment the pile can be subjected to extreme temperatures and cracked on purpose to see if the simulation are correct.

**Freezing soil**
The soil was subjected to temperatures of below freezing, however the numerical model did not model ice. It was simply water with a below 0 °C. The freezing soil will influence the behaviour of the soil and the pile-soil interface. Energy piles are not generally used at temperatures that low, but knowing what happens when they are is a good precaution.

**3D analysis of cross-section stresses**
In the cross-section there is a hot pipe and a cold pipe, these temperature differences cause a difference in strain and therefore a shear stress. This is another stress in an energy pile that is not present in conventional non-energy piles. Knowing the magnitude of these shear stresses will give some more insight into whether or not the strength of the concrete is sufficient.

**DIANA soil modelling**
DIANA FEA has proven itself in that it can be used to model complicated multi-physics model. It is however not very user-friendly when modelling soil. A phased model of a soil body without a pile at first and then with a pile installation later is difficult, But necessary to get the stresses right in the soil and the pile.

# Bibliography


H. M. Abuel-Naga, D. T. Bergado, S. Soralump, and P. Rujivipat. Thermal consolidation of soft Bangkok clay. *Lowland Technology International*, 7(1):13–21, 2005. ISSN 13449656. doi: 10.1016/S0020-7462(00)00035-4.

B. L. Amatya, K. Soga, P. J. Bourne-Webb, T. Amis, and L. Laloui. Thermo-mechanical behaviour of energy piles. *Géotechnique*, 62(6):503–519, 2012. ISSN 0016-8505. doi: 10.1680/geot.10.P.116. URL http://www.icevirtuallibrary.com/doi/10.1680/geot.10.P.116.

T. Amis, P. J. Bourne-Webb, C. Davidson, B. Amatya, and K. Soga. The effects of heating and cooling energy piles under working load at Lambeth College, UK. *Proceedings of the 33rd Annual and 11th International Conference on Deep Foundations*, (April):10, 2008. URL http://scholar.google.com/scholar?hl=en{&}btnG=Search{&}q=intitle:THE+EFFECTS+OF+HEATING+AND+COOLING+ENERGY+PILES+UNDER+WORKING+LOAD+AT+LAMBETH+COLLEGE+,+UK{#}0{%}5Cn+.

O. Boënnec and F. Maunsell. Shallow ground energy systems. *Energy*, 161(EN2):57–61, 2008. ISSN 1751-4223. doi: 10.1680/ener.2008.161.2.57.

P. J. Bourne-Webb, B. Amatya, K. Soga, T. Amis, C. Davidson, and P. Payne. Energy pile test at Lambeth College, London: geotechnical and thermodynamic aspects of pile response to heat cycles. *Géotechnique*, 59(3):237–248, 2009. ISSN 0016-8505. doi: 10.1680/geot.2009.59.3.237.

P. J. Bourne-Webb, K. Soga, and B. L. Amatya. A framework for understanding energy pile behaviour. *Geotechnical Engineering*, 166(GE2):170–177, 2013. ISSN 1353-2618. doi: 10.1680/geng.10.00098.

J. E. Bowles. *Foundation analysis and design*. McGraw-Hill Higher Education, 5th edition, 2007.

H. Brandl. Energy foundations and other thermo-active ground structures. *Géotechnique*, 56(2):81–122, 2006. ISSN 0016-8505. doi: 10.1680/geot.2006.56.2.81.

H. S. S. Carslaw and J. C. Jaeger. *Conduction of heat in solids*. Oxford University Press, Oxford, second edition, 1959. ISBN 0198533683. doi: 10.1016/0022-5096(59)90029-8.

C. Cekerevac and L. Laloui. Experimental study of thermal effects on the mechanical behaviour of a clay. *J . Numer . Anal . Meth . Geomech*, 28(April 2003):209–228, 2004. ISSN 0363-9061. doi: 10.1002/nag.332.

B. G. Clarke, A. Agab, and D. Nicholson. Model specification to determine thermal conductivity of soils. *Proceedings of the ICE - Geotechnical Engineering*, 161(3):161–168, 2008. ISSN 1353-2618. doi: 10.1680/geng.2008.161.3.161.

Fugro. Cone Penetration Testing, 2017. URL https://www.fugro.com.

K. A. Gawecka, D. M. G. Taborda, D. M. Potts, W. Cui, L. Zdravkovi, and M. S. Haji Kasri. Numerical modelling of thermo-active piles in London Clay. 2016. doi: 10.1680/jgeen.16.00096.

O. Ghasemi-Fare and P. Basu. A practical heat transfer model for geothermal piles. *Energy and Buildings*, 66:470–479, 2013. ISSN 03787788. doi: 10.1016/j.enbuild.2013.07.048. URL http://dx.doi.org/10.1016/j.enbuild.2013.07.048.

GSHP Association. Thermal pile design, installation and materials standards. *Ground Source Heat Pump Association, Milton Keynes*, (1):82, 2012.

L.R. Ingersoll, O.J. Zobel, and A.C. Ingersoll. *Heat conduction with Engineering Geological and Other Application*. University of Wisconsin Press, Madison, 2nd editio edition, 1954.

C. Knellwolf, H. Peron, and L. Laloui. Geotechnical Analysis of Heat Exchanger Piles. *Journal of Geotechnical and Geoenvironmental Engineering*, 137(10):890–902, 2011. ISSN 1090-0241. doi: 10.1061/(ASCE)GT.1943-5606.0000513.

L. Laloui, M. Nuth, and L. Vulliet. Experimental and numerical investigations of the behaviour of a heat exchanger pile. *International Journal for Numerical and Analytical Methods in Geomechanics*, 30(8):763–781, 2006. ISSN 03639061. doi: 10.1002/nag.499.

J. E. Low, F. A. Loveridge, W. Powrie, and D. Nicholson. A comparison of laboratory and in situ methods to determine soil thermal conductivity for energy foundations and other ground heat exchanger applications. *Acta Geotechnica*, 10(2):209–218, 2015. ISSN 18611133. doi: 10.1007/s11440-014-0333-0.

J. E. Low, W. Powrie, and F. A. Loveridge. Error analysis of the thermal cell for soil thermal conductivity measurement. *Geotechnical Engineering*, 170(GE3):191–200, 2017.

T. Mimouni. *Thermomechanical Characterization of Energy Geostructures with Emphasis on Energy Piles PAR*. Phd thesis, EPFL, 2014.

MWH B.V. TU Delft - Green Village Geotechnische beschouwingen. Technical report, Delft, 2015.

NEN. *NEN 9997-1*. Nederlands Normalisatie-Instituut, Delft, 2016.

C. W W Ng, Q. J. Ma, and A. Gunawan. Horizontal stress change of energy piles subjected to thermal cycles in sand. *Computers and Geotechnics*, 78:54–61, 2016. ISSN 18737633. doi: 10.1016/j.compgeo.2016.05.003.

Rijksdienst voor Ondernemend Nederland. Bodemenergie/aardwarmte, 2016. URL `http://www.rvo.nl/onderwerpen/duurzaam-ondernemen/duurzame-energie-opwekken/bodemenergie/aardwarmte`.

Z. S. Spakovszky. Thermodynamics notes, 1993. URL `http://web.mit.edu/16.unified/www/FALL/thermodynamics/notes/node117.html`.

M. E. Suryatriyastuti, H. Mroueh, and S. Burlon. A load transfer approach for studying the cyclic behavior of thermo-active piles. *Computers and Geotechnics*, 55:378–391, 2014. ISSN 0266352X. doi: 10.1016/j.compgeo.2013.09.021. URL `http://dx.doi.org/10.1016/j.compgeo.2013.09.021`.

# A

# CPT data

This appendix contains the CPT data from the site investigation in Delft. Four were taken in a straight line around the exact location of the proposed energy pile experiment. The interpretation of these is in chapter 4.

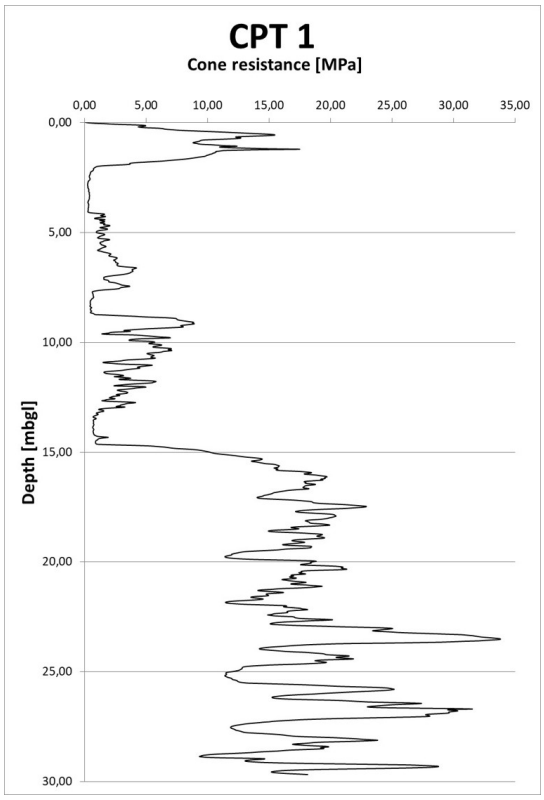



Figure A.1: CPT 1, cone resistance

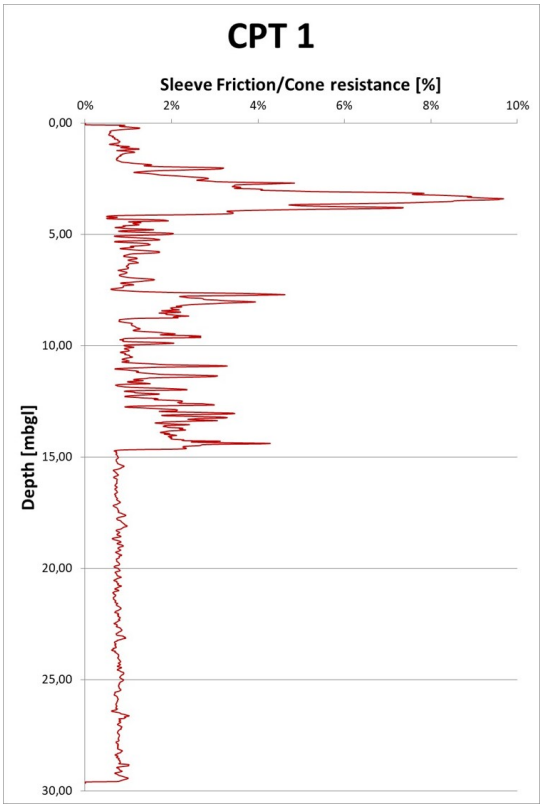



Figure A.2: CPT 1, sleeve friction/cone resistance

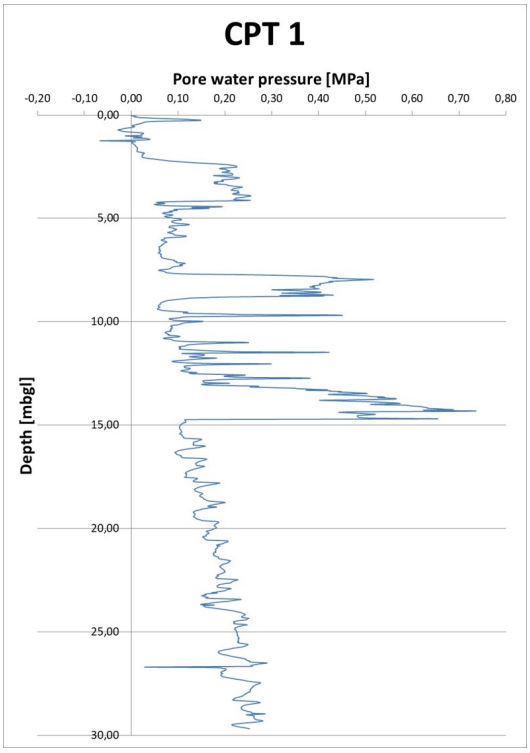



Figure A.3: CPT 1, pore water pressure

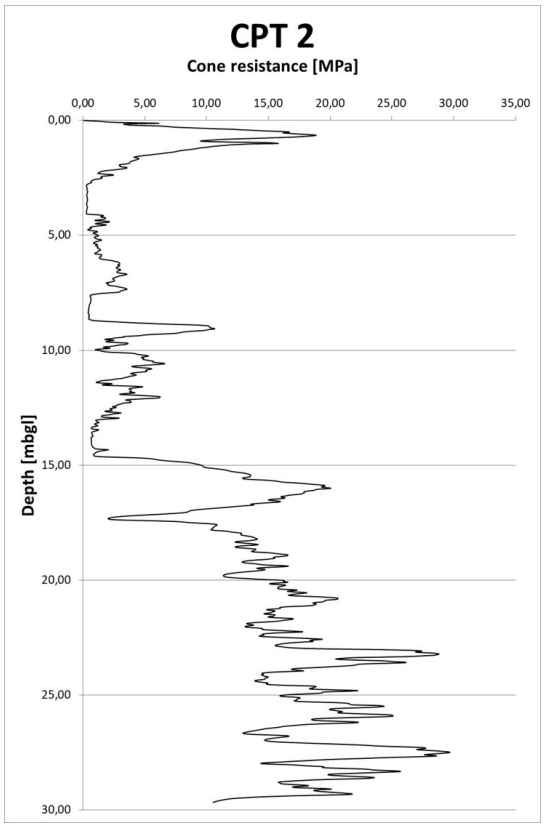



Figure A.4: CPT 2, cone resistance

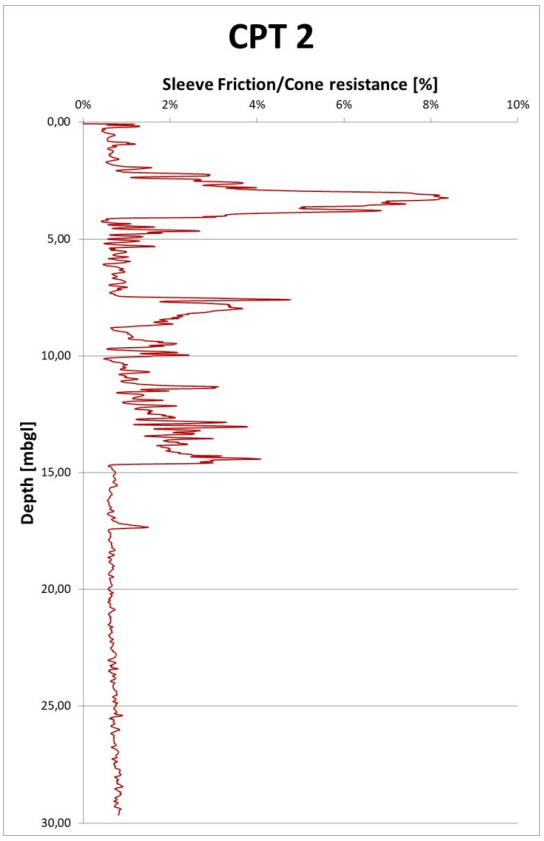



Figure A.5: CPT 2, sleeve friction/cone resistance

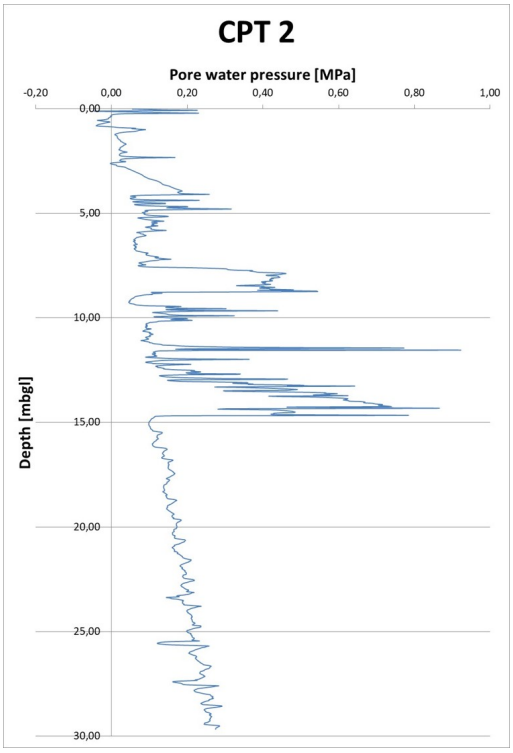



Figure A.6: CPT 2, pore water pressure

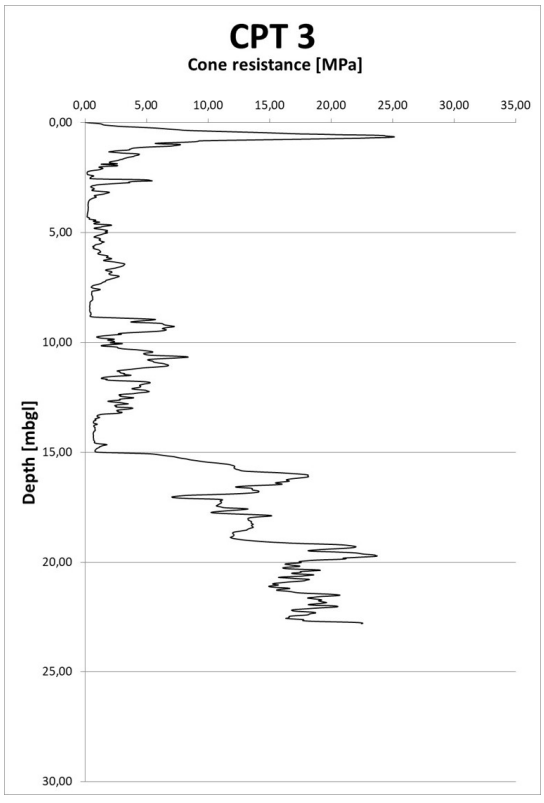



Figure A.7: CPT 3, cone resistance

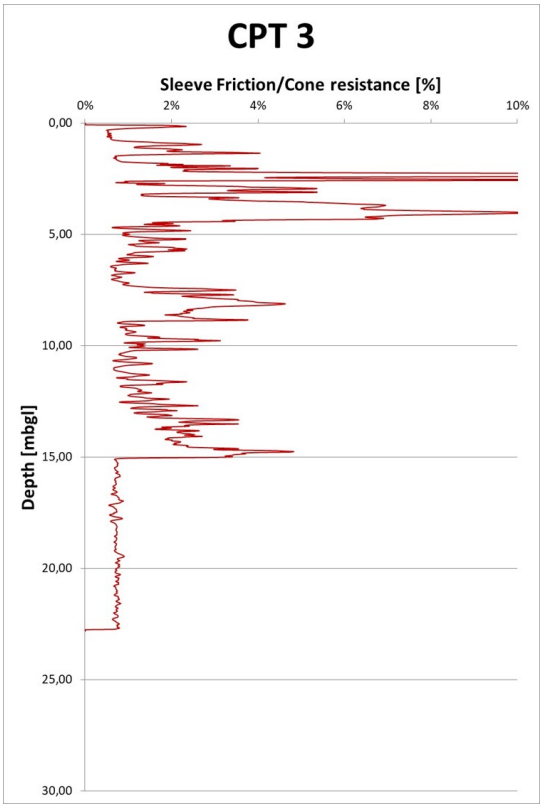



Figure A.8: CPT 3, sleeve friction/cone resistance

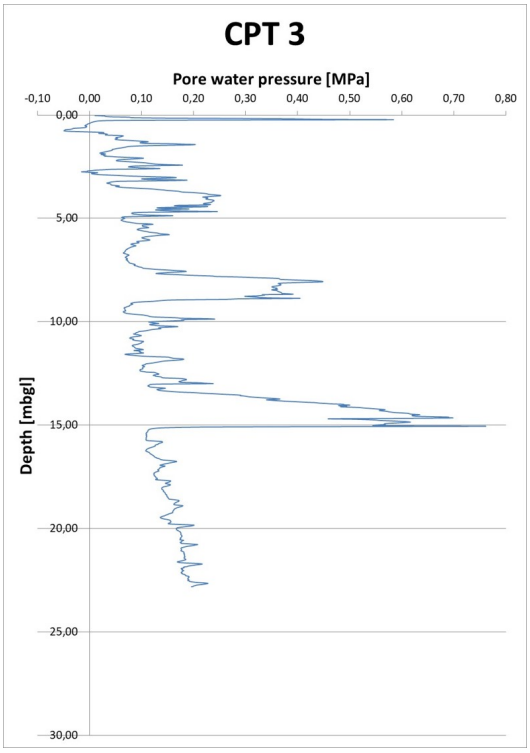



Figure A.9: CPT 3, pore water pressure

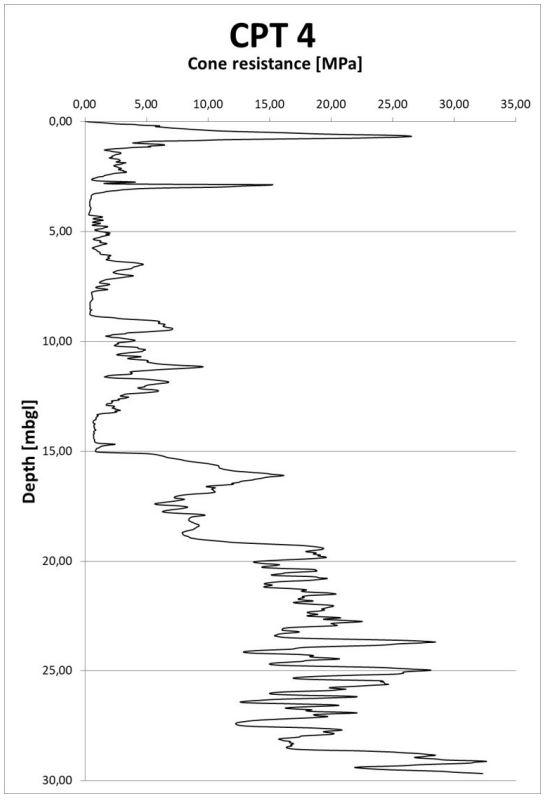



Figure A.10: CPT 4, cone resistance

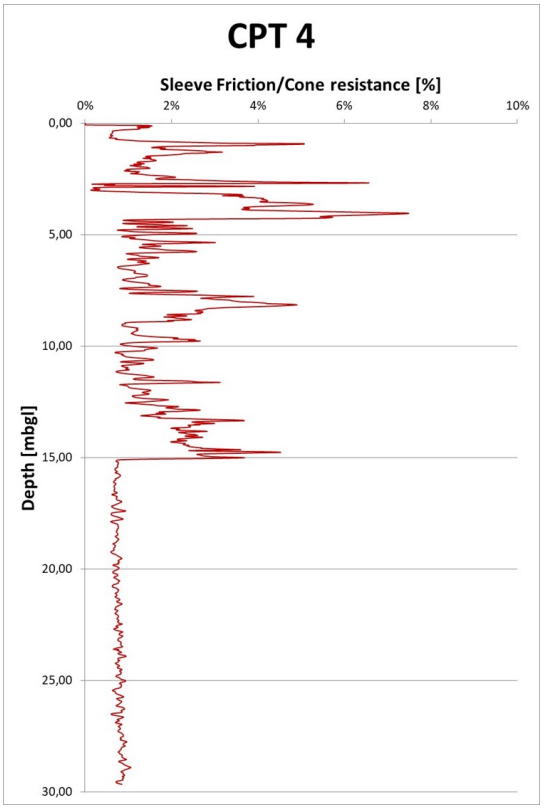



Figure A.11: CPT 4, sleeve friction/cone resistance

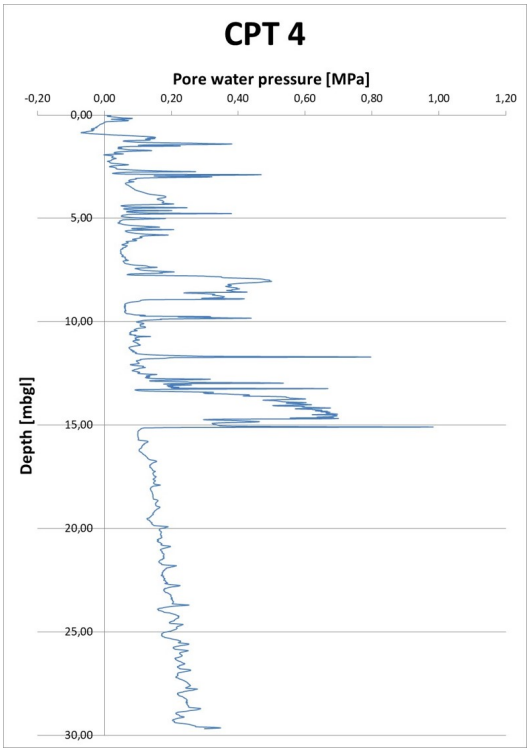



Figure A.12: CPT 4, pore water pressure

# B

# Results for 24 degrees

These are the results for the Delft pile run at a $\Delta T = 24°C$. In the graphs, day 7 is the cooling cycle at -12 $°C$, day 40 is the heating cycle at 36 $°C$.


- Axial strain B.1
- Axial stress B.2
- Shear stress B.3
- Vertical displacement B.4
- Maximum thermally induced axial stress B.5
- Vertical pile head displacement B.6
- Ground level displacement B.7

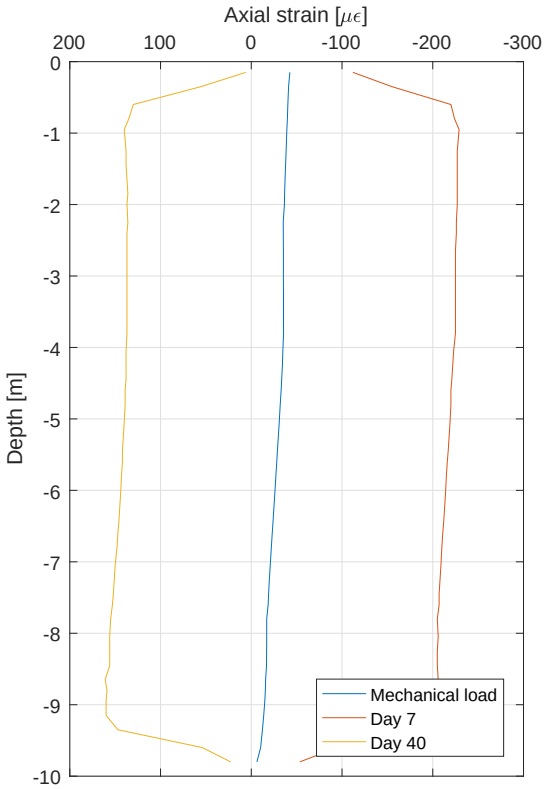



Figure B.1: Axial strain, heating and cooling

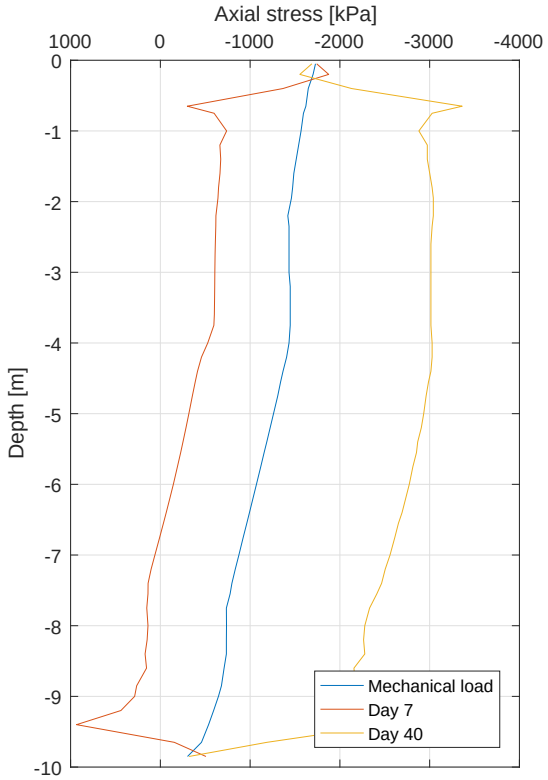



Figure B.2: Axial stress, heating and cooling

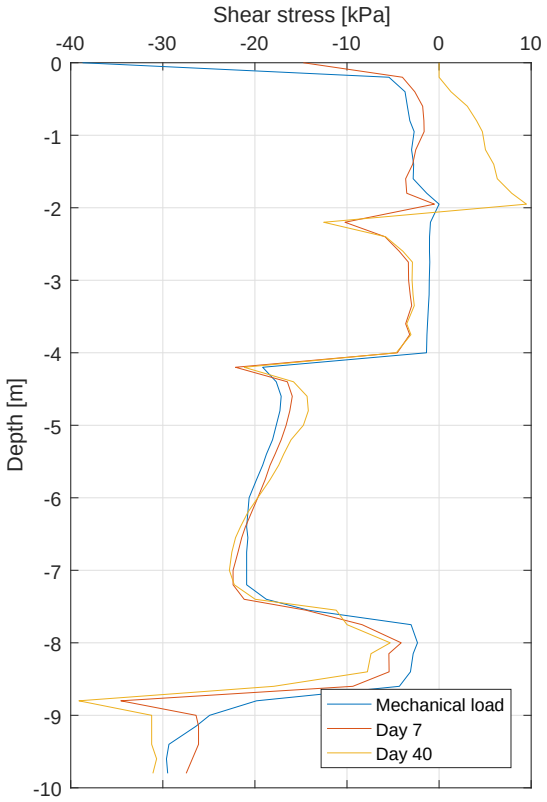



Figure B.3: Shear stress, heating and cooling

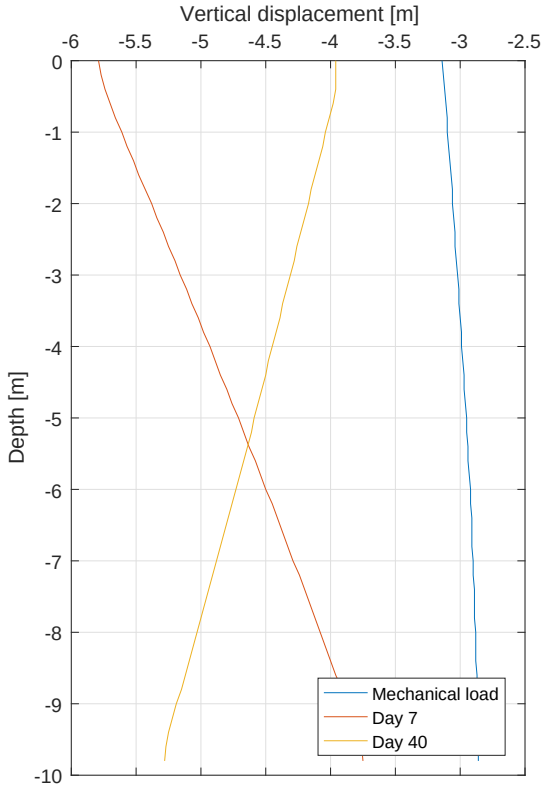



Figure B.4: Vertical pile displacement, heating and cooling

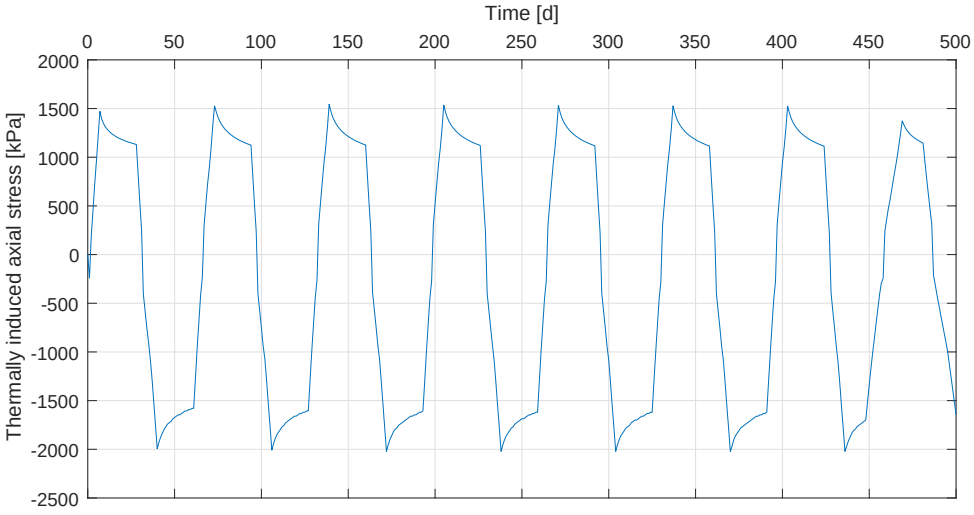



Figure B.5: Maximum thermally induced axial stress, first 500 days

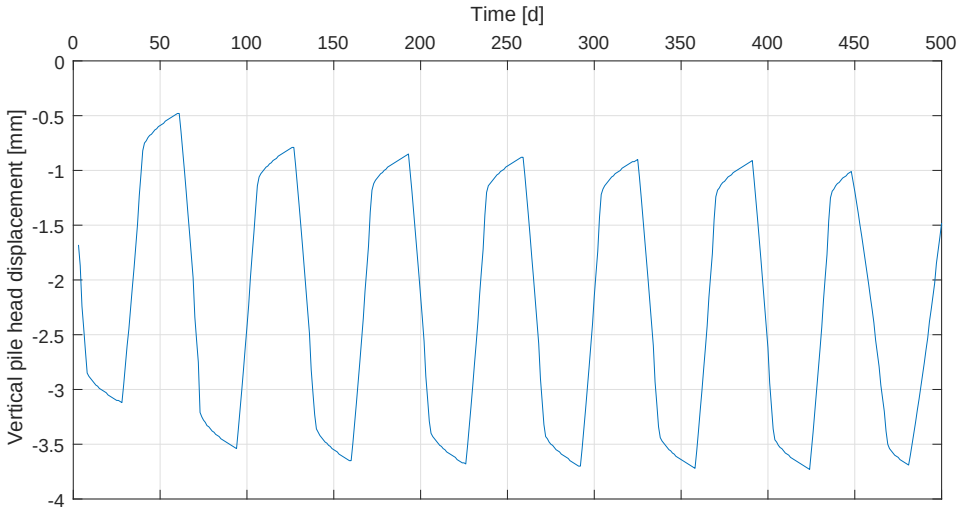



Figure B.6: Pile head displacement, first 500 days

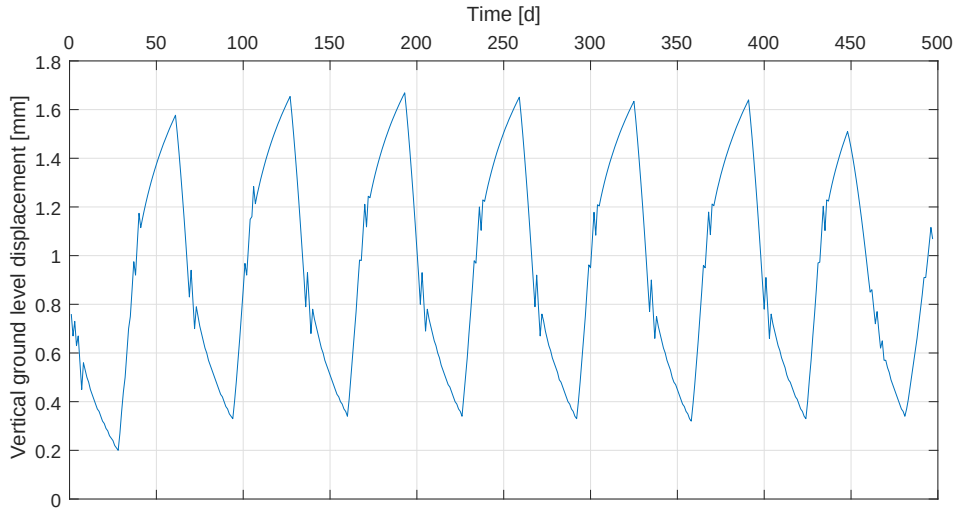



Figure B.7: Ground level displacement 1.0 m from the pile, first 500 days